The unstable phyllitic rocks in Stampa – Flåm, western Norway:

Compilation, scenarios, risk and recommendations

35
2013

RAPPORT

The unstable phyllitic rocks in Stampa – Flåm, western Norway: Compilation, scenarios, risk and recommendations

Norwegian Water Resources and Energy Directorate
2013

NVE Report no. 35 – 2013

The unstable phyllitic rocks in Stampa – Flåm, western Norway: Compilation, scenarios, risk and recommendations

Published by: Norwegian Water Resources and Energy Directorate

Editor: Lars Harald Blikra (ÅTB)

Co-authors: Martina Bøhme (NGU), John Dehls (NGU), Reginald L. Hermanns (NGU), Thierry Oppikofer (NGU), Tim Redfield (NGU), Jan Steinar Rønning (NGU), Freddy Yugsi Molina (NGU), Ulrik Domaas (NGI), Andreas Pfaffhuber (NGI), Helge Henriksen (HSF), Jarle Hole (ÅTB), Lene Kristensen (ÅTB)

Other contributors: Jørn Vatn (SINTEF); Hallvard Berg (NVE); Michel Jaboyedoff (University of Lausanne); students at Sogn & Fjordane University College

Print: Norwegian Water Resources and Energy Directorate

Cover photo: Top: Overview of the Flåm – Stampa area (www.norgei3d.no); Lower left: Steep cliffs at Stampa (Photo: R.Hermanns, NGU); Lower right: Ground-based InSAR monitoring from Otternes with view towards Stampa (Photo: L.H. Blikra, ÅTB)

ISSN/ISBN: 1501-2832 / 978-82-410-0904-4

Abstract: The report presents a compilation and summary of all existing data on the unstable slopes in the Stampa-Flåm area, presents a risk classification and gives recommendations for the future risk handling. The unstable area is characterized by relatively small movements without any signals of increased deformations, and a follow-up in terms of a revision of existing displacement measurements is considered to be sufficient in order to handle the risk in the Stampa area. Based on the relatively low risk connected to the largest scenarios and the limited knowledge on the hydrological conditions, it is in the present situation not recommended to initiate any mitigation measures in terms of larger drainage systems. This conclusion follows the recommendations from the international expert panel.

Key words: Risk, hazard, monitoring, stability, landslides, rockslides, tsunami

Norwegian Water Resources and Energy Directorate
Middelthunsgate 29
P.O. Box 5091 Majorstua
N 0301 OSLO
NORWAY
Telephone: +47 22 95 95 95
Fax: +47 22 95 90 00
E-mail: nve@nve.no
Internet: www.nve.no

August 2013

Contents

Preface

Landslides pose a serious risk in large parts of Norway. The Norwegian Water Resources and Energy Directorate (NVE) is the governmental authority for the prevention of damage caused by landslides. The steep and unstable slopes in Flåmsdalen and along Aurlandsfjorden have been of large concern for a long time both from the local inhabitants, the municipality, the County Governor, Sogn og Fjordane County, and governmental institutions. The potential of a large rock collapse triggering a rockslide that can generate a destructive tsunami has been of particular attention. Several measures for risk reduction have been proposed. Before deciding on further action, NVE saw the need for compilation of all available knowledge. This report presents a full compilation of all existing investigations and research that have been performed in the Flåm-Stampa area, and gives recommendations for further action.

It is the aim of NVE that the present report will provide a good basis for the management of landslide risk in the area.

Oslo, August 2013

Per Sanderud
Director General

Anne-Britt Leifseth
Director
Department for Landslides, Flood and River Management

Summary

The unstable rockslopes is located at the southern end of Aurlandsfjorden, a branch of Sognefjorden in Western Norway, along Flåmsdalen and Aurlandsfjorden (Stampa-Flåm area) and represents one of the largest active rockslide areas known in Norway. Large rockslide deposits have been mapped in the fjord below, and displacements of about 1 cm/year have been documented from parts of the unstable area. The municipality of Aurland, Sogn og Fjordane County, the County Governor and institutions on the governmental level have been concerned about the stability conditions, and especially the potential of getting a major collapse that can generate large rockslides and tsunamis.

This report presents a compilation and summary of all existing data on the unstable slopes in the Stampa-Flåm area, presents a risk classification and gives recommendations for the future risk handling. This work is done in close corporation with persons and institutions that have performed investigations in the area. The report has been the basis for an international evaluation and will be an important document for the future handling, led by the Norwegian Water Resources and Energy Directorate (NVE).

Several possible scenarios have been evaluated and used for the risk classification. There are still large uncertainties connected to this classification and there is a need for further investigations in terms of getting better knowledge on displacements, geological structures, run-out and tsunamis. The risk analysis show that the scenarios related to the steep cliffs north of Stampa (scenario 2a and 3a) has the highest risk. These areas need to be followed up in more detail in order to reduce the uncertainties in the risk classification.

At the moment, with relatively small movements and without any signals of increased deformations, a follow-up in terms of a revision of existing displacement measurements is considered to be sufficient in order to handle the risk in the Stampa area.

Physical mitigation in terms of large scale drainage systems would possibly have an effect on the largest scenarios. However, the present data show limited displacements and the present analysis indicate a low hazard for these scenarios. The knowledge of the unstable area is too limited in order to evaluate the effect of drainage, for example the coupling between the hydrological system, displacement and stability. Based on the relatively low risk connected to the largest scenarios and the limited knowledge on the hydrological conditions, it is in the present situation not recommended to initiate any mitigation measures in terms of larger drainage systems. This conclusion follows the recommendations from the international expert panel.

1 Introduction

The unstable rockslopes is located at the southern end of Aurlandsfjorden, a branch of Sognefjorden in Western Norway, along Flåmsdalen and Aurlandsfjorden (Stampa-Flåm area), Figure 1. It represents one of the largest active rockslide areas known in Norway (Braathen et al. 2004). An area of up to 11 km^2, along the eastern slope, shows signs of active and postglacial gravitational deformations (Bøhme et al., 2013). Large rockslide deposits have been mapped in the fjord below (Blikra et al., 2006), and displacements of about 1 cm/year have been documented from parts of the unstable area (Hermanns et al., 2011). The municipality, the county and institutions on the governmental level have been concerned about the stability conditions, and especially the possibility of a major collapse that can generate large rockslides and tsunamis.

It has been performed a series of studies and investigations related to the unstable phyllitic rocks along Flåmsdalen and Aurlandsfjorden. This includes a research project in the period 2000-2003 focusing on mapping and detailed investigations on specific topics like stability and ground-water conditions. The project participants were Aurland municipality, Norwegian Geotechnical Institute (NGI). Geological Survey of Norway (NGU), Institute for Energy Technology (IFE), E-CO Energi and Spilde Entrepenør. NGU in corporation with the Sogn & Fjordane county have made geological mapping and displacement measurements in a project going on between 2005 and 2009 (Henderson & Blikra, 2008), a work that has been continued through the governmental mapping program (NVE/NGU). NGU together with NORUT have processed and evaluated satellite-based InSAR in order to detect displacements, and NGU in corporation with Åknes/Tafjord Beredskap (ÅTB) have performed periodic ground-based InSAR campaigns). NGI have performed relatively extensive geophysical measurements with use of 2D resistivity and airborne electromagnetic mapping (AEM) in a research project organized within International Centre for Geohazards (ICG). SINTEF has been involved with evaluation of existing reports and made proposals for investigations and further approach connected to stability analysis in the area. Sogn og Fjordane University College (HSF) has performed some research activity related to groundwater and geophysics. NGU and NTNU in corporation with University of Lausanne have a PhD project on the stability of rock slopes, which also include the Stampa-Flåm area (Böhme et al., 2013). E-CO Energi has made evaluations of the possibility of performing large-scale drainage in order to reduce the stability problems in these areas.

This report aims to make a compilation and summary of all existing data on the unstable slopes in the Stampa-Flåm area. It gives a summary of the most important data, evaluates geological models/scenarios, presents the new risk classification from NGU and gives advice for the future risk handling. All data is compiled and integrated on an ArcGIS platform. This work is done in close corporation with persons and institutions that have performed investigations in the area. The report has been evaluated by an international expert panel and will be an important document for the future handling, led by the Norwegian Water Resources and Energy Directorate (NVE).

Figure 1. Overview of the area. From Norkart (www.norgei3d.no).

2 Bedrock and structures

2.1 Regional geology

The regional geological background presented here is based on an internal NGU document (Redfield, 2012). The most important geological history of importance for the Flåm-Stampa area goes back to more than 400 million years ago when Laurentia (e.g. Greenland) collided with Baltica (e.g. Norway), forming Euramerica. During the collision, large sheets or nappes, were thrust over the deep basement rocks, helping thicken the crust and forming the Caledonide mountain range. In many ways comparable to today's Himalaya, the Caledonide mountains became unstable near the peak of their growth. Perhaps as early as 400 Ma the range began undergoing extensive gravitational collapse (e.g. Andersen and Jamtveit, 1990; Fossen, 2000).

Although the mountains had collapsed, Euramerica remained intact. During the Late Carboniferous and Early Permian the Oslo Graben underwent rifting and volcanism, but supercontinent amalgamation continued as Euramerica joined with the rest of Pangaea. A series of extensional events began stretching the crust between Laurentia and Baltica. Thinning began in Permian time, achieved a crescendo in the Late Jurassic or Early Cretaceous, and culminated in continental breakup and sea floor spreading around the earliest Tertiary, circa 55 Ma. Today's map pattern and today's potential large volume rock slides reflects this sequence of events.

A simplified geological map of southern Norway is shown in Figure 2. The Baltic shield basement is covered by Lower Paleozoic platform rocks and three Caledonian nappe stacks (e.g. Bryhni and Sturt, 1985). Two major structural zones, the Møre og Trøndelag Fault Complex (MTFC) and the Hardangerfjord Shear Zone-Lærdal Gjende Fault System (HSZ-LGFS), run southwest across the map. The MTFC and the HSZ were also active during Caledonian orogenic collapse (Osmundsen et al., 2006; Fossen & Hurich, 2005). Subsequently, the MTFC has undergone multiple episodes of post-Caledonian reactivation in brittle mode (e.g. Redfield et al., 2005), and similar episodes of brittle activity along the HSZ is also known from the offshore (Andersen et al., 1999; Fossen & Hurich, 2005). Work in the Lærdal area, northeast of Flåm,

documents similar reactivation on the LGFS (Andersen et al. 1999), as illustrated by formation of thick zones of fault breccia end even some occurrences of unconsolidated breccias.

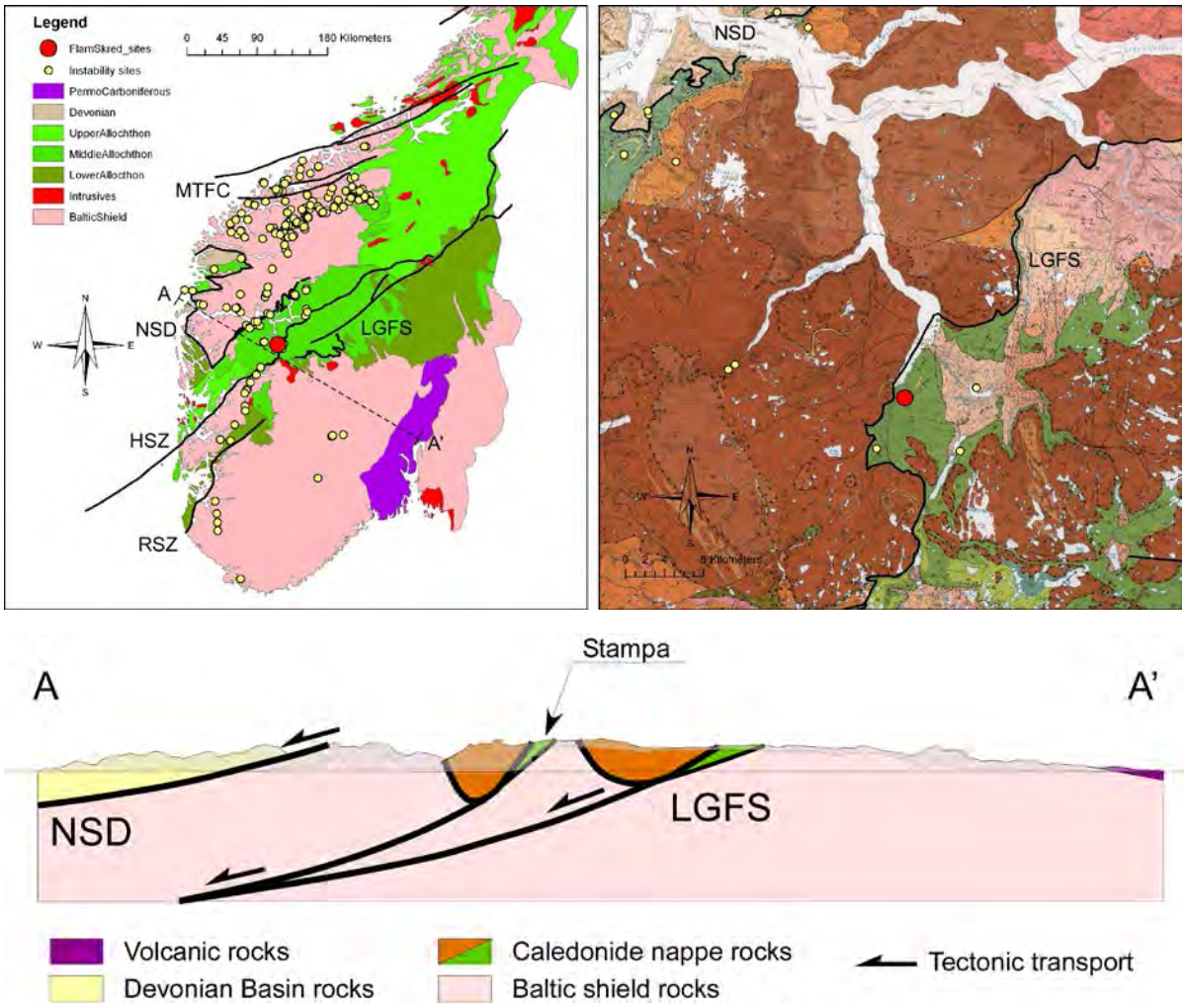

Figure 2: Left: Generalized geological map of southern Norway. MTFC = Møre og Trondelag Fault Complex. NSD = Nordfjord Sogn Detachment. HSZ = Hardangerfjord Shear Zone. LGFS = Lærdal Gjende Fault System. RSZ = Røldal Shear Zone.Yellow circles denote potential rock instability sites from the NGU database. Red circle indicates the rock instability site at Stampa. Note the majority of instabilities occur in faulted and heavily-incised terrains proximal to or NW of the HSZ-LGFS. A-A' marks the cartoon at bottom. Right: Local geological map of the Stampa area after the NGU 1:250000 series. Below: Generalized tectonic cartoon modified from Fossen and Hurich (2005). Large black arrows show direction of overall tectonic transport during collapse and subsequent extension. Note the brown-colored nappe rocks (Jotun nappe) are thrust over the green colored nappe rocks (phyllites) in the Stampa vicinity. Light grey shading shows a typical topographic envelope. Mylonite fabrics not shown.

The fault complexes mark zones of weakness that are obvious candidates for structural reactivation, and it has been shown that some of the large-volume rockslides in Norway can be associated with structurally reactivated faults, e.g. both from the Troms County (Osmundsen et al., 2009, 2010) and in Møre (Redfield and Osmundsen, 2009). The documented fault zones that helped guide events such as the 1756 Tjellefonna and the 2008 Ålesund rockslides are much more common in the heavily-incised regions to the NW of the HSZ-LGFS-RSZ. This "Escarpment Zone" appears to have undergone a series of significant fault-related rock-column uplifts throughout the latest Mesozoic and the Cenozoic (Redfield et al., 2005; Redfield and Osmundsen, 2009). Although the individual mechanisms of failure may differ significantly,

their existence is likely controlled by a few simple fundamentals that are rooted in Norway's tectonic history. It is thus clear that the unstable rockslopes at Stampa are influenced by the tectonic history and the regional extensional detachments and faults as indicated in Figure 2. However, as no systematic mapping of such fault zones has been undertaken in the Flåm area, for example close to and along the contact of the Jotun nappe, their importance there for rock-slope stability remains poorly constrained.

2.2 The Stampa area

The studied unstable rock slopes are situated on the eastern slope above the fjord and the village of Flåm. The data presented here is mainly based on Hermanns et al. (2011) and Bøhme et al. (2013). The bedrock consists of Lower Palaeozoic and Precambrian metamorphic rocks (Figure 3). The instability is located within phyllites that are thrusted over the Precambrian basement cropping out north and east of the study area. Caledonian thrust boundary forms the contact between the phyllites and the overlying Jotun Nappe to the west (Figure 4).

Detailed structural field mapping was performed in the period from 2008 to 2010, including more than 2500 measurements of joints and foliation (Böhme et al., 2013), Figure 3. Also a LIDAR survey (TLS) was carried out at two locations and a structural analysis was done. A DEM based on an airborne laser scanning was used for interpretations of lineaments and open fractures.

The field data show that the foliation in the phyllites is strongly folded, ranging from cm-scale to m-scale open folds, with a shallow fold axis plunging on average 274/12 $\pm 10^0$ (Hermanns, 2011; Böhme et al., 2013). The orientation of the foliation changes a bit, but have an average of 264/18 ± 15°, slightly oblique towards the fjord. This is in accordance with the TLS data as presented in Bøhme et al. (2013) (261/18 ± 16°). In southern area, south of Ramnenosi, the TLS data also show the same orientation, but the foliation dip angles were found to be significantly steeper, around 35°. Bøhme et al. (2013) discuss that this could also be an effect of the different scale used (10x10 cm for field data; 50x50 cm for TLS data). The reason might also be that the TLS data is from steeper slopes, including vertical cliffs, in contrast to the field measurements performed on the top of the plateau. Since there are limited data in the steep areas, and no borehole data exists, it is difficult to know if the foliation dip changes downslope and with depth.

The field data has no indications of larger fault zones, for example related to the thrust fault occurring in Flåmsdalen (Figure 4).

The specific TLS analysis of the foliation at and around the block at GPS AU 12 north of Stampa (named scenario 3a in later sections) shows the following results of the dip directions and dip angle (Hermanns et al., 2011):

1. The steep backscarp inside, in the southwest: 262°/19° ± 16° and 298°/44° ± 20°
2. The southwest steep part: 246°/27° ± 12° and 278°/33° ± 12°
3. The block in northwest, downslope: $229^0/30^0 \pm 10^0$

Grimstad et al. (2008) reported foliation in the front of the steep cliffs outside Joasete to be between 16 and 24^0, and 25-27^0 at Joasete and lower part of Stampa, with exceptions of up to 36^0.

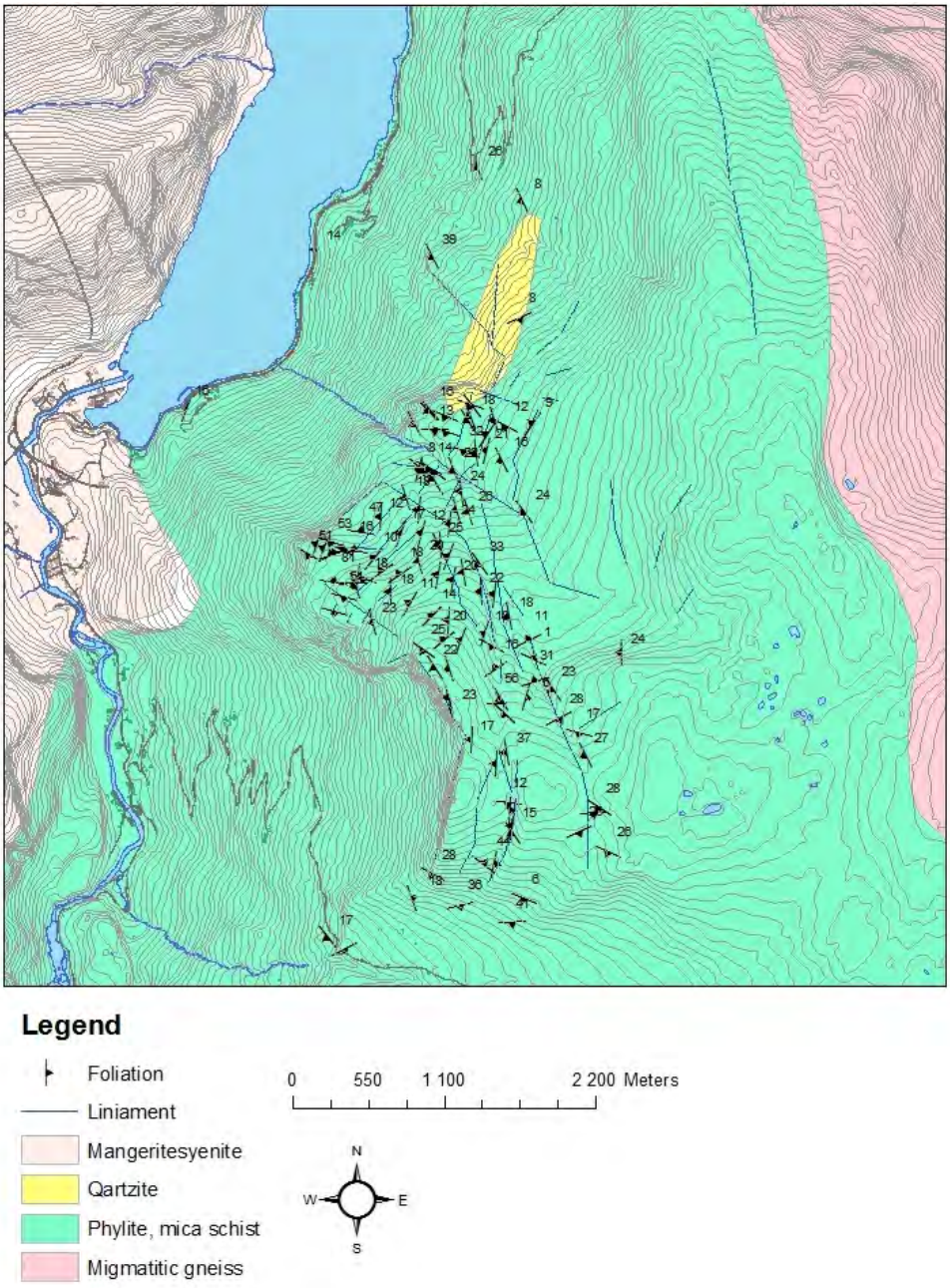

Figure 3: Bedrock map including lineaments and foliation measurements. The migmatitic gneiss is the basement rocks and the mangeritesyenite belongs to the thrusted Jotun nappe.

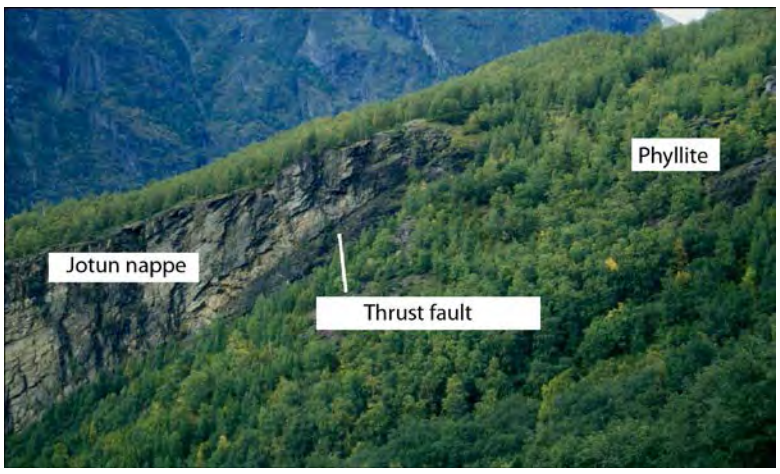

Figure 4: The thrust fault of the Jotun Nappe with The underlying phyllitic rocks. View towards north.

In conclusion, it seems that the foliation outside the plateau and in lower altitudes can be steeper than those found on the plateau, but this needs to be investigated in the field.

The field data, TLS data and detailed DEM demonstrate the occurrence of three main steep joint set with a constant orientation in large areas (J1: NNW-SSE; J2: WNW-ESE; J3: NNE-SSW). Most of the open fractures and direction of instabilities like slide scars are developed along these joint sets (Figure 3). In the Stampa area, the major open fractures follow the NNW-SSE joints (J1), while the northernmost area has prominent normal faults and slide scars following the NNE-SSW joints (J3).

Altogether, the different data show a relatively consistent picture, with the mapped instability features having a strong structural control, at least for the joint sets. The foliation direction is also consistent, but the conclusions regarding the dip in the steepest area of the slope is still questionable. There are indications that the dip may change and possibly be steeper downslope. However, more measurements in this area are needed, and it is important to have in mind that there are no data of the geological structures in the subsurface. The regional geological data also raise the questions about the possible occurrence of major fault zones linked to the post-caledonian and younger Devonian/Permian reactivation. Such zones are not found in the field-data set, but may be important in the subsurface, close to and along the Jotun nappe. Such zones may explain the long and persistent trend of the SW-NW back-bounding structures at Stampa (Figure 3 and Figure 5).

3 Geomorphology

The research project performed in the period 2000-2003 also included geomorphological mapping of the area (Domaas et al., 2002), recognizing that a considerable part of the slope above Flåm shows signs of active gravitational deformation (Braathen et al., 2004; Blikra et al., 2006). The investigations also included collection of bathymetric and seismic data in Aurlandsfjorden. All datasets indicate that large areas of the slopes, valleys and fjord bottom are covered by thick rockslide and rock avalanche deposits. Prominent slide scars are present along the entire front of the unstable area.

A detailed air-based LIDAR scanning was performed by Aurland municipality, giving a detailed DEM, which is very valuable for geomorphological interpretations. The old data has been evaluated and some revised interpretations of the detailed DEM have been done in order to produce an updated geomorphological map (Figure 5 and Figure 6).

A long and persisting back-bounding structure has been mapped starting in Gudmedalen in south, cutting through the Ramnanosi mountain and continuing in the north towards the Stampa river and Joasete were it separates into segments that are slope-parallel and W-dipping. The structure is a more than 4 km long normal fault, seen as a more or less distinct 1-2 m high scarp (Braathen et al., 2004: Fig 11d). Large parts of the structure seem to show down-slope shear movements by reactivation of the foliation. On the plateau, some faults can be followed in a linear shape by the formation of sinkholes (Braathen et al., 2004: Fig. 11d). In the north, several N to NNW striking faults and joints, parallel to the steep mountainside, interact with a series of E-W, transverse fractures. The deformed mountain plateau is characterized by a series of normal faults and associated half-grabens, locally with an enechelon pattern.

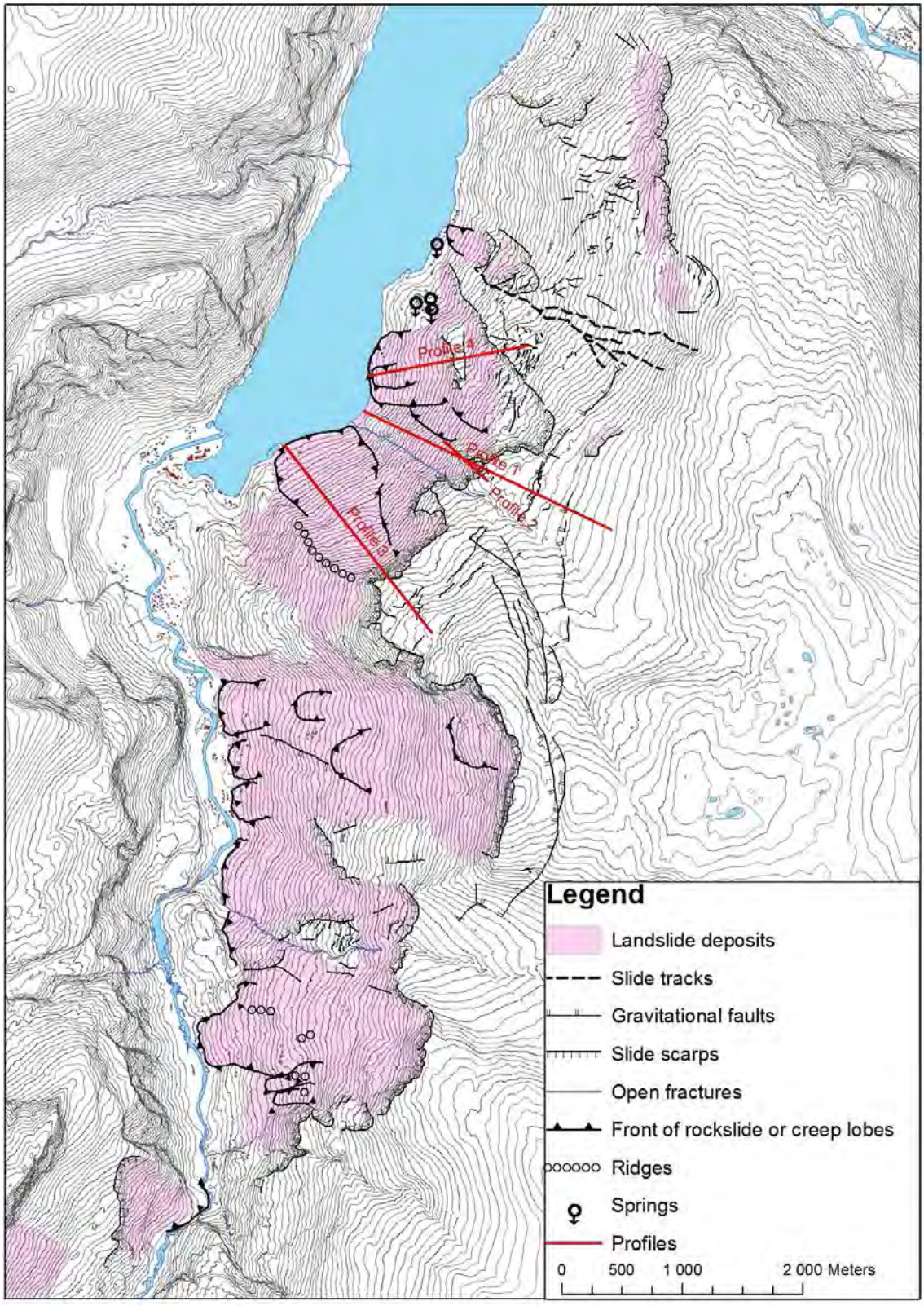

Figure 5: Geomorphological map Flåmsdalen – Aurlandsfjorden.

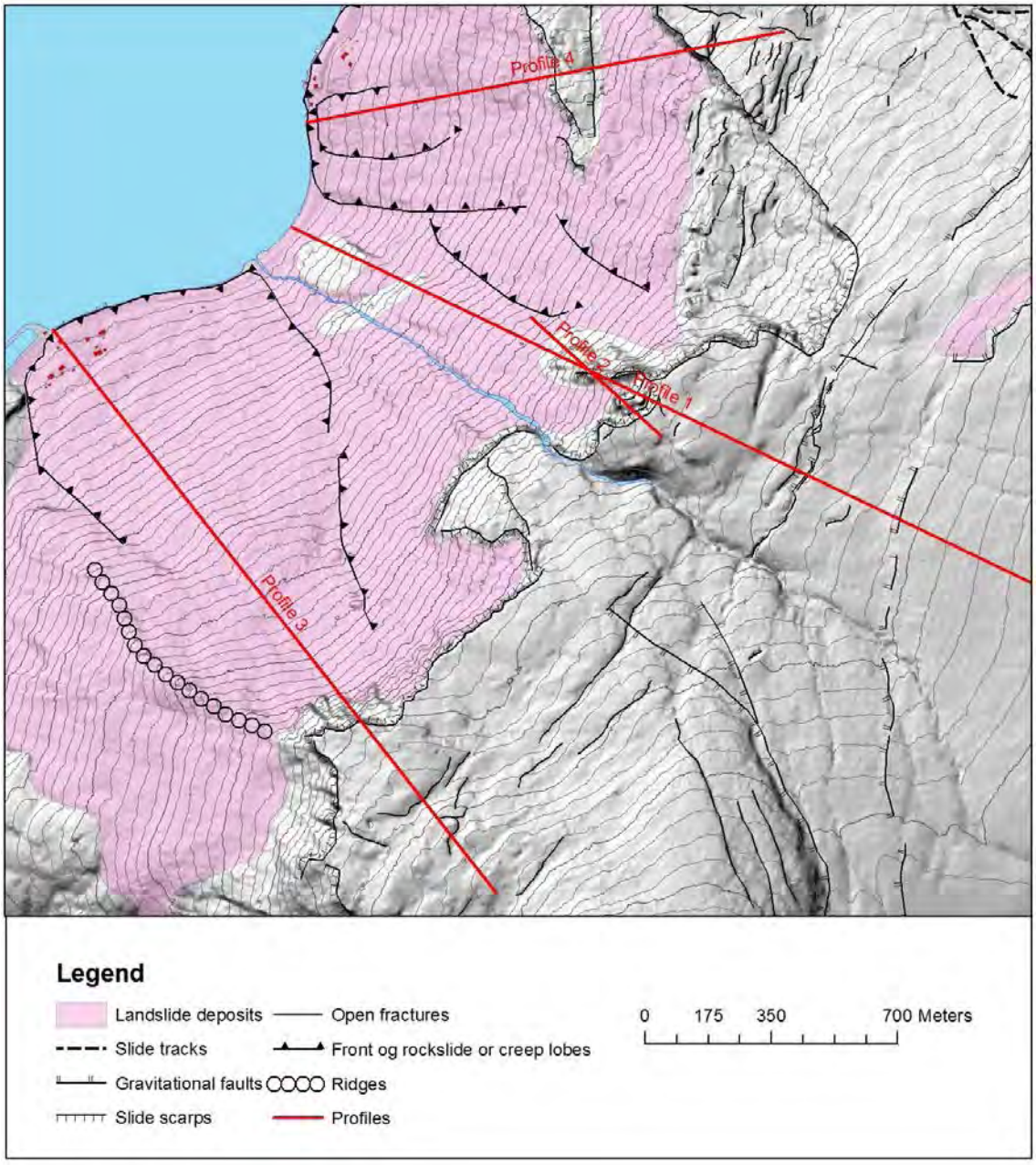

Figure 6: Geomorphological map Stampa area. Profiles used later in the report are shown.

The area below the mountain plateau is characterized by a very large number of open fractures, slide blocks and slide scars. Large parts of the back scarps of slide blocks and slide scars formed by rock avalanches follow the steep joint sets (Figure 5 and Figure 6). However, the northern area between Joasete and Otternes has a prominent back scarp that seems to be controlled by the NW-SE trending foliation.

The lower part of the mountain slopes, near the valley floor and fjord is dominated by 100- 700 m wide bouldery lobes, which are most likely formed by creep of rock-avalanche deposits (Figure 5 and Figure 6). Many of them are active today, and in 1980, a creeping lobe moved into the fjord in the northern part of the area, just south of Otternes (Domaas et al., 2002).

4 Subsurface data: Geophysics, drilling and excavations

The research project in 2000-2003 included some geophysical investigations. Some refraction seismic profiles and ground-penetrating radar measurements were performed on the lower creeping boulder lobes in Flåmsdalen, and some profiles also across the large back-bounding normal faults in Gudmedalen (Domaas et al., 2002). Some drillings were also performed at Holo in Flåmsdalen in order to investigate sediment types, sediment depths and hydrological conditions. Also some excavations were performed in the creeping landslide to map their internal characteristics.

NGI has performed a relatively extensive airborne electromagnetic mapping (AEM) survey in 2009 and an Electrical Resistivity Tomography (ERT) campaign in 2010 (Pfaffhuber et al., 2010, 2011). We have got access to all data from NGI and these are integrated into the ArcGIS platform in order to do interpretations together with the other data sets.

The University college of Sogn & Fjordane have performed some georadar profiles at Joasete, and also some few drillings in order to investigate potential water level.

The road authorities have performed a large number of ground investigations along the shore of Aurlandsfjorden in connection with the planning of a new road (Skotheim, 1993).

4.1 Resistivity data (AEM and ERT)

The AEM data has been processed and presented in depth intervals (Figure 7 and Figure 8) and in two selected profiles (Figure 9 and Figure 10). The data shows the following main characteristics:

- The phyllites seems to have low resistivity values, and Pfaffhuber et al. (2010, 2011) demonstrate the transition to the underlying Precambrian metamorphic rocks showing higher resistivity in the east. The extreme low resistivity values can be due to the content of graphite, which have been observed in the phyllitic bedrock in this area (Henriksen, pers. comm.).
- There is a relatively clear transition within the phyllitic rocks between the undeformed low resistivity phyttlitic rocks and the deformed and unstable phyllitic rocks with higher resistivity to the west (Figure 7 and Figure 8). The unstable area has undergone major deformations characterized by open fractures, which seem to influence the resistivity conditions. This high resistivity zone is especially evident at the slope break going from the plateau and down the steep slope, where the zone seem to be about 100 m thick (Figure 9). Furthermore, this indicates that the area is well drained.
- Some areas within the unstable rocks shows much lower resistivity, especially a zone starting in the Joasete area, and can be followed towards and along the Stampa river. The resistivity in the upper Joasete area seems to increase again from about 60-80 m depth, while the low values along the Stampa river is relatively persistent throughout the entire depth section from the surface to 180 m below surface.
- A low resistivity zone is evident east of Joasete, at the end of the 2D resistivity profile, below 100-110 m depth.
- A smaller low resistivity zone occurs in the depth interval 50-110 m just outside GPS point 14 north of Joasete.

- Relatively high resistivity characterizes the surface of lower slopes covered by landslide debris. If this indicates the debris coverage, it shows that the landslide debris thickness can be up to 50 m thick, but locally with thin cover or exposed bedrock (Figure 9 and Figure 10).

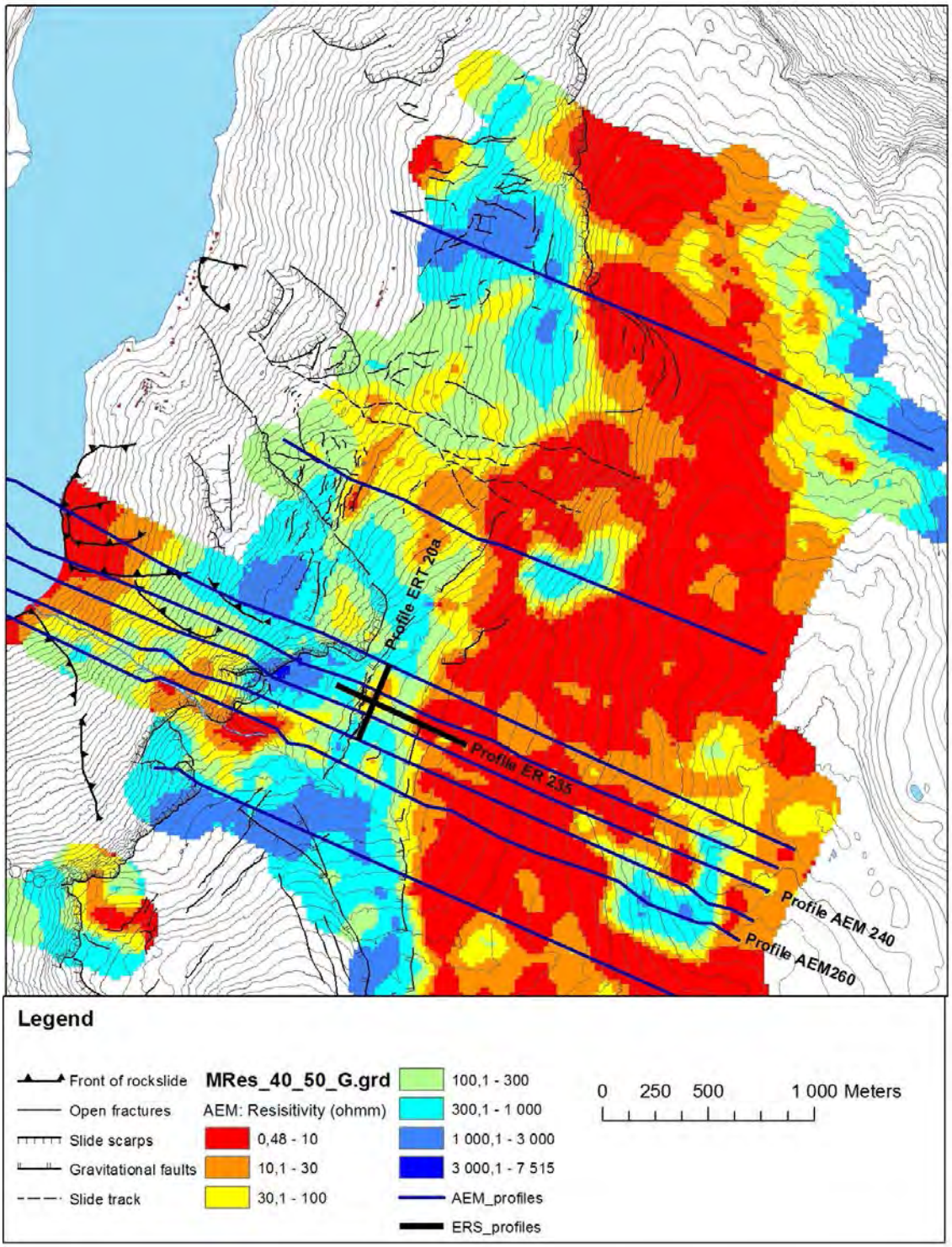

Figure 7: AEM data at 40-50 m depth

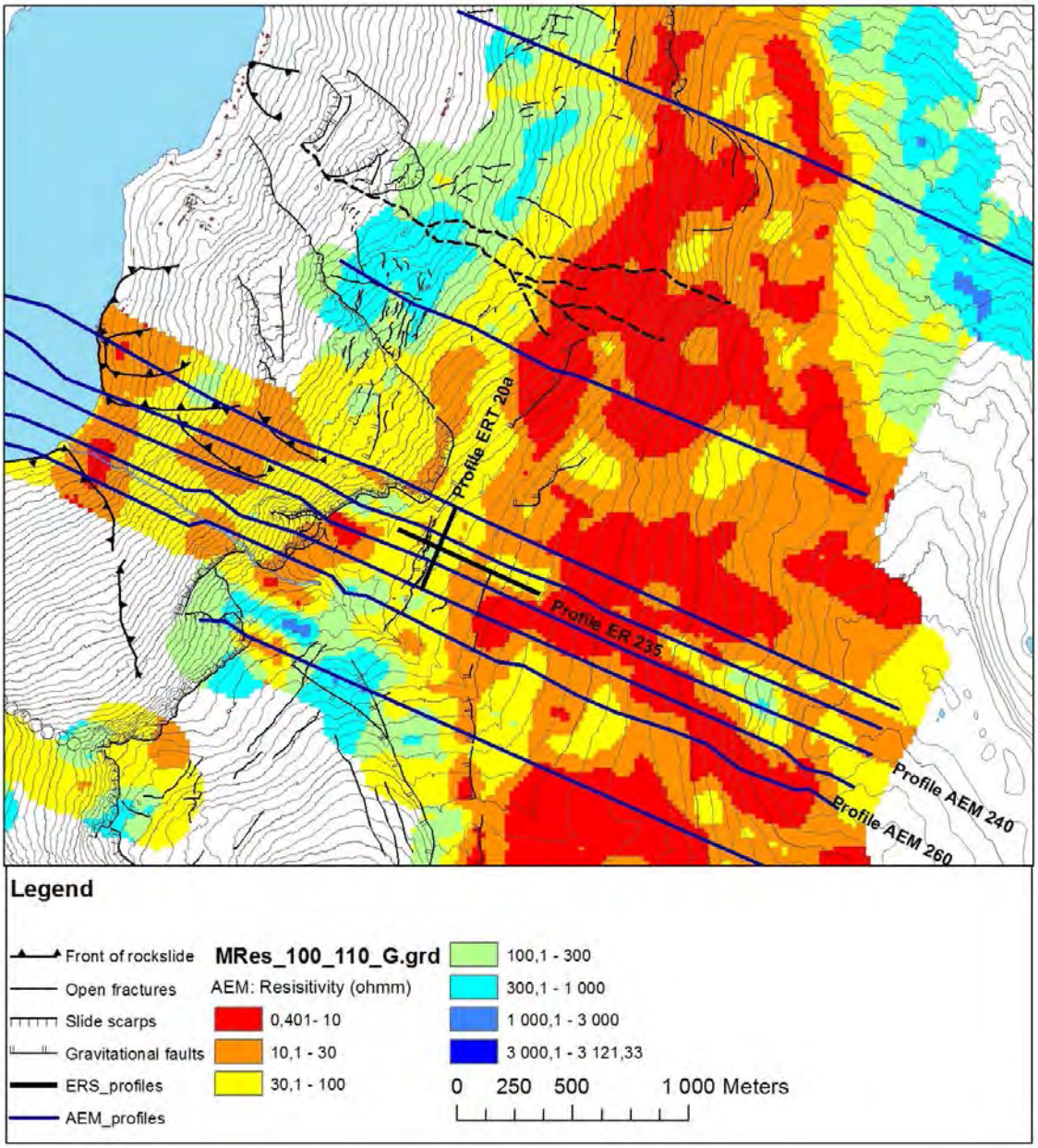

Figure 8: AEM data at 100-110 m depth.

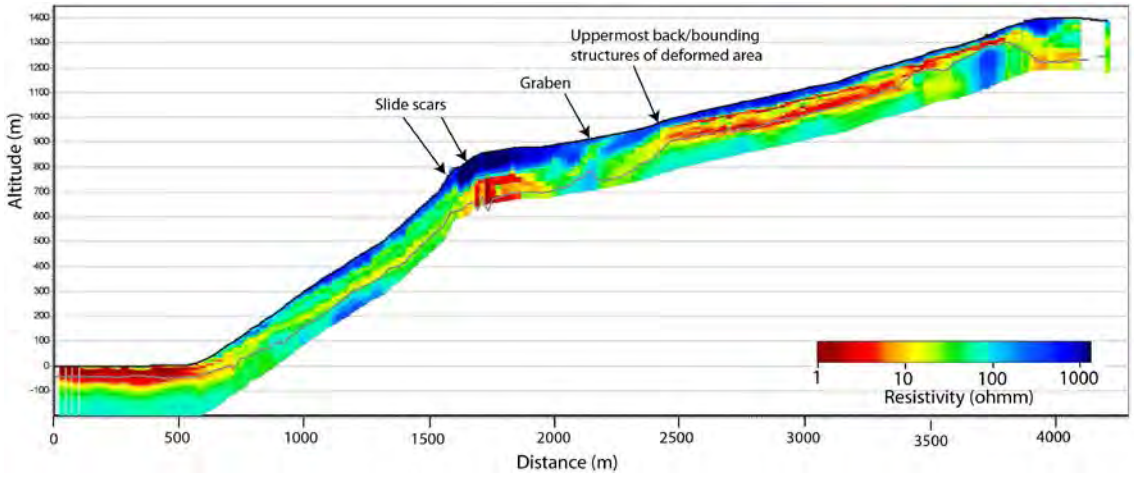

Figure 9: AEM data from profile 240. Location in Figure 7.

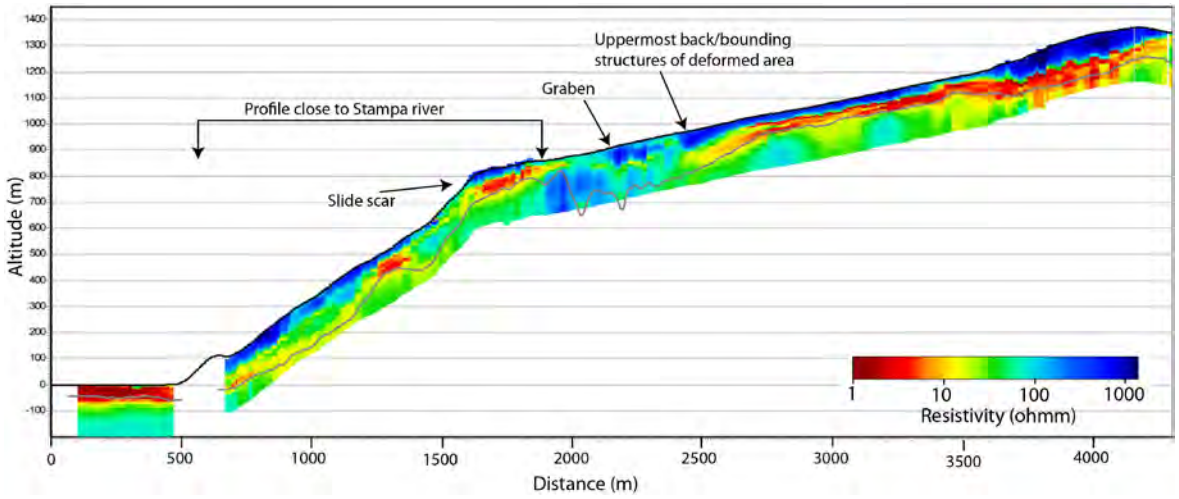

Figure 10: AEM data from profile 260. Location in Figure 7.

The two ERT profiles support to a large degree the AEM data in terms of the pattern and changes in resistivity, but shows generally much higher resistivity values. The ERT data show the distinct low resistivity zone at Josete and Stampa (Figure 11). The low resistivity zone at Joasete seems to start as a point source at the surface, and continues below 60-70 m depth. Interestingly, this zone does not continue out to the steep slope, but goes as a relatively narrow and deep "channel" from Joasete towards the Stampa river and turns the direction towards west. The low-resistivity zone is thought to be caused by water-rich parts of the deformed phyllitic rocks. Several small streams drain towards the Joasete river, and the Stampa river will also support the subsurface with water. This is also indicated by the observations of Stampa river that several times have been dry in its lower portion.

The ERT profile also show a low resistivity zone along the uppermost back-bounding structure of the deformed area.

There is a quantitative mismatch between ERT and AEM values, and a clear understanding of this has not been verified. Anisotropy and 3D effects can be the explanation, but only a synthetic study could confirm or reject such assumptions.

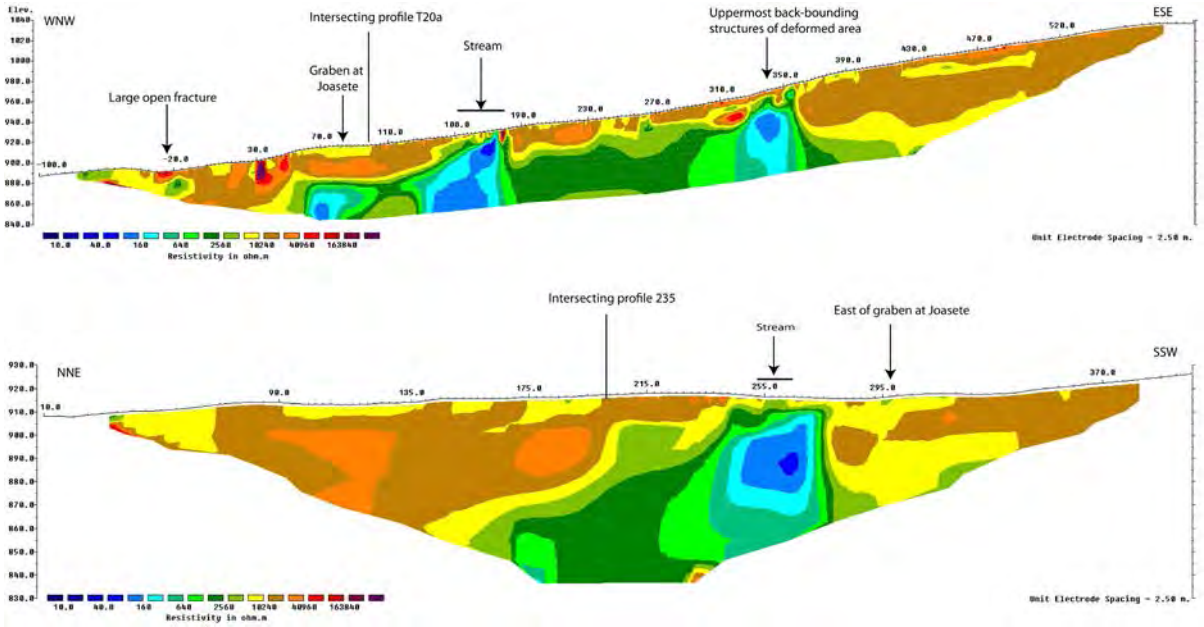

Figure 11: ERT profiles from NGI. The text explanation is done for the present report. See location in Figure 7.

4.2 The Joasete area: GPR and drillings

A ground penetrating radar (GPR) study was performed in the graben area at Joasete by students at the University College of Sogn og Fjordane (Brenne et al., 2011). The data show that the graben area is characterized by deformations including subsidence of blocks, large fractures and probably crushed areas in the entire penetrating depth down to 20-25 m (Figure 12). Also several percussion drillings were performed by the students, with maximum depth of 17 m. The main conclusion is that the graben area is characterized by displaced blocks, open spaces, crushed material and is well drained.

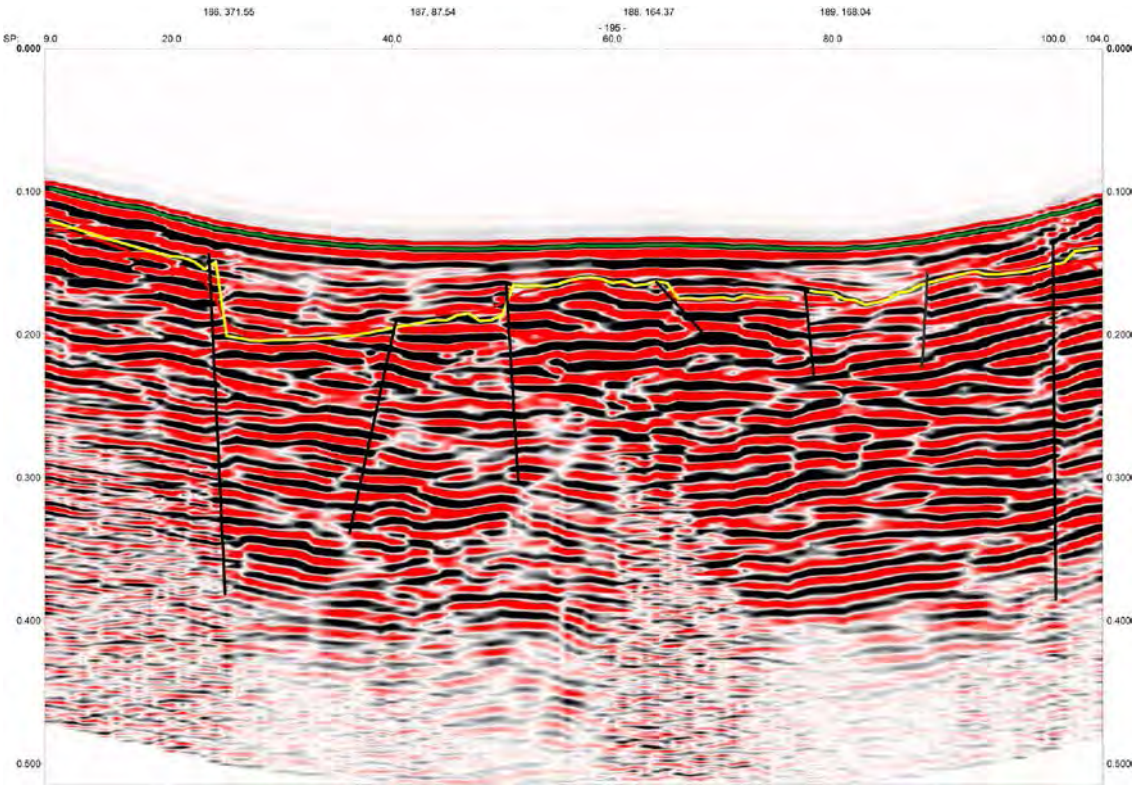

Figure 12: GPR profile 195 (Brenne et al., 2011). The depth penetration is 20-25 m.

4.3 Holo and Heimdal in Flåmsdalen: Refraction seismic, ER, drillings and excavations

The research project in 2000-2003 included some geophysical investigations, drillings and excavations. Some refraction seismic profiles and ground-penetrating radar measurements were performed on the lower creeping boulder lobes in Flåmsdalen, and some profiles were also measured across the large back-bounding normal faults in Gudmedalen (Domaas et al., 2002). Some drillings were performed at Holo in Flåmsdalen in order to investigate sediment types, sediment depths and hydrological conditions. Also some excavations were performed in the creeping landslide depths to map their internal characteristics. The data are not summarized here, but some of it is used in the chapter on hydrological investigations.

Some few refraction seismic profiles were measured in 2002 to evaluate the thickness of the lower creeping lobes at Heimdal in Flåmsdalen (Domaas et al., 2002).

4.4 Ground investigations along Aurlandsfjorden

The road authorities have performed a large number of ground investigations along the shore of Aurlandsfjorden in connection with the planning of a new road (Skotheim, 1993). The data generally shows that there are blocky rock avalanche deposits in large parts along the fjord, but in areas covered by some few metres of fine-grained deposits. In some areas more than 20 m of blocky material have been documented, interpreted to be rock-avalanche deposits. The data are in accordance with the geomorphic data.

5 Hydrological investigations

There were made some hydrological investigations in the research project performed in 2000-2002 (Domaas et al., 2002). This included pietzometer measurements in boreholes, tracer tests and resistivity measurements in the area around Holo in Flåmsdalen (see location in Figure 1). There were active movements in some of the landslide lobes in 2000. The main conclusions from these investigations were the following:

- Stratigraphy: Glacial till above bedrock (10-15 m thick) capped by a 5 to 10 m thick phyllitic debris (landslide lobe)
- The overlying phyllitic landslide deposits have a low permeability and tension fractures is important for effective infiltration of water
- The glacial till above the bedrock has higher permeability, leading to the possibility for water overpressure.
- High conductivity in shear zones and water-filled glacial till, measured to be less than 200 ohmm in the ERT investigation.
- Conductivity of between 130 and 200 µS/cm in one of the boreholes, measured in May to June.

These investigations and analyses made in Holo may give some important knowledge also for other areas in the entire unstable phyllitic area. It shows that the phyllitic landslide debris can be relatively impermeable and that there may be possibilities to get large overpressure during snowmelt and high precipitation. This can be important for the stability of the debris-covered slopes if they were impacted by smaller or larger rockfalls from above.

The Sogn & Fjordane University College have had a bachelor thesis (Brenne et.al. 2011) in the area in order to better understand the hydrological system. They performed some percussion drillings in the graben at Joasete and installed a pietzometer at 9,5 m depth in order to measure pore-pressure. Slug tests were performed and a temperature/depth datalogger was installed. The slug tests gave no results and no water level was recorded in the borehole from October 2010 to May 2011.

It has been observed that small streams are captured and subsurface drained at the Joasete area. The bachelor thesis (Brenne et.al. 2011) tried to quantify this. The discharge from the crossing stream was measured at two points, one above and one below the graben. They concluded that 100% of the water was infiltrated into the fractures during low discharge (4 l/s), while 16% of the water was infiltrated into the fractures during high discharge (30-100 l/s). During the period of highest water flow, the total water infiltration into the fractures in the graben was estimated

to be 17 l/s or ca. 1500 m^3 per day. The further travel route of the infiltrated water in the subsurface fracture system water was not mapped out and remains an open question.

The students also measured the electrical conductivity at two water springs at Otternes, located at 100 and 135 masl at the lower part of the slope. The springs are discharging through fractures in the phyllite. The high values between 225 and 273 µS/cm indicate a long residence time. These two springs are located just below and outside the unstable area (Figure 5). Another spring is discharging close to sea level (Figure 5). The mapped springs do not form a single horizon. Judged by the high conductivity, the water discharging from the springs could be deep seated groundwater travelled through fractures, or more shallow groundwater travelled for some distance in the scree-deposits upstream the springs.

University of Bergen have had some student excursions to the open fractures at Joasete, and it has been tried to climb down some of the large open cracks. Lauritzen (pers. com.) informed that they have been able to climb and go down to 30-40 m depth. They observed that water was coming into the open cracks, but there were no sign of any permanent water level.

According to Domaas et al. (2002) it has been observed that the water discharge of Stampa down at the fjord is often less than what has been observed on the plateau, above 800 m altitude. This has been interpreted to have been caused by water draining into open fractures in higher altitudes.

6 Displacements and deformations

There are numerous historical observations of deformations and stability problems in the phyllites along Flåmsdalen and Aurlandsfjorden. This includes rockfalls, debris flows, and creep in the lower landslide debris and active movements in areas with open fractures in higher areas (Domaas et al., 2002). This has caused problems related to roads, railway, agricultural land and buildings.

6.1 Historical events and meteorology

There are several historical landslide events in the area. Debris flows have been documented at Otternes in 1828 and 1872. A large bouldery phyllitic lobe moved across the road and into the sea just south of Otternes in 1979 (Domaas, et.al., 2002). The landslide deposits here was interpreted to be 5-20 m thick by use of refraction seismics, and part of it moved by 11 m during the summer 1979. Further south, the blocky landslide deposits have been interpreted to be even thicker, up to 40 m (Domaas et al., 2002).

Large parts of a steep phyllitic slope at Holo, south of Gudmedal, were displaced by creep in June 2000 (Domaas et al., 2002). This was caused by heavy precipitation and snowmelt, and the movement decreased when the precipitation was reduced. Pietzometers were placed in deep boreholes at the location showing overpressure.

In Flåmsdalen, there are numerous evidence of debris flows, rockfalls and active creep in the lowermost bouldery phyllitic landslide lobes. The creep can easily be seen by deformations in foundations of buildings, roads and the railway tracks. In general, observations of movements near the valley floor show periodical creep that is closely linked to precipitation (Domaas et al. 2002).

6.2 Differential dGNSS data

Differential GNSS surveys were initiated by NGU in 2005 and 2006 with 3 points in stable areas and 18 point in the deformed areas (Hermanns et al., 2011), see Table 1 and GPS vectors

in Figure 13 and Figure 14. Rates of displacements and directions vary significantly at many points due to the fact that the measurements are close to the accuracy level. However, only two of the dGNSS points have not a significant horizontal displacement. The movements range between 0.8 – 10.8 mm/year. The directions of these points and the other points reveal a constant downslope movement towards WNW to NW (Böhme et al., 2013). The largest displacement is in a highly deformed area in the northern sector (AU12 and AU14).

Only half of the dGNSS points have a significant vertical movement (Böhme et al., 2013). The movement plunge (dip of sliding) is very steep for points AU14, 15 and 16 (47-58^0) and between 24 and 31^0 for points AU 10 and 12 (Table 1). However, the vertical values needs to be used with caution, as the accuracy levels are not significant, except for point AU14.

Table 1. Summary of differential GNSS results. Average movement values as well as movement trend and plunge are calculated based on linear regression. Results that are not significant are shown I italics, and points showing consistent movement in bold. Table from Bøhme et al. (2013).

GNSS-point	Average horizontal movement [mm/year]	Average horizontal movement error $3\sigma_m$ [mm/year]	Significant horizontal movement	Average vertical movement [mm/year]	Average vertical movement error $3\sigma_m$ [mm/year]	Significant vertical movement	Average 3D movement [mm/year]	Average 3D movement error $3\sigma_m$ [mm/year]	Movement trend [°]	Movement plunge [°]
AU2	0.8	0.7	Yes	−1.2	1.1	Yes	1.5	1.3	287	56
AU3	*0.9*	*1.7*	*No*	*−0.8*	*2.9*	*No*	*1.2*	*3.4*	*255*	*42*
AU4	1.2	0.7	Yes	−1.6	1.2	Yes	2.0	1.3	301	53
AU5	1.4	0.7	Yes	−1.5	1.2	Yes	2.1	1.4	297	48
AU6	**1.7**	0.7	Yes	*−1.1*	*1.2*	*No*	*2.0*	*1.4*	**303**	*33*
AU7	**2.3**	0.8	Yes	*−1.3*	*1.4*	*No*	*2.6*	*1.6*	**290**	*30*
AU8	2.2	0.8	Yes	*−1.2*	*1.4*	*No*	*2.5*	*1.6*	314	*28*
AU9	2.1	0.9	Yes	*−0.7*	*1.5*	*No*	*2.2*	*1.7*	315	*18*
AU10	**4.0**	0.9	Yes	−1.8	1.5	Yes	4.4	1.8	**306**	24
AU11	*2.0*	*2.6*	*No*	−4.3	3.9	Yes	*4.7*	*4.7*	*308*	65
AU12	**8.5**	2.2	Yes	−4.4	3.4	Yes	9.5	4.0	**301**	31
AU13	2.1	0.9	Yes	*−1.0*	*1.5*	*No*	*2.4*	*1.8*	322	*25*
AU14	**10.8**	1.1	Yes	**−10.7**	1.8	Yes	15.2	2.1	**324**	**47**
AU15	2.3	1.0	Yes	−3.1	1.8	Yes	3.9	2.1	330	53
AU16	1.9	1.1	Yes	−3.1	2.0	Yes	3.6	2.3	326	58
AU18	1.6	1.3	Yes	*−0.9*	*2.2*	*No*	*1.8*	*2.6*	322	*31*
AU21	1.8	0.9	Yes	*−0.9*	*1.5*	*No*	*2.0*	*1.8*	308	*25*
AU22	1.4	0.6	Yes	*−1.0*	*1.1*	*No*	*1.7*	*1.2*	317	*35*

6.3 Satellite based InSAR

NGU has in corporation with NORUT processed satellite-based InSAR data from the Flåm-Stampa area. This includes both Radarsat-2 Ultrafine data and high-resolution TerraSAR-X data (Dehls et al., 2012). We have got access to the TerraSAR-X data from 2010 and 2011 (Figure 13). Most of the slope is vegetated, so the density of measurements is low. There are no clear indications of any large area with significant displacements, however several smaller areas show displacements, but these are most probably due to creep in debris. Relatively large displacements are shown on the landslide debris just below the steep cliff below Ramnanosi.

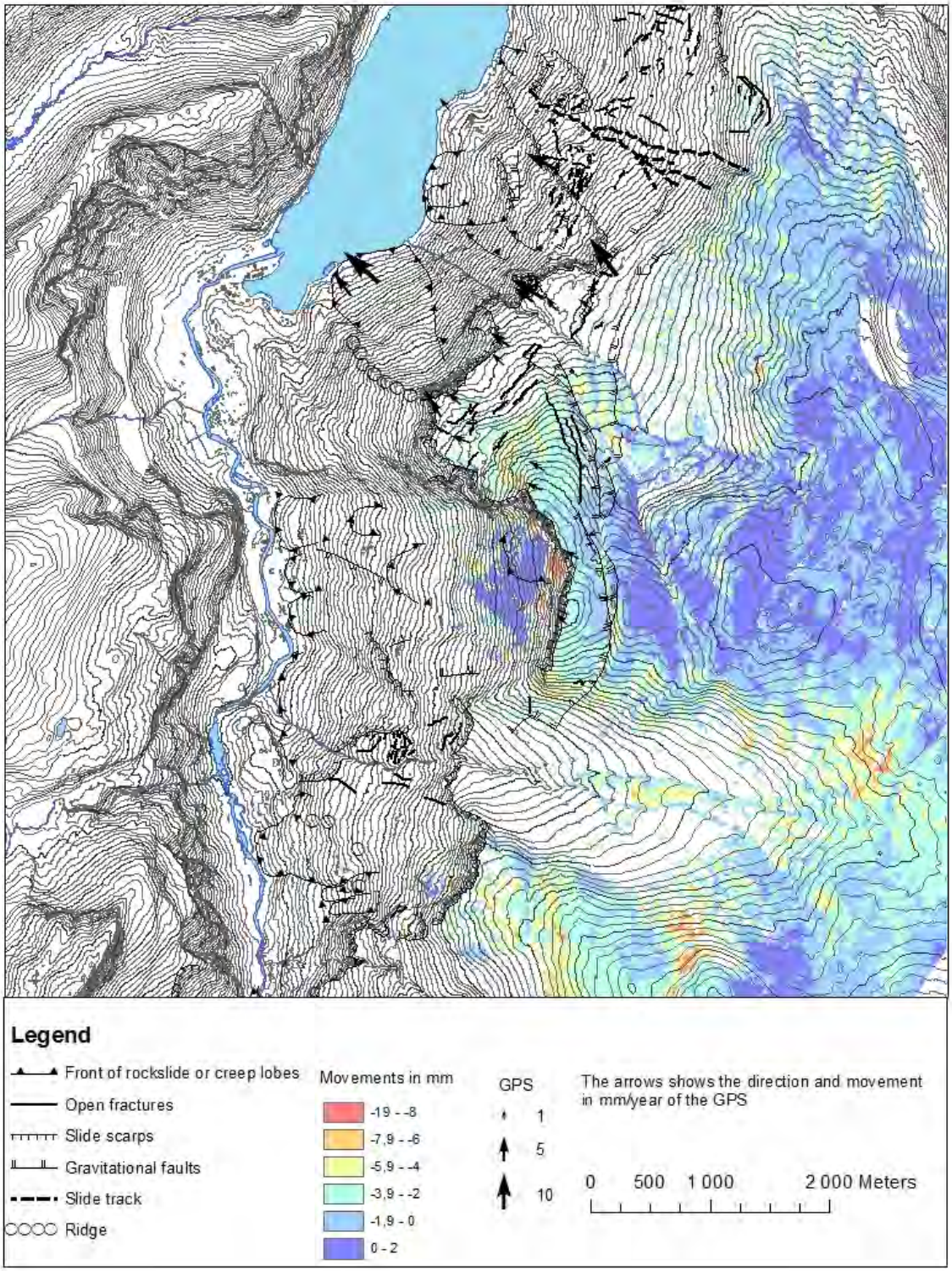

Figure 13: The average line of sight (LOS) velocity (mm/year) obtained using the TerraSAR-X images from 2010 and 2011. GPS vectors with displacements are also shown.

6.4 Ground-based InSAR

ÅTB has, on commission from NGU, used a Ground Based INSAR system (LiSALab system) to measure distributed displacement of the unstable area at Joasete/Furekamben. The foundation was established at Otternes, and one spring and one autumn campaign were performed in 2011

(Kristensen, 2011) and one longer period in the spring 2012 (Kristensen 2012), Figure 14. The coverage, return signal and coherence on the near vertical upper parts of the rock-slope were good, while the vegetated scree slope gave a weaker and less coherent return signal. Quite strong atmospheric disturbance affect the data from 2011, but the 2012 data were much better. The vertical cliff areas seem to be stable during the campaign, but some major displacements occur in lower areas in the boulder landslide deposits.

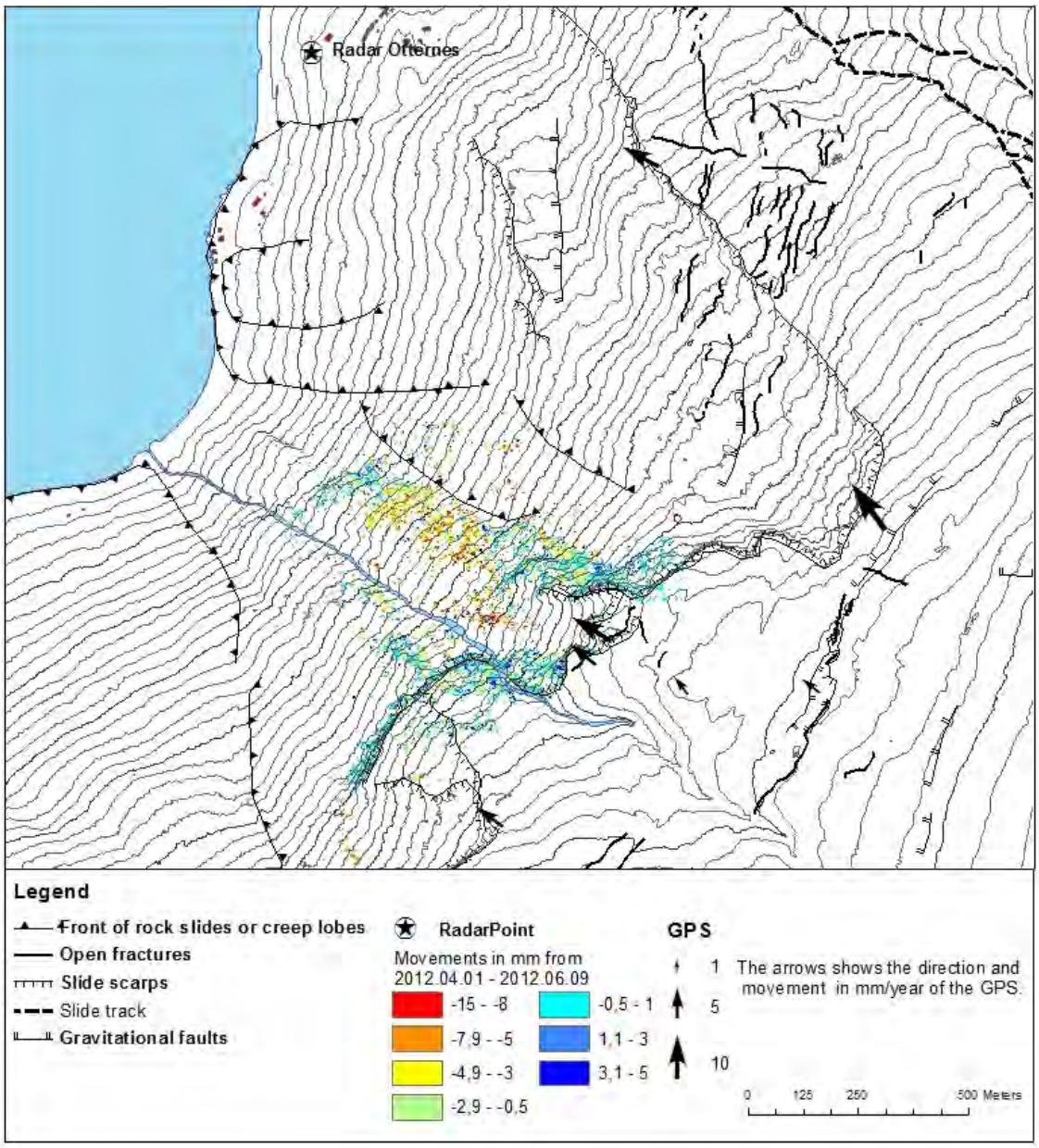

Figure 14: Ground-based InSAR data from 2012 (1th of April – 9th of June). From Kristensen (2012).

7 Stability analysis

A stability analysis for the area just north of Stampa was done by Grimstad (2008) in connection with the evaluation of possible drainage measures. However, the limited information about the subsurface conditions, and especially the hydrological conditions, make this analysis difficult to use. The potential sliding planes was set to between 16 and 24°, and the water in fractures was allowed to increase up to the terrain surface. The safety factor was calculated to 1.3 in dry conditions, and goes down to about 1 at maximum water pressure. The conclusion was that the rock mass was stable in dry conditions, but can be unstable with maximum water pressure in fractures. A situation with water in fractures being totally filled up to the surface seems to be unrealistic in these highly fractured rocks, also demonstrated by the resistivity data (e.g. Figure 9).

Two numerical models were performed by Böhme et al. (2013), including a 2D continuum model (Phase^2) and a discontinium model (2D UDEC). The Phase^2 model was used to model the rock mass before and after a prehistoric rockslide (two stages), in order to investigate the stress distribution and the influence of the former rockslide. The vertical joint sets and the foliation were implemented in the model, in addition to rock-mass parameters. The results indicate that the presence of the discontinuities was necessary in order to develop the prehistoric failure. Furthermore, the analysis shows that there are only minor regions along the slope with strength factors below one after the prehistoric failure.

The 2D UDEC model was used in order to evaluate the failure mechanisms. Testing of different geometrical configurations confirmed that all observable structures need to be included into the model in order to get the highest deformation at the slope crest and to be able to reproduce today's morphology. Also, the implementation of weak structures defining the large graben structure on the plateau was needed in order to form these features. A complex failure mechanism was proposed based on the numerical modelling (Figure 15):

1. A toppling component operating in the entire unstable area
2. Formations of several graben structures based on subsiding bilinear wedges (between joint sets J1 and J3)
3. Planar sliding along foliation on different horizons at the toe of the slope

Based on field observations, kinematic analysis and the numerical modelling, this model is proposed by Böhme et al. (2013) to be the most reliable explanation for the failure mechanisms controlling the entire unstable area.

Stability analysis, including numerical models, is strongly depending on reliable structural data, rock-strength parameters and the groundwater conditions. Especially important is the understanding of these factors in the subsurface. In the present case, there are limited information and data on the hydrological conditions, foliation measurements in the steep areas and structures in the subsurface. Grimstad (2008) seem to have used unrealistic high water pressure, while the modelling by Bøhme et al. (in rev.) did not introduce water pressure in the model. It is also a question about the used foliation structures, which are used as sliding planes in the models. Grimstad (2008) used foliations (sliding planes) with dip of 16 and 24°, while Bøhme et al. (op cit.) used a foliation dip down to about 10°. The present modelling approach has not introduced different foliations as a part of a sensitivity test. The possible occurrence and

importance of larger regional fault systems for the gravitational failures in this area are also unknown (see Figure 2).

On the background of the lacking structural field data in the steep cliffs, lacking data of structures in the subsurface and the lack of using reliable hydrological conditions in the stability analysis/modelling, it is concluded that the understanding of the stability conditions and the failure mechanisms is still not well understood. SINTEF made some proposals for stability analysis and risk evaluation based on existing reports from NGU and NGI (Vatn et al., 2009; Vatn, 2011). These documents describe some of the large uncertainties in different key parameters in the stability analysis, and conclude that there is a need for a combination of different stability models. They also stress that there is a substantial lack of knowledge on several important key areas, especially linked to the overall geological model and the hydrological conditions.

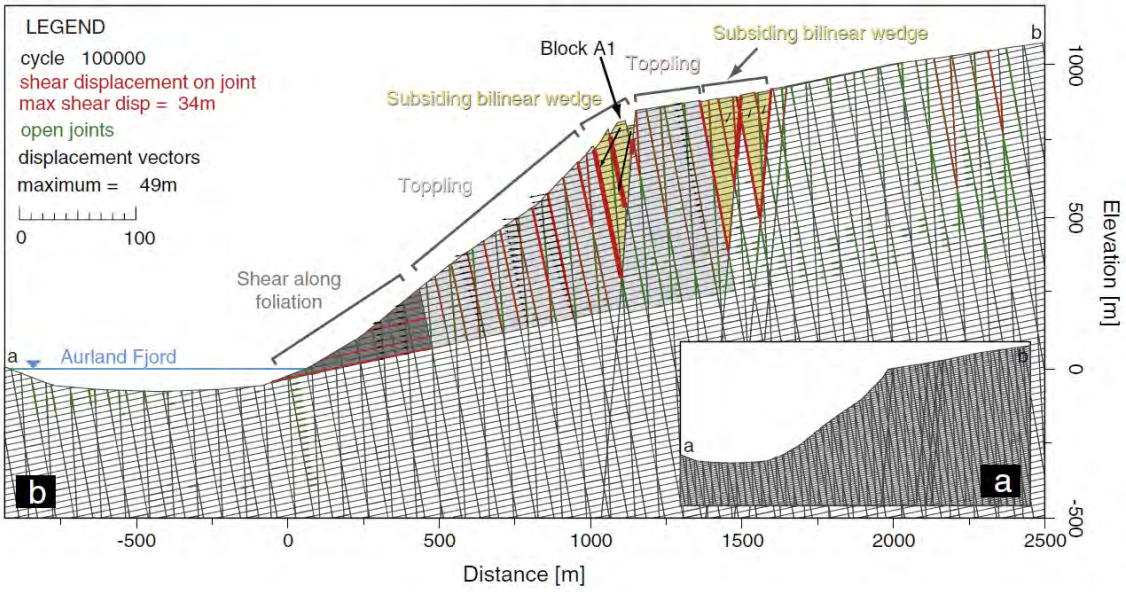

Figure 15: Stability model (Bøhme et al., 2013). Block A1 is sceanrio 3a in Figure 16.

8 Geological model and scenarios

The evaluated area is large and complex, and it is challenging to present reliable geological models. From the new compilation, some geological profiles from the unstable area are proposed from some selected areas. These are discussed together with existing proposed models and scenarios. It is proposed new numbering of scenarios in this report. These are summarized in the subchapter on Scenarios, but are also introduced in the first subchapter on Geological profiles. The scenarios are divided into 3 main scenarios, 1, 2 and 3, with 1 being the largest and 3 the smallest. These are again subdivided into different areas (Scenario 1a and 1b; Scenario 2a and 2b; Scenario 3a, 3b, 3c and 3d). These scenarios (Figure 16) are the basis for the new risk classification presented in this report.

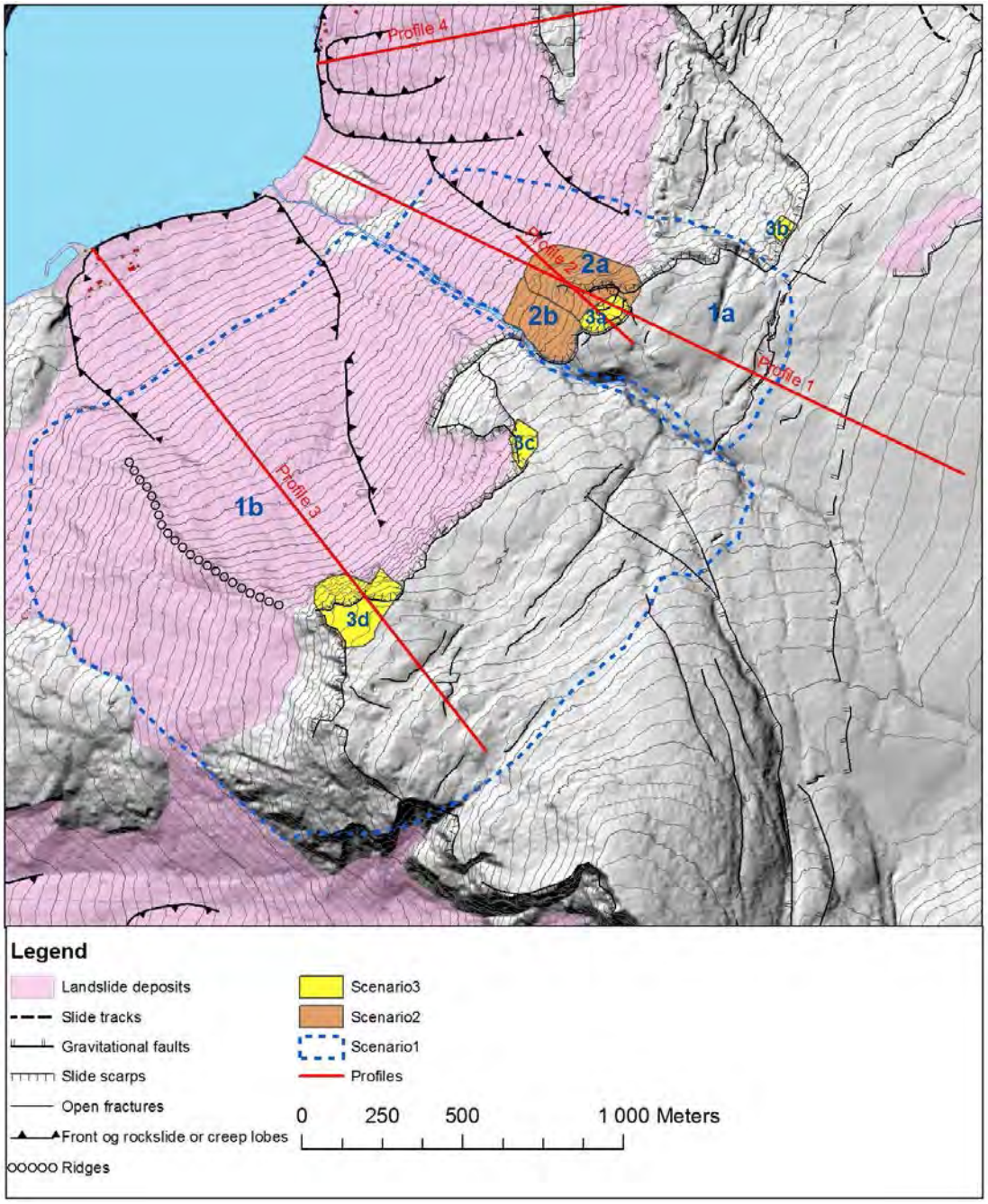

Figure 16: The scenarios used in this report. The location of profiles is shown.

8.1 Geological profiles

8.1.1 Joasete – Stampa (Profile 1 and 2)

This profile is located north of Stampa, from Joasete, and includes the scenario 1a, 2a and 3a (Figure 16).

Bøhme et al. (2013) have suggested a complex model for the basal failure surface in the area (Figure 17). Evaluation of possible failure surface is based on the assumption that the foliation is gentle (12º) throughout the potential unstable areas and that there is a need for large steps and deformation processes to destruct large rock bridges.

Figure 17. A complex basal failure surface as proposed by Bøhme et al. (2013). (a) A schematic profile indicating that the failure surface follows foliation in some parts, but steps down along pre-existing joints or fold hinges. (b) and (c) Step-path failures observed in smaller scale in the field.

Profile 1 is going from the plateau area at 1080 masl, crossing the Joasete area and the unstable area at GPS AU12 and down to the fjord (Figure 18). The profile direction is following the movement direction of GPS AU12, towards west-northwest (300º). A possible sliding plane of about 30º, including the unstable block at GPS AU12 (scenario 2a), will daylight at 550 masl (Figure 18 and Figure 19). See also a detailed profile 2 from this area (Figure 21). This is just at the transition between rocks and the blocky landslide debris, and the sliding plane located just at the lower part of the high resistivity zone. It has been argued that the plunge of the foliation is too gentle in order to get sliding planes along foliation. However, the structural analysis of TLS data indicates steeper foliation in the back wall of scenario 3a (261/18 ± 16º), and with steeper dips in the sliding block of scenario 3a itself (246/27 ± 12º; 278/33 ± 16º) (Hermanns et al., 2011; Bøhme et al., 2013). Hermanns et al. (2011) also argued, based on a rotational analysis of TLS data, that the displacement seen cannot be explained by toppling alone, but by a combination of sliding and toppling. The method is based on a comparison between structures on the back crack (number 1 in stable area, Figure 20) and data from the same structures on the moving block (point 3 and 4 in scenario 3a, Figure 20). Based on this analysis, they concluded that most of the displacements at scenario 3a must be explained by sliding mechanisms.

The InSAR and ground-based InSAR data show no movement in the steep cliff areas and on the plateau area, although there are limited data points due to dense forest. Substantial areas show quite large displacements in the bouldery landslide deposits, especially around and below the area of scenario 2a (Figure 14).

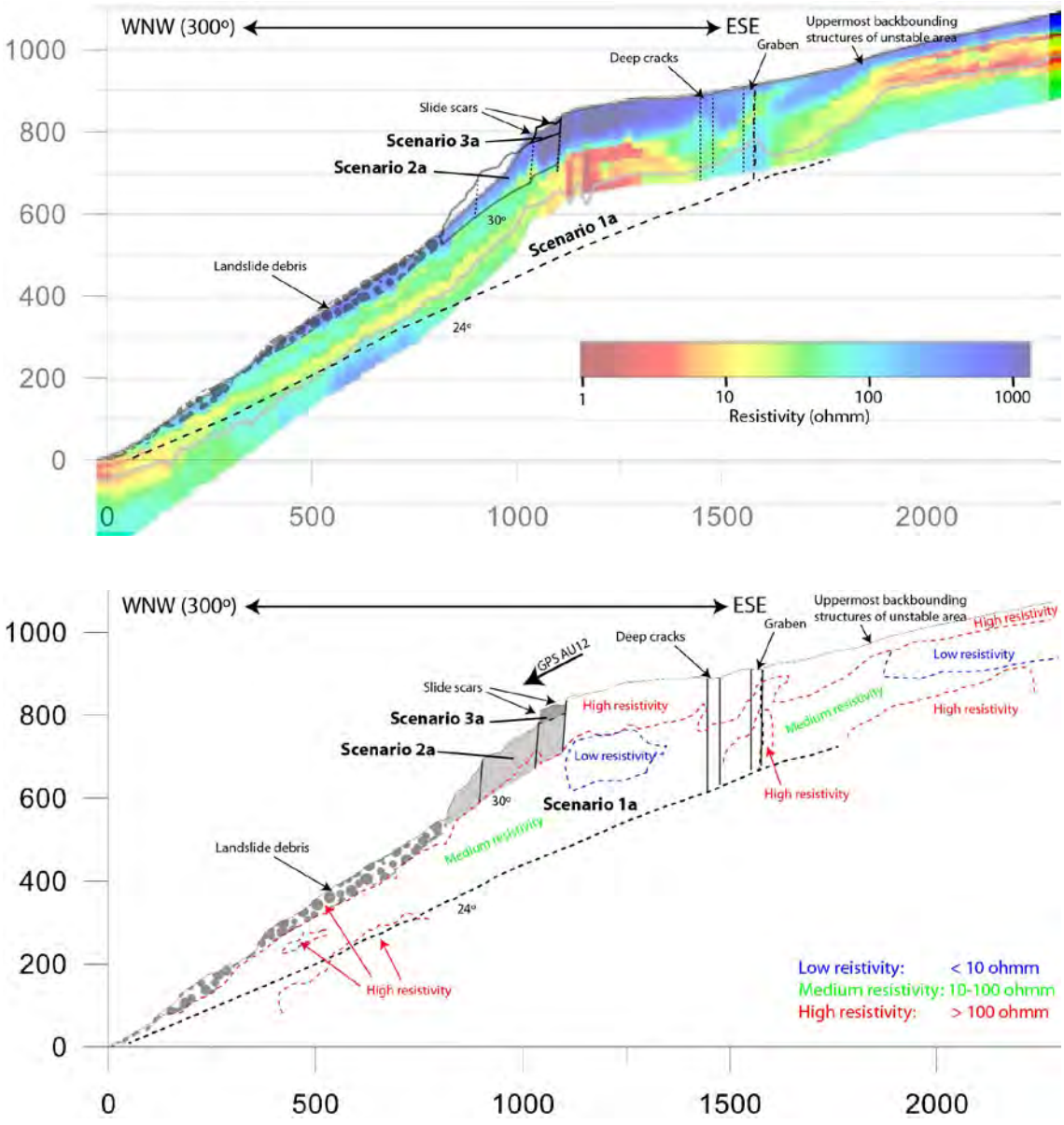

Figure 18: Profile 1 with main geomorphological features and resistivity data from AEM. The upper figure shows the resistivity data from profile 240. It is not entirely covering the same profile as profile 1, especially on the edge of the unstable area. The scenarios 1a, 2a and 3a are indicated. The upper high-resistivity zone can reflect dry areas with large open fractures, with a possible water level below.

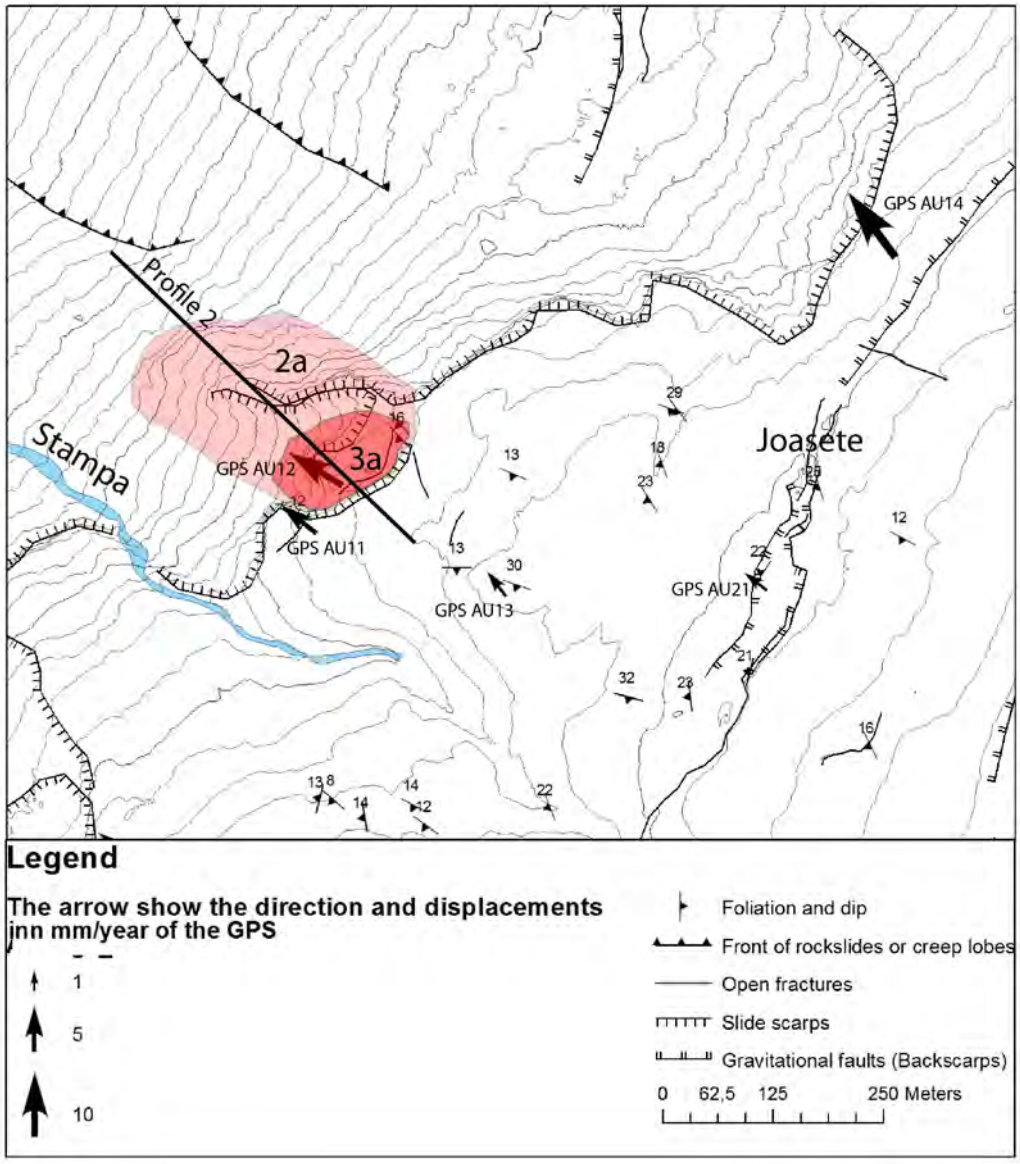

Figure 19: Structural measurements and location of profile 2 together with GPS measurements and scenario 2a and 3a in the Stampa – Joasete area.

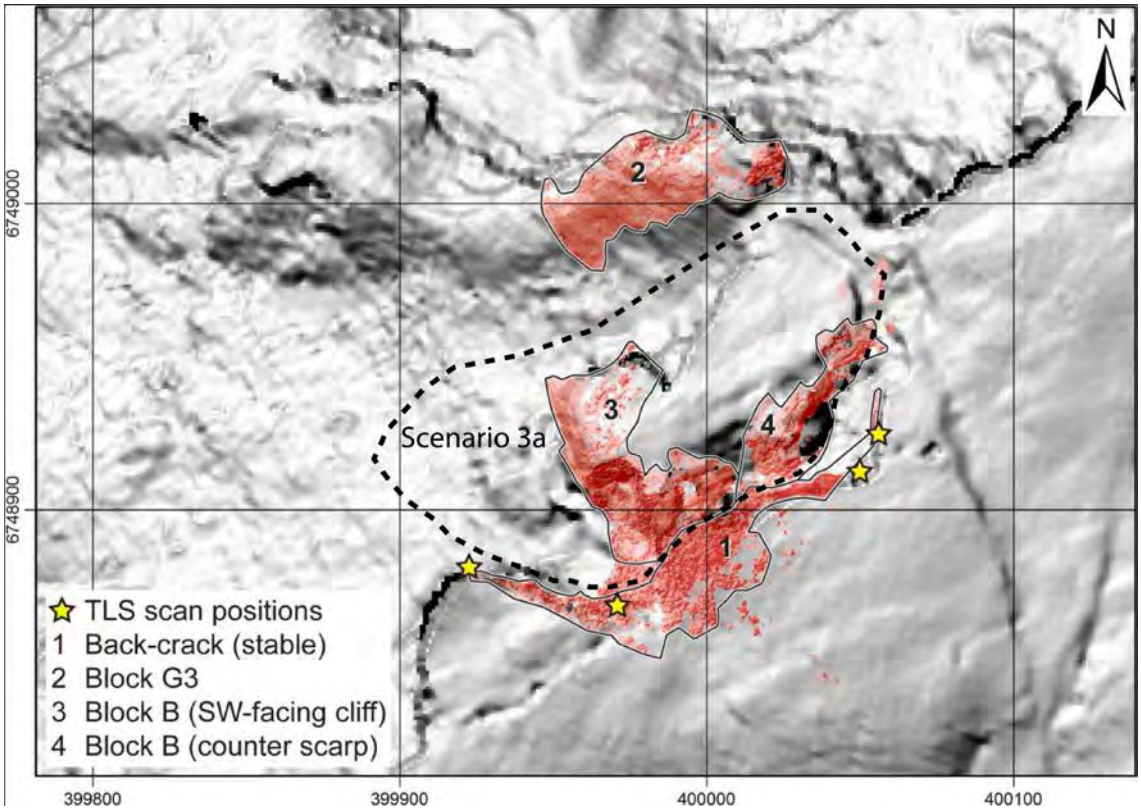

Figure 20: Location of The TLS scans performed by NGU (red) in the area of scenario 3a north of Stampa (modified from Hermanns et al., 2011).

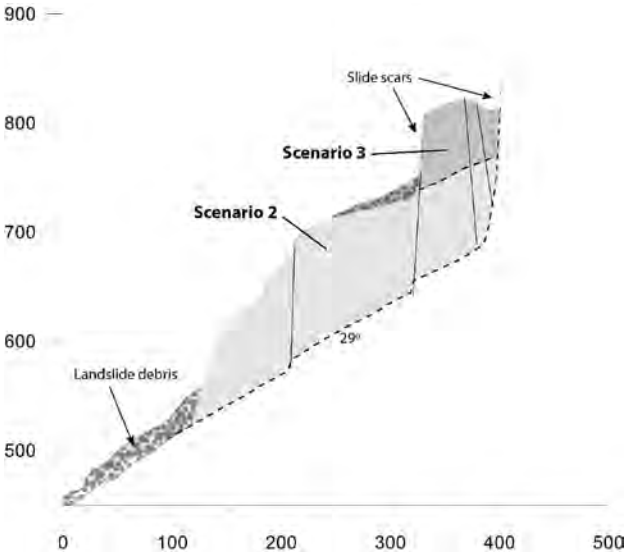

Figure 21: Profile 2 north of Stampa, see location in Figure 16 and Figure 19.

8.1.2 Furekamben (Profile 3)

Profile 3 shows the area from the plateau at Furekamben and towards the fjord (Figure 22, location in Figure 16). The foliation measurements on the plateau show quite different orientations, but it seems that the general trend is a dip direction downslope towards WNW, and with dips of 10 to 20º (Figure 3). Potential failures need to have detachments that are much steeper than the measured foliation, but the major uncertainties are the lack of structural measurements in lower areas or in the subsurface. Possible detachments linked to fault zones cannot be excluded. The displacement measured at GPS AU15 and AU16 shows average rates of 3.5-4 mm/year. The movement direction is 326-330º and with a plunge of between 53 and 58º (Table 1). This steep plunge is different from other GPS points nearby on the plateau (e.g.

AU10) and is difficult to interpret in terms of a geomorphic feature on the surface or a reliable geological model. The possible sliding surfaces for scenario 3d, indicated in profile 3 (Figure 22), is gentler than the plunge seen from the GPS measurements. However all the GPS measurements show relatively consistent movement directions downslope towards WNW.

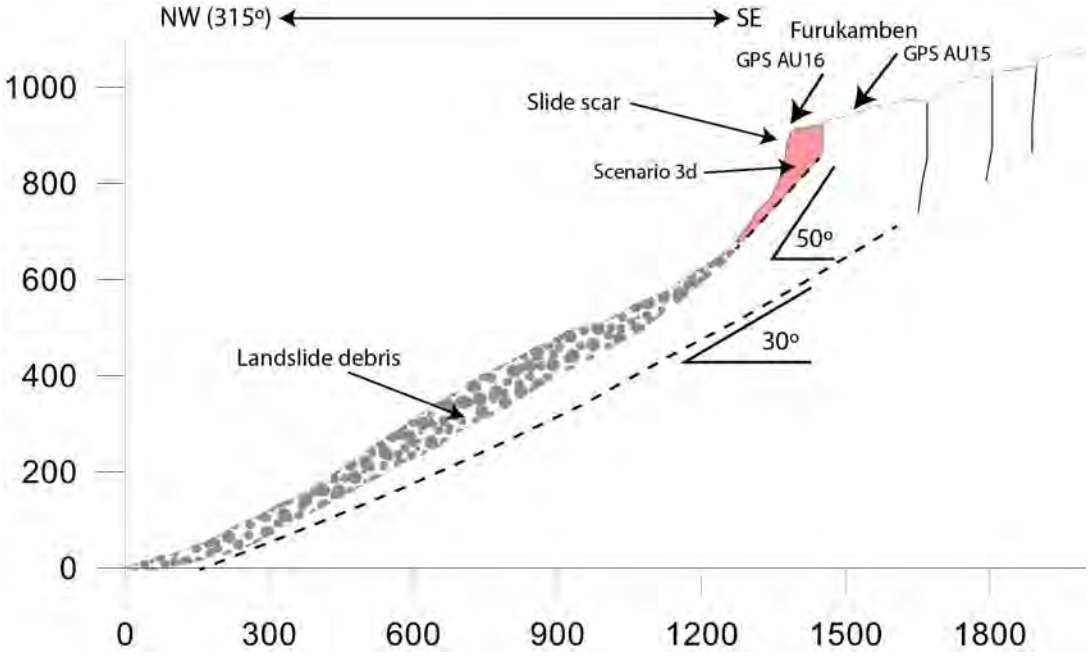

Figure 22: Profile 3 from Furukamben. See location in Figure 16. The plunge of the GPS points is indicated.

8.1.3 Southeast of Otternes (Profile 4)

A major back scarp with large slide blocks developing into landslide debris is mapped southeast of Otternes (see profile 4 in Figure 23). The lower part of the blocky landslide debris was active in 1979 and moved about 11 m and passed the main road at the shoreline. Foliation measurements show direction and dip that can be consistent with sliding surface. A GPS point along the back scarp also indicates movements. The topographic conditions and the geological/geometrical model indicate that the detachment zone is relatively gentle and that the most probable landslide behaviour is slow movements with a less probability of evolving into a rapid landslide (Figure 23). This will probably also be the case for the area further to the east at GPS AU14 (scenario 3b), north of Joasete (Figure 16 and Figure 19).

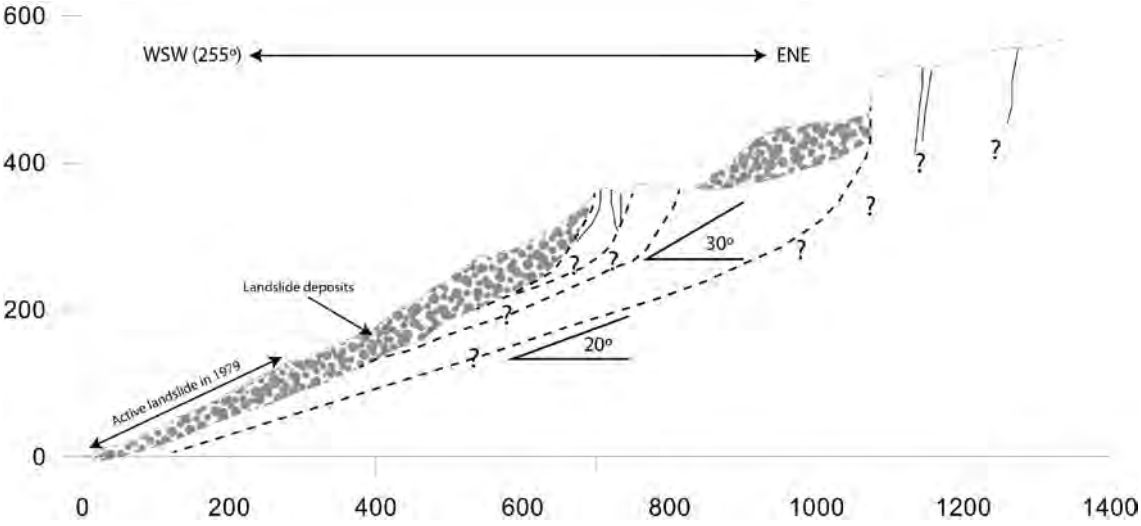

Figure 23: Profile 4 from the northern area southeast of Otternes. See location in Figure 16.

8.2 Thickness of deposits

The rockfall and rock-avalanche deposits from Stampa were mapped in detail based on the hillshade of the ALS-DEM and field mapping (Fig. 10 in Hermanns et al., 2011), Figure 5 and Figure 6. There are also some few drillings and refraction seismic profiles in some areas given data on the thickness of landslide debris, in addition to the AEM data (Figure 7 and Figure 8). For the data input to run-out analysis, the thickness of the delimited slope deposits is computed using the sloping local base level algorithm (Jaboyedoff et al., 2004). This algorithm allows computing a smooth second-order surface between the limits of the deposits, which gives an estimate of the topography before the rockfall and rock avalanche deposits. Different curvature parameters are tested in order to obtain different deposits thicknesses. Using several cross-sections allows choosing the plausible deposits thickness model for the Stampa area.

8.3 Comparable active rockslides in phyllites

The Ruinon rockslide in Upper Valtellina in Italy is a comparable active landslide in pyhyllitic rocks (Figure 24 and Figure 25). A minor part of a large, dormant deep-seated gravitational slope deformation, is today active with especially large displacements during periods of high precipitation (Crosta & Agliardi, 2003). The slope failures are located in a glacial valley, deeply cut by a river. The active Ruinon rockslide is developed in highly folded pre-Permian metamorphic phyllites, and the lowermost part of the system includes also landslide debris (surficial cover), see profile in Figure 25. Even though most of the large system is thought to be dormant, InSAR data demonstrated that the entire slope is subjected to displacement velocity ranging from 7 to 25 mm/year (Crosta & Agliardi, 2003).

The Ruinon rockslide is thought to be characterized by translational and rotational sliding of ca. 13 Mm^3 with a sliding surface at c. 70 m depth. Crosta & Agliardi concludes that it may originate into a fast moving rock avalanche and that it does not need to be affected by basal erosion. A ring-shear test of cataclastic material (sliding zone) gave internal friction angel of between 26º (peak value) and 24.5º (residual). The presented profile (Figure 25) shows that the sliding surface have dips of 21º in the lower part, increasing to above 30º in upper part.

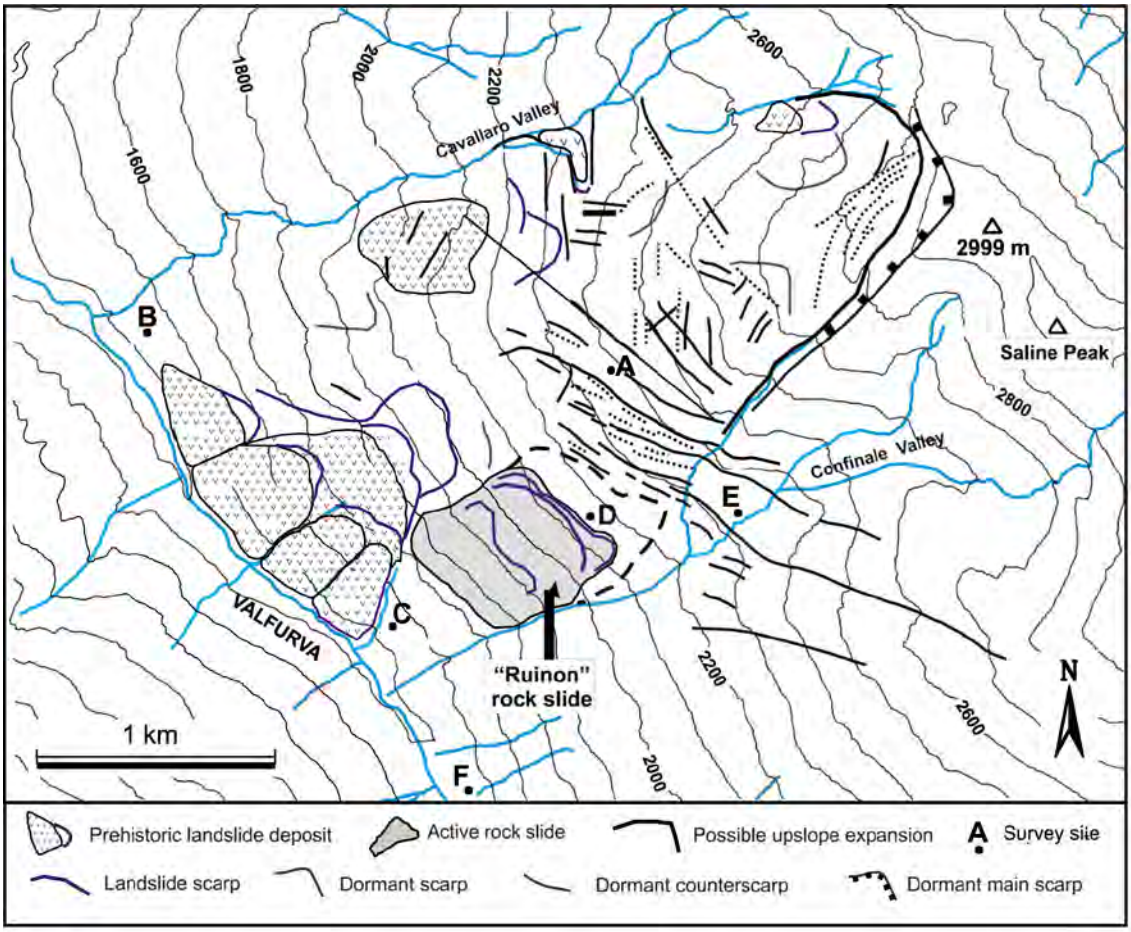

Figure 24: Geomorphological map of the Ruinon rock slide area (Crosta & Agliardi, 2003). It shows the location of the main active Ruinon rockslide and the main features of the dormant deep-seated gravitational slope deformation involving the entire slope.

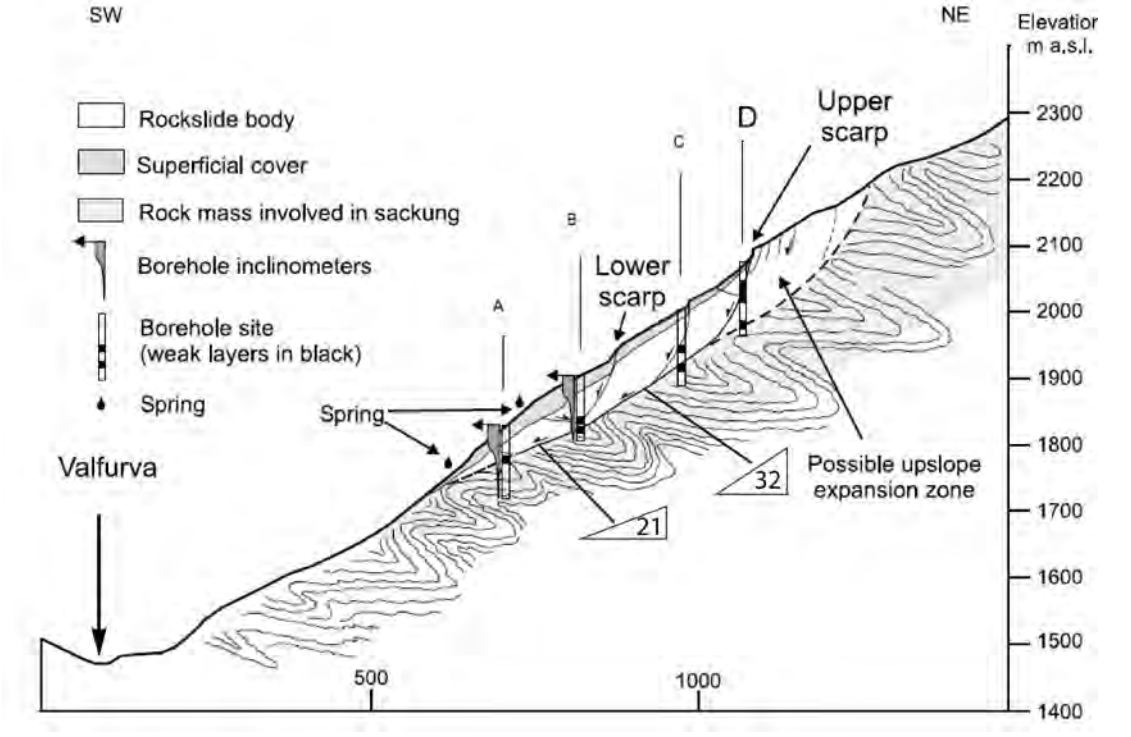

Figure 25: Geological cross section of the Ruinon landslide (Crosta & Agliardi, 2003). Slope gradients are indicated.

8.4 Scenarios

The different projects and investigations that have been performed during the last 10-12 years have suggested several different scenarios. Domaas et al. (2002) concluded that large rockslides of several million m^3 cannot be excluded and that several areas of 20-160 000 m^3 are unstable. This research also concluded that water infiltration in fractures and in the blocky landslide debris is a key for the creep processes in lower areas. Especially critical is the possibility for establishing overpressure in underlying permeable glacial tills capped by more fine-grained phyllitic landslide debris.

The stability evaluation of a large scenario from the Joasete – Stampa area performed by NGI (Grimstad, 2008) seem to be based on unrealistic water pressure, and too gentle sliding planes. The resistivity data and other field measurements indicate relatively large water infiltration into fractures on the plateau, but it seems not possible to achieve the high water levels that are used in this model.

NGU (Hermanns et al., 2011) evaluated the Flåm -Stampa area and proposed several scenarios. Scenario 1 is a collapse of a large segment of the unstable area (10-100 Mm^3), but the probability for this was evaluated to be low (annual probability less than 1/10 000). Scenario 2 included a medium collapse of a segment from 100 000 to some few million m^3, that could reach the fjord and initiate a tsunami. This included a possible collapse in the Stampa-Joasete area of about 280 000 m^3, and the annual probability was estimated to be between 1/3000 – 1/10 000. The last scenario was smaller volumes of between 10 000 and 100 000 m^3 which could not reach down to the fjord. The annual probability for these events was estimated to be between 1/100 and 1/1000.

Bøhme et al. (2013) has further analysed and evaluated the possible scenarios and volumes of subareas presented in Hermanns et al. (2011) (Table 2). It was concluded that the collapses of large volumes is not realistic, however several smaller areas were evaluated more carefully, especially the area just north of the Stampa river at GPS AU12. A possible volume of 280 000 m^3 was estimated for scenario 3a (Table 2).

Table 2: An overview of subareas and different unstable blocks as evaluated by Böhme et al. (2013). Volumes are calculated based on limiting structures except for Scenario 1a were the SLBL method was used to estimate the volume. Note that the areas/scenario has been renamed from those used by Böhme et al. (2013).

	GNSS-point	3D movement vector		Volume [m³]	Limiting structures		
		Value [mm/year]	Direction (trend/plunge)		Back bounding fracture	Lateral release fractures	Basal limit
Scenario 1a	AU21	2.0	308/25	31 Million	285/80 (J3)	-	300/27
	AU13	2.4	322/25		310/80 (J3)		
	AU12	9.5	301/28				
Scenario 3a	AU12	9.5	301/28	280 000	281/75 (J3)	226/46 331/74	302/38
Scenario 3b	AU14	15.2	324/45	130 000	120/90 (J3)	247/74 (J1) 036/80 (J2)	259/18 333/29
Scenario 1b	AU7	2.6	290/30	300 Million	-	-	-
	AU8	2.5	314/28				
	AU9	2.2	315/18				
	AU10	4.4	306/24				
	AU15	3.9	330/53				
	AU16	3.6	326/58				
Scenario 3c	AU10	4.4	306/24	380 000	300/76 (J3)	258/80 (J1)	005/18
Scenario 3d	AU15	3.9	330/53	280 000	310/40	240/80	310/40
	AU16	3.6	326/58				

The present report presents a new evaluation and compilation of possible scenarios. It will be given some few representative scenarios for the risk classification, since it is not possible to give

all possible scenarios in this large and complex area. The following important points have been used during this evaluation:

1. The present understanding of the geological model including geomorphology and structural geology. The geomorphology shows that a very large area has undergone major deformations, and that there still are large areas with open fractures that can be a potential for future failures. Uncertainties are related to structures (directions and dip) in lower areas and in the subsurface and especial possible fault zones linked to the post-caledonian and younger Devonian/Permian reactivation. Brittle deformation structures are found several places in the area (Helge Henriksen, pers. com.). The distinct and persistent open fractures showing extension towards WNW are not well understood.

2. Displacement data shows only some few areas of significant movements in the outer edge of the unstable plateau (top of slide scars), but many of the GPS points showing smaller movements indicate a consistent horizontal displacement direction towards WNW. This fits with the direction of the distinct and continuous SSW-NNE trending open fractures demonstrating extension towards WNW. InSAR and ground-based InSAR data do not show movements in the plateau areas. However relatively large areas of the landslide debris is active. The major uncertainty is here related to the possibility for large annual and seasonal differences. The GB InSAR data is only collected during two years, and may not be representative for year with extreme precipitation and/or rapid snowmelt.

3. Infiltration of water in fractures in the Joasete and Stampa area may have influence on the water level, and the interpretations of resistivity data indicate that the water level is located at relatively large depths in the most critical areas (>100m). Also visual observations in deep cracks points to water levels at least deeper than 30 m. The water infiltration during snowmelt and heavy rainfall events has shown to greatly control the creep and displacements in the lower landslide lobes, but in the Joasete – Stampa area this could also affect the stability conditions at larger depths.

4. Stability analysis is always difficult to use in large and complex landslides, especially due to lack of structural data in the subsurface and the hydrological conditions. Also the complexity of the structures limits the models, since the model needs to be greatly simplified. This limits the use of stability evaluations in the evaluation of scenarios.

5. Data from the fjord area evidence some major past rock avalanches from the unstable area. One event is dated to be older than c. 3000 years BP.

6. It is important to separate between areas characterized by slow movements (creep) that cannot evolve into an accelerating landslide, and steeper areas that have the possibility to create large collapses and rapid rock avalanches. It is important to include run-out modelling in the evaluation of scenarios, and especially the role of entrainment for some of the smallest scenarios. Run-out evaluation is generally lacking for most of the scenarios.

7. Comparison of the present rockslope failures with similar slope failures elsewhere. The Ruinon rockslide in Italy is a comparable area in phyllitic rocks

Based on the issues listed above, three main scenarios have been suggested to be part of the risk analysis. Scenario 1 is the largest scenario, scenario 2 of medium size and scenario 3 the smallest scenario. Letters are used to name different areas that are classified into these main scenarios (Figure 16 and Figure 19).

8.4.1 Scenario 1

The largest scenario is composed of a major section of the unstable area, leading to a very large rock avalanche of volumes of several tens or millions of m^3 (see scenario 1a and 1b in Figure 16). These scenarios are to a large degree controlled by the distinct and persistent extension fractures trending SSW-NNE. The present data from periodic GPS, InSAR and ground-based radar demonstrate that there are not any significant movements. However, the GPS data going back to 2004 indicate some small movements, and consistent directions of displacements downslope towards WNW. This includes the scenario 1 proposed by NGU in Hermanns et al (2011) and subarea A and B (Bøhme et al., 2013), see Figure 26. They estimated the volumes to be between 10 and 300 Mm^3. Both NGU and the following work by Bøhme et al. (2012) concluded that this scenario is not very likely. A significant increase of the displacement rates is needed before a catastrophic failure. In this report these scenarios are named 1a and 1b (Table 3). This scenario can be compared with what has been termed the dormant part of the Ruinon rockslide, were large areas shows sign of deformations, but were the present displacements are very low (Crosta & Agliardi, 2003).

Table 3. Scenario 1 with volume estimates and displacements in inner areas. From Bøhme et al. (2013).

Scenario	Volume (Mm^3)	Horizontal displacements (mm/year
1a	30	1
1b	300	1

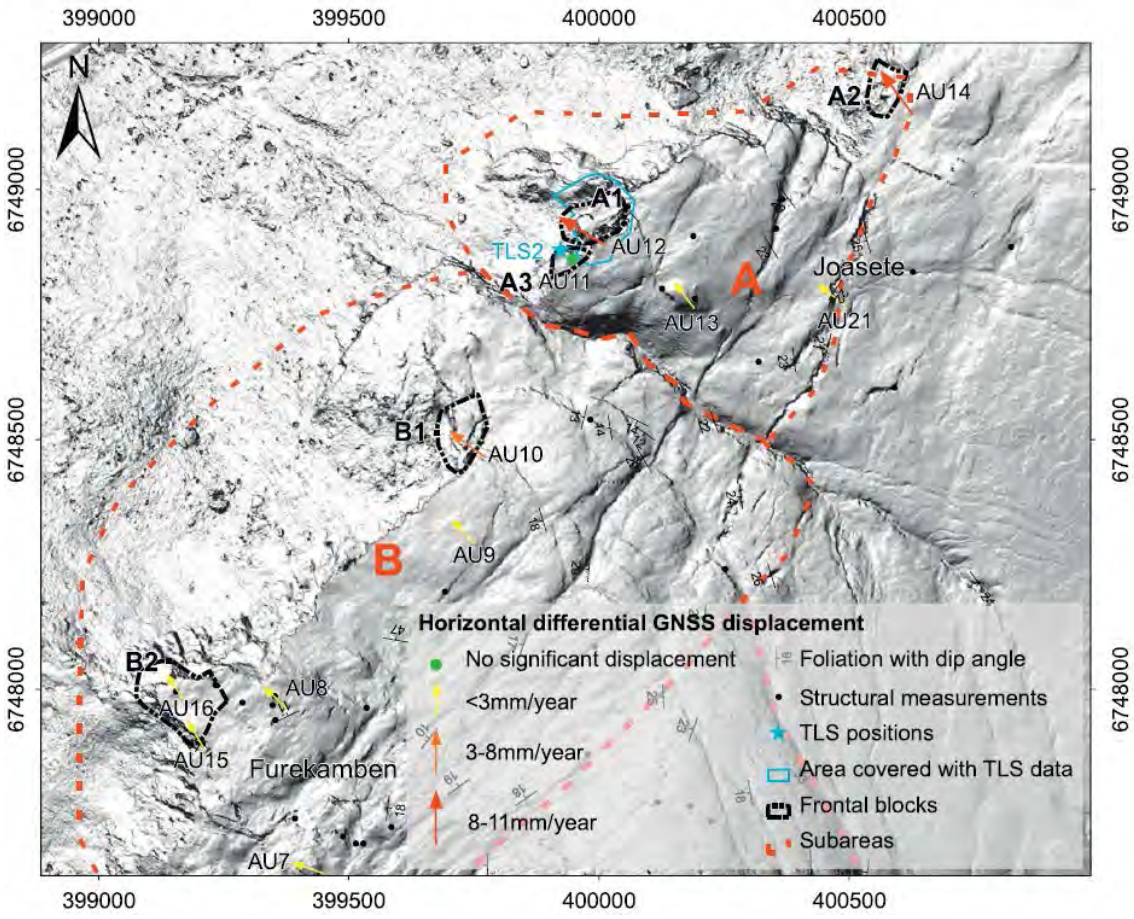

Figure 26: Map from Bøhme et al. (2013), showing scenario A and B and scenarios A1, A2, B1 and B2. Scenario A and B are scenario 1a and 1 b in this report. A1 is scenario 3a, A2 is 3b, B1 is 3c and B2 is 3d.

8.4.2 Scenario 2

This include scenarios were a large portion of the outer plateau area west of Joasete and north of Stampa river fail and evolve into a large rock avalanche (Figure 16, Figure 18, Figure 19 and Figure 27). The scenarios are based on the following:

- Documented displacement at GPS AU12 of about 1 cm/year in a west-northwest direction, plunging 31º.
- Relatively large displacement in landslide debris below the scenarios (Figure 14).
- Sliding along steep foliation planes or other weak structural zones not documented in the field data, probably in combination with steps and rock bridges.
- Resistivity data from the AEM campaign show a high resistivity zone of up to 100 m with underlying zones of much lower resistivity, which may indicate a transition between highly fractured rocks with underlying water-saturated portions. The data also indicate that water infiltration in the Joasete and Stampa area may be important for drainage of water into the highly fractures high-resistivity zone of scenario 1a. This is further documented by water discharge measurements in the Joasete area.
- A sliding plane of about 30º dip fits relatively well with the topographic conditions, delighting at the base of the steep cliff, in the transition to landslide debris.

These scenarios have not been evaluated before and NGU has made a more detailed volume estimates for this report. Two different subareas have been considered for scenario 2, **scenario 2a** in the north that includes the area of GPS12, and **scenario 2b** in the south including GPS11 (Figure 27). GPS point AU12 has a documented displacement of c. 1cm/year in horizontal and 4,4 mm in vertical direction, while GPS 11 have 4.3 mmm/year vertical movement and a much lower and not significant horizontal displacement (2 mm/year). It is not known if the movement at GPS 12 is representative for the entire scenario 2a, and it is questionable if the back-bounding structure is fully developed.

The volume of scenario 2 was estimated using the Sloping Local Base Level (SLBL) technique (Jaboyedoff et al., 2004), which computes a second-order surface as basal surface. Different curvature parameters are tested in order to obtain minimum, maximum and mean volume estimations for both extents of scenario 2 (Table 4). Both the SLBL model and the profile in Figure 28 indicate maximum depth of approximate 100 m for scenario 2a, and the area has been estimated to 40 000 m^2. The estimated volumes range from 0.93 to 1.95 Mm^3 for scenario 2a and from 1.12 to 5.09 Mm^3 for scenario 2b. Inspection of the cross-section in Figure 28 shows, however, that both minimum volumes and the maximum volume for scenario 2b are not plausible. Thus, the likely volume is 1.51 to 1.95 Mm^3 for scenario 2a and 3.20 M m^3 for scenario 2b.

Table 4: Volume estimations of scenario 2 using the SLBL technique with different curvature parameters resulting in different mean and maximum thicknesses ΔH and volumes.

Scenario	Curvature parameter [m]	Area [m²]	ΔH_{max} [m]	ΔH_{mean} [m]	Volume [Mm³]
Scenario 2a minimum	0.00000	39975	90.2	23.3	0.93
Scenario 2a mean	-0.06116	39975	104.8	37.9	1.51
Scenario 2a maximum	-0.12231	39975	121.5	48.9	1.95
Scenario 2a minimum	0.00000	74575	90.2	15.0	1.12
Scenario 2b mean	-0.06116	74575	112.2	42.9	3.20
Scenario 2b maximum	-0.12231	74575	156.7	68.3	5.09

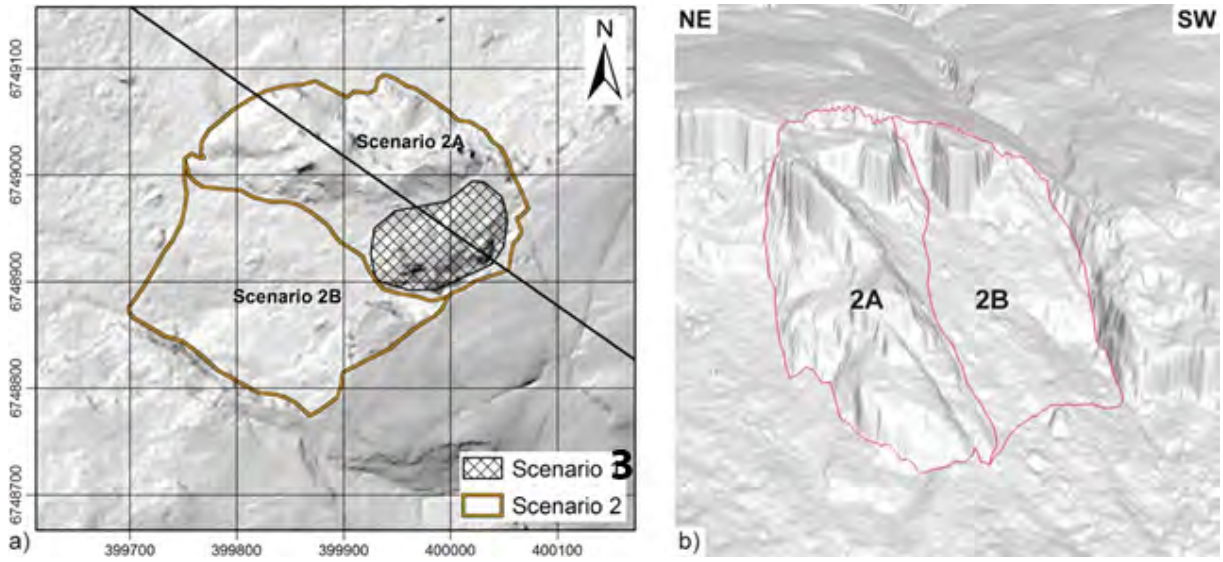

Figure 27: (a) Hillshade map of scenario 2 with two possible extents (scenario 2a and scenario 2b), which both include the detached frontal block of scenario 3a (coordinates in UTM 32N); (b) 3D view of scenario 2. Note that the scenario in the text is named 2a and 2b (not 2A and 2B).

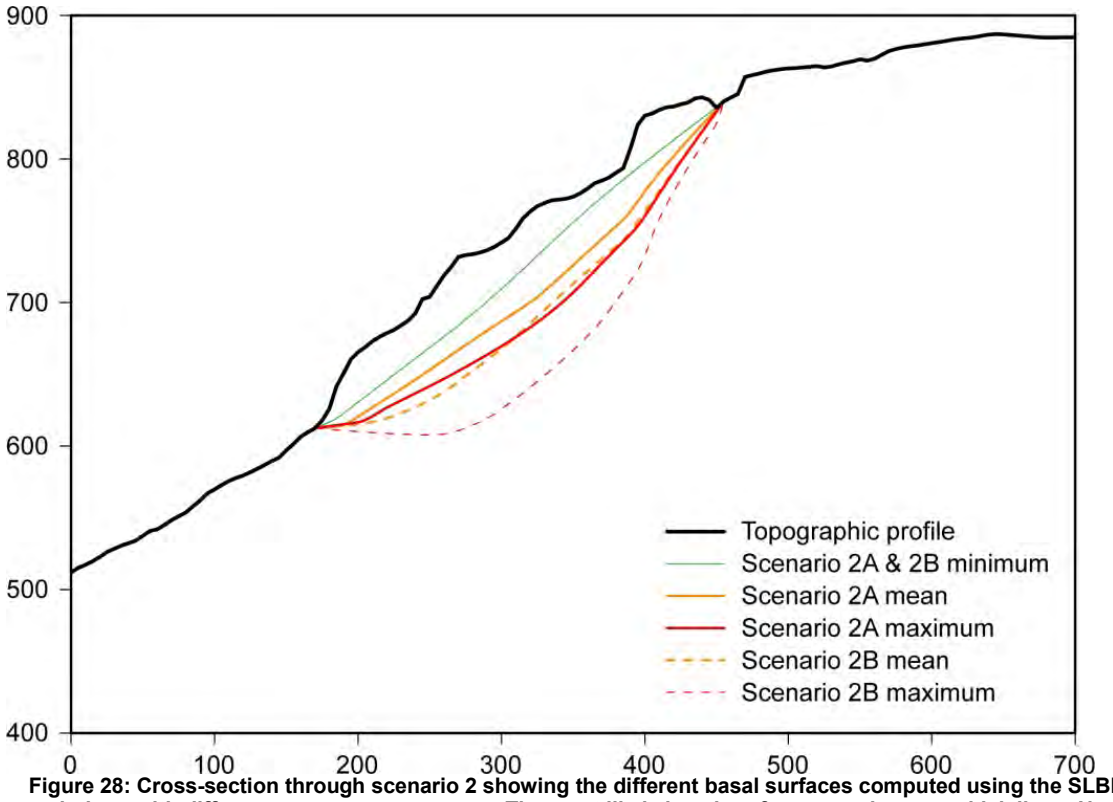

Figure 28: Cross-section through scenario 2 showing the different basal surfaces computed using the SLBL technique with different curvature parameters. The most likely basal surfaces are shown as thick lines. Note that the numbering is 2a and 2b in the text.

Large parts of the landslide debris undergo slow displacements, documented by the GB InSAR in 2012 (Figure 14). An additional volume would thus be entrained by incorporating and collapsing the creeping landslide mass below. This could increase the volume of a landslide initiating from scenario 2a and 2b. The thickness of the landslide debris could be from 5-10 m to more than 50 m locally. However, the area below the potential failures of scenario 2a and 2b have relatively thin landslide deposits and several areas of bedrock outcrops (Figure 5 and Figure 6). If we estimate that a rock avalanche from these two areas will affect a total area with

landslide deposits of 500x300m (150 000 m^2) and with a mean thickness of 2m, the total volume entrainment would be about 0.3 Mm^3 (Table 5). The table shows an overview of the scenarios, the initial volumes and possible volume of entrainment (landslide deposits). A total volume of a major failure in scenario 2 could then be in the order of 2-4 Mm^3. Compared to the Ruinon landslide, the dip of detachment zone is in the same order, but steeper in its frontal part.

Table 5: Scenario 2 with volume estimates (Mm^3) and displacements.

Scenario	**Back-bounding release surface**	**Initial volume**	**Landslide debris**	**Total volume**	**3D Displacements** (mm/year)
2a	Partly	1,7	0.3	2.0	0-9.5
2b	Partly	3,2	0.3	3.5	4,7 (not significant)

8.4.3 Scenario 3

Scenario 3 includes collapse of clearly defined blocks of less volume that have documented displacements of around 10 mm/year (Hermanns et al., 2011; Bøhme et al., 2013), see Table 2 and Figure 16, Figure 19 and Figure 29. Scenario 3a include the block with GPS 12 showing displacements of 9,5 mm/year (Figure 18, Figure 19, Figure 21 and Figure 29), and scenario 3b in the north having displacements of 15 mm/year. The estimated volumes are 280 000 and 130 000 m^3 respectively. An additional volume will be entrained during an event due to the landslide deposits below. The GB InSAR data show that large parts of these deposits are active and show displacements (Figure 14). For scenario 3a we have estimated that the run-out affects areas of thin landslide deposits of 150 x 600 m. If we assume a mean thickness of 2 m this gives a considerable increase in the total volume (see estimated numbers in Table 6). For scenario 3b it would be an even larger entrainment, since the run-out will include areas of thick landslide deposits (Figure 16). However, the slope below the unstable area here is gentler and it should be performed run-out modelling, including entrainment, in order to further evaluate possible increased volumes. It is not recommended to perform risk classification for scenario 3b until a proper run-out analysis has been performed.

Two small areas have been evaluated by Bøhme et al. (2013) south of Stampa (Figure 26). These scenarios have been named 3c (at GPS 10) and 3d (at GPS14), Figure 16. The initial volumes and displacements are given in Table 6. The scenario 3d has been a bit revised compared to the scenario proposed by Bøhme et al. (2013). There are limited structural measurements on scenario 3c. Large landslide deposits are situated in the run-out zone for these areas, and the entrainment can thus be substantially. The entrainment volume has been given twice the volumes as the original failure. The displacements measured on these two areas are small (3-4mm/year), and there is not any clear continuous and open back-bounding release structure.

Figure 29: View towards scenario 3a. Note the possible detachment surface. Location of GPS 12 with an annual displacement of 9,5 mm/year is shown together with the possible detachment surface. Photo: Reginald Hermanns (NGU).

Table 6: Scenario 3 with volume estimates and displacements.

Scenario	**Back-bounding release surface**	**Initial volume (Mm^3)**	**Landslide debris**	**Total volume**	**3D Displacements** (mm/year)
3a	Yes	0.28	0.22	0.50	9.5 (GPS12)
3b	Yes	0.13	?	>0.13	15.2 (GPS14)
3c	No	0.38	0.8	0.78	4.4 (GPS10)
3d	No	0.40	0.6	1.00	3.6 (GPS16)

8.4.4 Scenario 4

Scenario 4 includes the areas of slow deformations of landslide debris and larger slide blocks. Especially large systems have been documented in the northern area between Stampa and Otternes (Figure 5 , Figure 6 and Figure 16). The ground-based InSAR data shows relatively large displacements in the landslide debris in several areas (Figure 14). The landslide debris involves large volumes, but it seems that the plunge of possible larger-scale detachments will be too gentle in order to generate a rapid rock avalanche (see example of profile in Figure 23).

Compared to the Ruinon rockslide, the possible detachment zones for scenario 4 are much gentler. Continuous slow displacements in large areas are thought to continue, and with the possibility to get smaller landslides of larger velocities during heavy precipitation and/or snowmelt, like the event south of Otternes in 1979.

9 Evaluation of run-out, tsunamis and consequences

Detailed run-out analysis from the potential unstable areas is limited, but NGI used the PCM code for the evaluation of velocity and run-out distance for the use in the tsunami modelling. Also, NGU has performed a new run-out analysis for scenario 3a for this report (DAN 3D code). Experience from other events and the rockslide deposits in the fjord give some indications of potential run-out distance. However, most of the landslide debris on the subaerial slope is interpreted to be developed by slow moving deformations (creep), and will thus not tell us much about future run-out of high-speed rock avalanches. The tsunami analysis is based on NGI (Domaas & Glimsdal, 2009). NGU have for the present report made an evaluation of consequences and potential loss of life on the background of the existing tsunami analysis.

9.1 Run-out modelling of scenario 3a

NGI has presented 2D run out analysis for different scenarios of the area (Domaas & Glimsdal, 2009). Modeling was here done in order to estimate input parameters for tsunami wave modeling (volume and velocity) using the PCM model (Perla et al., 1980). The main results for scenario 3a (volume 200.000 m^3) and input parameters for the tsunami analysis are shown in Table 7.

NGU has for this report carried out a 3D run-out simulation in the area of Stampa-Joasete for a small rock cliff of approximately 280.000 m^3 (scenario 3a, Figure 29), see appendix 1. The DAN 3D Beta Version 2 (Hungr Geotechnical Engineering Inc., 2010) has been used, trying to include the effects of lateral spreading of the rock mass along the potential run-out track. A 1,35 m resolution DEM was used to represent topography, but no submarine topography was used during simulations as it was considered that DAN 3D cannot simulate sub-aquatic flow. 16 different starting conditions were simulated taking in account different input parameter values (see figures 3 to 6 in Appendix 1in this report). It is stressed that the modeling is stopped at the fjord and the results presented are for the arrival time of the mass into the fjord. A summary of the results are presented in Table 7. The results show important differences compared to the analysis done by Domaas & Glimsdal (2009) in terms of both block geometry and velocity at the fjord impact time. Differences can be explained due to the effect of lateral spreading of the rock avalanche during run out, the presence of topographical asperities along the track, and material entrainment and longitudinal expansion due to topographic roughness. A significant change in the run-out pattern occurs at a narrow rock cliff underneath the unstable source area of scenario 3a (Figure 30). It leads to a split of the whole mass into three separated compartments. Two compartments continue to flow down-slope with a clear independent behavior, reaching the shoreline at different times but near to each other. A larger portion of the mass goes into the southern mass. The third compartment stops at higher elevations with only a short run out distance.

Large differences between the models show some of the challenges related to run-out models of complex landslides, especially related to velocities, thickness of flow and the dimensions

(length/width). However, it is difficult to directly compare the results since the DAN 3D model stops at the fjord margin, while the NGI analysis also include the impact and run-out into the fjord. The most important input factors for tsunami analysis is the frontal area (thickness and with), velocity at the water impact and the total length of the rock avalanche moving into water (Domaas & Glimsdal, 2009). It is concluded that several critical factors for the run-out modeling, especially connected to the land-water impact, needs to be further analyzed in order to get reliable input for the tsunami analysis.

Table 7: Summary of the results of run-out analysis/modelling of scenario 3a (from NGI and NGU).

Model	Volume (Mm^3)	Length (m)	Width (m)	Thickness at the fjord (m)	Thickness on land (m)	Velocity impact (m/s)	Velocity max. (m/s)	Run-out in fjord (m)
PCM (NGI)	0.2	200	200	5	--	40	55	400
DAN 3D (NGU)	0.28 – 0.46	900-1100	512-765	≈0	0.83-1.55 (mean) ≈5 (max)	--	21-32	--

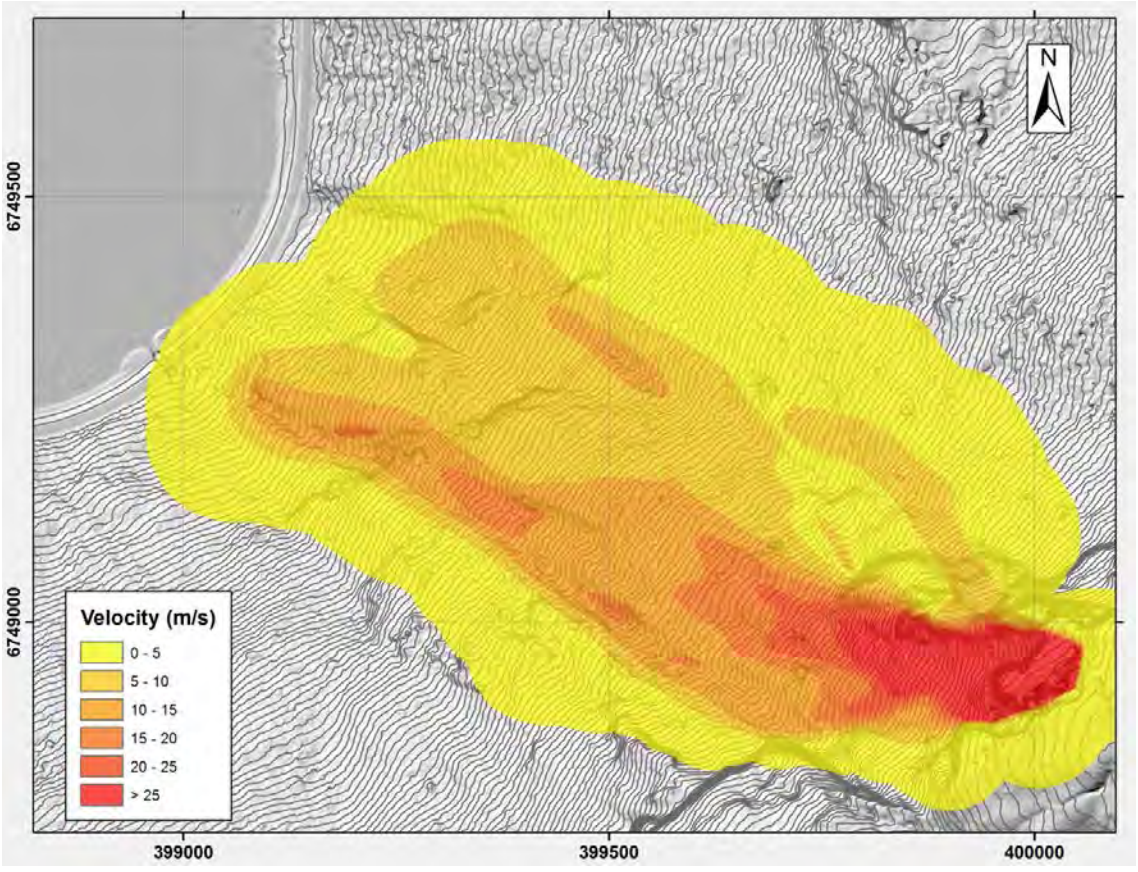

Figure 30: Results from the 3D DAN modelling showing maximum thickness along the run-out zone for the case of sliding mass with no entrainment (see also appendix 1). It shows the maximum thickness of material that has passed along the track cell by cell.

9.2 Tsunami analysis

NGI (Domaas & Glimsdal, 2009) have estimated tsunamis based on 3 different scenarios (Table 8). The scenarios included volumes of 40 Mm^3, 5 Mm^3 and 0.2 Mm^3. The 3 scenarios are

comparable with scenario 1, 2 and 3 described above. NGI used the PCM code for the evaluation of velocity and run-out distance for the use in the tsunami modelling. Entrainment is not included in this modelling. The 40 Mm^3 scenario (scenario 1a in this report) will have a travel distance of 1 km in the fjord and will be stopped at the other side of the fjord. The 5 Mm^3 scenario (almost comparable with scenario 2 in this report: 2 and 3,5 Mm^3) will have a travel distance of 750 m in the fjord, while a rockslide of 200 000 m^3 (a bit less than the volumes in scenario 3 in this report) will have a run-out distance in the fjord of 400 m.

There are several critical issues related to input parameters for the tsunami modelling that needs to be better defined, as also demonstrated by the new run-out modelling by use of the DAN 3D code (Table 7 and Appendix 1). Especially important is the velocity at water impact, dimensions of the landslide when entering the water and the length of the flow into water.

Table 8: Run-up heights from 3 rockslide scenarios as estimated by Domaas & Glimsdal (2009).

Place	Scenario: 200.000 m^3	Scenario: 5 Mm^3	Scenario: 40 Mm^3
Flåm	3-4 m	20-40 m	40-80 m
Aurlandsvangen	1-1.5 m	8-10 m	20-30 m

9.3 Exposed population in tsunami run-up areas

This subchapter have been made by Thierry Oppikofer (NGU) for this report. Based on NGI's tsunami run-up modelling for the villages of Flåm and Aurlandsvangen, NGU have estimated the number of inhabitants in the affected area based on population data from Statistics Norway. The uncertainties linked to the input parameters of the tsunami modelling and thus the final run-out height is stressed, and thus the present evaluation of possible exposed population needs to be revised when a new evaluation of run-out and tsunami analysis have been performed.

The tsunami run-up maps were digitised and intersected with the population data for the three different scenarios considered by NGI for the modelling (Domaas & Glimsdal, 2009). The total exposed population in Flåm and Aurlandsvangen, W_P, is 5 persons for a displacement wave triggered by a 0.2 Mm^3 rockslide from Stampa and 106 persons for a 5 Mm^3 rockslide (Table 9). 325 people are living in the run-up area of a displacement wave created by a 40 Mm^3 rockslide from Stampa. We assume that the inhabitants are constantly present in the exposed area (exposure of inhabitants E_P = 100%), which is a conservative value.

Table 9: Number of inhabitants in Flåm and Aurlandsvangen exposed to displacement waves created by rockslides from Stampa with different volumes.

NGI scenario	Volume [Mm^3]	Exposed inhabitants	
		Flåm	Aurlandsvangen
1	0.2	5	0
2	5	36	70
3	40	58	267

This number however does not account for the large number of tourists visiting the village of Flåm and the Flåm Railway each year. In 2012 a total of 152 cruise ships navigate into the Aurlandsfjord with a maximum of 229'930 passengers on board (Table 10) (Aurland Havn, 2012). The first boat arrive already end of March, but the main cruise season lasts from mid-April to end of September. The total number of visiting tourists is more than 450'000 per year (en.wikipedia.org/wiki/Fl%C3%A5m). We assume that the temporal distribution of other tourist

visits follows that of the cruise ship passengers. This gives a daily number of tourists coming by land transportation of 2100 for the month of June, which appears to be busiest based on cruise ship arrivals (Table 10).

Table 10: Tourist visits in Flåm based on cruise ship arrivals in 2012 (data from Aurland Havn, 2012).

Month	Number of days	Cruise ships		Other tourists	
		Number of ships	Max. passengers per month	Per month	Per day
April	15	4	2359	2268	150
May	31	28	43482	41804	1350
June	30	40	65560	63029	2100
July	31	39	55707	53557	1730
August	31	26	42160	40533	1310
September	30	15	20160	19382	650
Total		**152**	**229428**	**220572**	
			450000		

Based on these data and assumptions, we propose three scenarios for the number of exposed tourists, W_T: 1. A minimum scenario when no tourists are present ($W_T = 0$ persons); 2. A worst-case (maximum) scenario taking the maximum of cruise ship passengers on a single day (6837 passengers on 5 June 2012) and the number of other tourists for June ($W_T = 6837 + 2100 \approx 9000$ persons); 3. A mean scenario distributing the tourist visits over the entire year (W_T = 450'000 persons / 360 days= 1250 persons/day).

The tourists mainly visit the harbour area and the railway station and their associated buildings (museums, shops, restaurants etc.) in the vicinity. This area is likely overrun by a displacement wave created by a >5 Mm^3 rockslide from Stampa (Scenario 1 and 2; NGI scenarios 2 & 3). In contrast, a displacement wave created by a 0.2 Mm^3 rockslide from Stampa (Scenario 3; NGI scenario 1) only would affect the coastal area (about 40% of the area visited by tourists, reducing the number of exposed tourists, W_T, accordingly.

In order to incorporate these numbers in the potential exposed population, we must assume the mean duration of a stay in the exposed area. Six hours is chosen as conservative value for the mean tourist scenario #3 given that cruise ships in average stay 9.3 hours (Aurland Havn, 2012) and that most tourists take a train trip out of the exposed area in the meantime (exposure of tourists: E_T = 25%). This exposure value is in agreement with the value used by Blikra et al. (2006) in the risk analysis for the Åknes rockslide. For the maximum tourist scenario #2, the exposure E_T is set to 50% in order to take into account that cruise ships are present in the fjord mainly at daytime.

The total number of persons, W_{TOT}, exposed to displacement waves triggered by rockslides from Stampa is obtained by multiplying W_P and W_T with the respective exposure E_P and E_T and summing the resulting products. Depending on the rockslide scenario and the tourist scenario W_{TOT} ranges from 5 to 4825 (Table 11). Using the yearly mean value for W_T gives a total number of exposed persons of 130 for a 0.2 Mm^3 rockslide from Stampa. The larger rockslide scenarios of 5 and 40 Mm^3 would affect 419 and 638 persons, respectively (Table 11).

In their risk assessment for the Åknes rockslide Blikra et al. (2006) assume a vulnerability of 70% for people affected by a rockslide-triggered displacement wave (survival rate of 30%). This reduces the mean potential life loss to 91 for a 0.2 Mm^3 rockslide from Stampa and to 293 and 446 persons for the larger rockslide scenarios of 5 and 40 Mm^3, respectively (Table 11). These values for the potential life losses will be used in the subsequent risk classification for the different rockslide scenarios.

Table 11: Number of inhabitants and tourists exposed to displacement waves created by rockslides from Stampa with different volumes.

Volume [Mm^3]	Inhabitants W_P	Tourists W_T			Total exposed persons, W_{TOT}			Potential life loss		
		Min.	Max.	Mean	Min.	Max.	Mean	Min.	Max.	Mean
0.2	5	0	3600	500	5	1805	130	4	1264	91
5	106	0	9000	1250	106	4606	419	74	3224	293
40	325	0	9000	1250	325	4825	638	228	3378	446

10 Risk classification

A risk classification has been performed in order to have a best possible basis for decisions regarding further investigations and possible mitigation measures.

The risk classification was carried out in collaboration of NGU (R. Hermanns) and ÅTB (L.H. Blikra) for the present report, by using the newly developed hazard and risk classification system that will be used for all Norwegian unstable rockslopes in order to more objectively compare risk levels over the different sites in Norway (Hermanns et al., 2012). An overview of the scenarios used for the risk classification is given in Table 12. All the scenarios described in chapter 8 have been classified, except for scenario 3b which need a run-out analysis before the consequences can be evaluated. The geological input data of the classification are summarized in this report and the specific input parameters for each scenario used are given in *Appendix 2*. The risk matrix for scenario 1 (1a and 1b) and 2(2a and 2b) is given in Figure 31 and the classification for scenario 3 (a, c and d) in Figure 32.

The classification shows that the mean consequences of all scenarios plot into the medium risk class. However, the uncertainties for consequences and hazard classes are large for most of them. If we take the worst case consequences into account, most of the scenarios come into the t high risk zone (red), Figure 31and Figure 32. This means that there is a need for further follow-up in order to reduce the uncertainties. Special focus needs to be put on scenario 3a plotting in the transition zone between medium (yellow) and high (red) risk with the mean consequences (Figure 32). Also scenario 2a plot relatively high in the transition zone between medium and high risk class (Figure 31).

The risk classification for Stampa is compared with a preliminary risk classification for the Åknes rockslide (Figure 33), based on the data in the NGU reports on risk classification of unstable rockslopes in Norway (Hermanns et al., 2012) and the hazard and risk analysis of the Åknes rockslide (Blikra et al., 2006).

Table 12: Overview of the scenarios used in the risk classification.

Scenario	Landslide type	Volume (Mm^3)	Displacement (mm/year)	Tsunami run-up Flåm
Scenario 1 (a, b)	Rapid	30-100	0-2	40-80 m (40 Mm^3)
Scenario 2 (a, b)	Rapid	3-5	0-10	20-40 m (5 Mm^3)
Scenario 3 (a, c, d)	Rapid	0.2-1	4-15	2-4 m (0.2 Mm^3)
Scenario 4	Slow	0.1-50	10-40	0

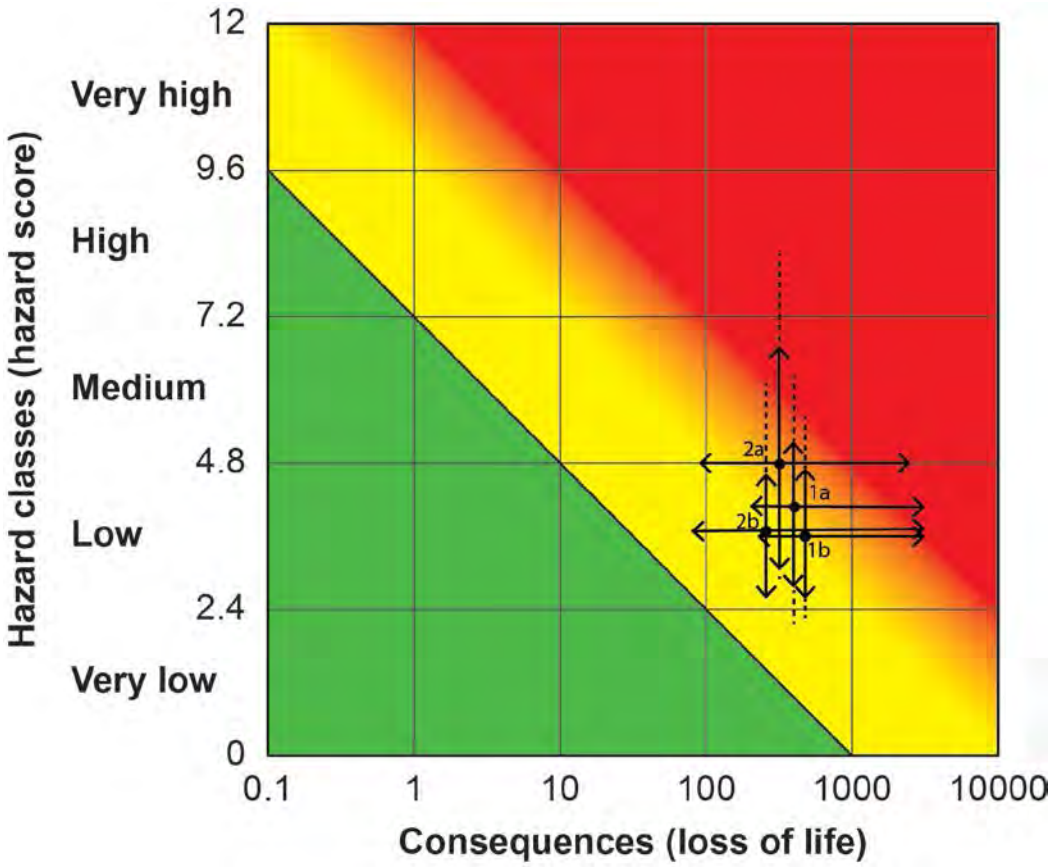

Figure 31: Risk matrix Stampa scenario 1 and 2. The points show the mean values, the black lines with arrows 5th and 95th percentile, and the stippled lines the minimum and maximum values.

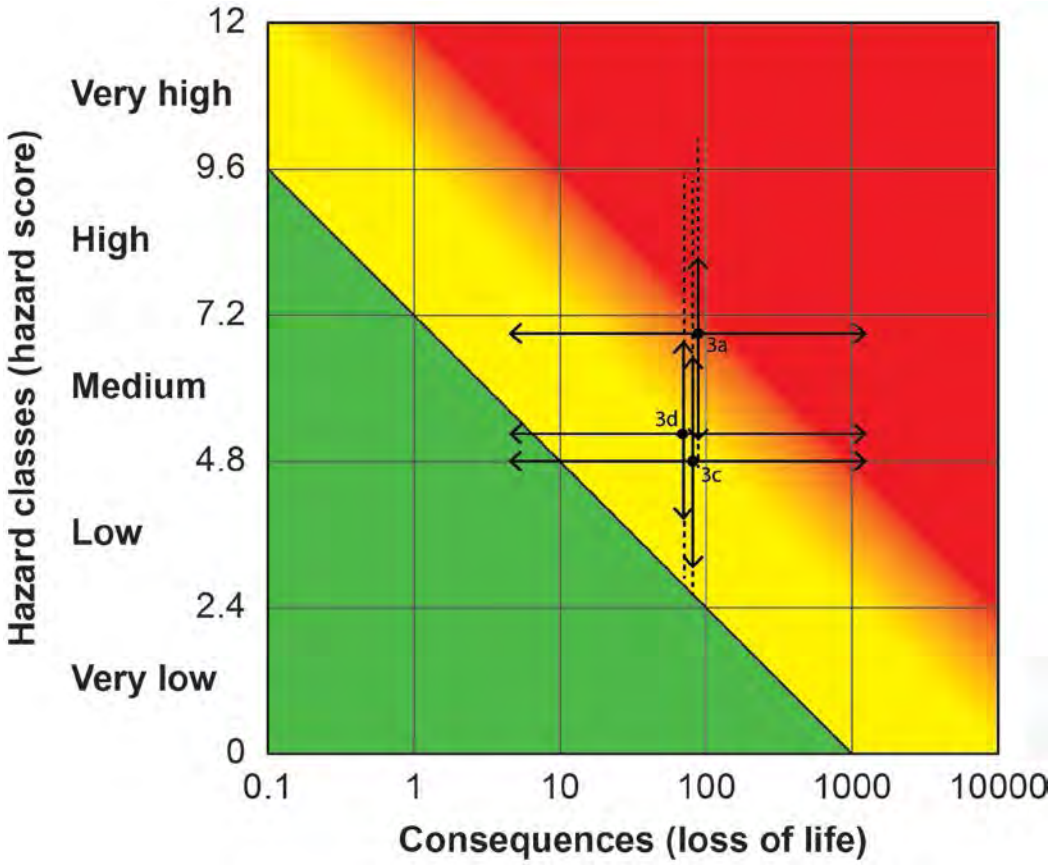

Figure 32: Risk matrix Stampa scenario 3.

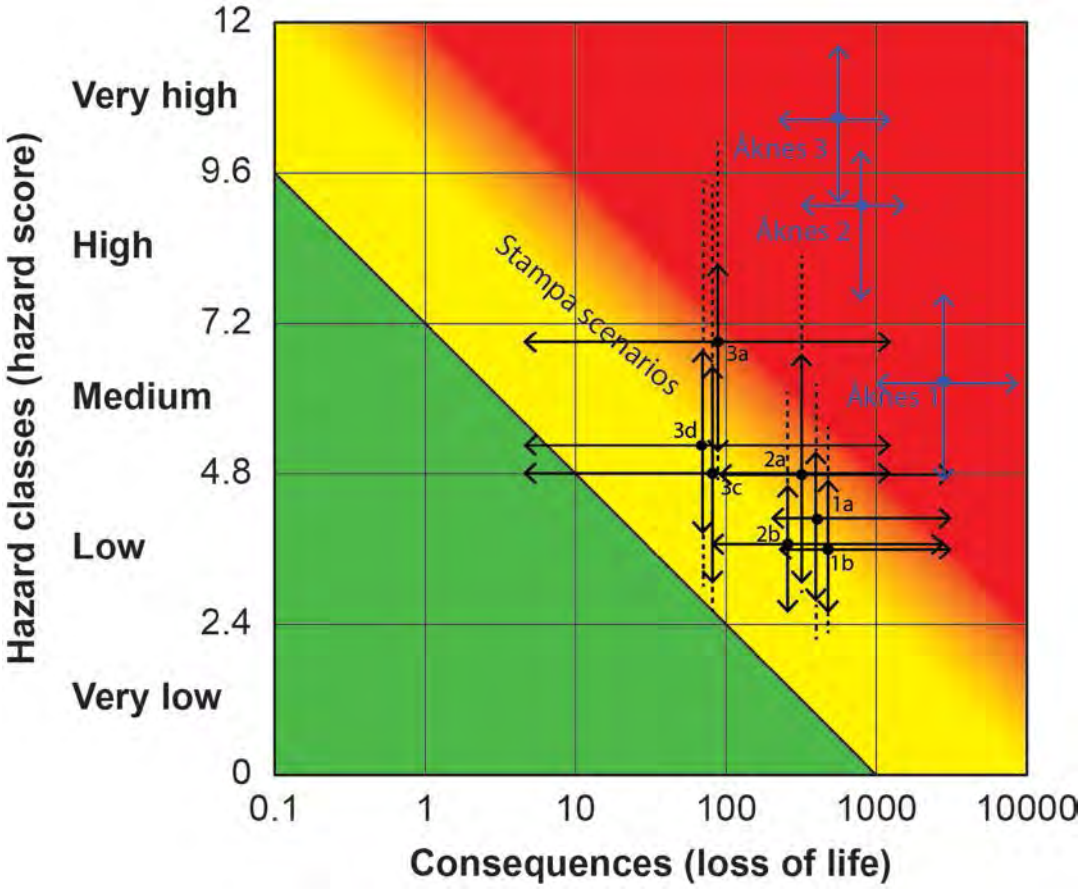

Figure 33: Risk classification from Stampa compared with a first classification of 3 scenarios of The Åknes rockslide. Åknes 1: Maximum scenario of 54 Mm^3; Åknes 2: Scenario 18 Mm^3; Åknes 3: Scenario 6-11 Mm^3 with highest displacements rates .

11 Recommendations

The evaluated rockslope failures in the Flåm-Stampa area have a large extent and are complex. The present compilation and evaluation have taken all earlier work into account and present some possible scenarios that have been the basis for the risk classification. The recommendations are based on the data presented in this report, the discussions during the meeting in the expert panel in Flåm in September, and the final recommendations from the expert panel.

The classification of the scenarios from Stampa shows that it has a distinct lower risk than the scenarios from the Åknes rockslide (Figure 33). Several of the scenarios are classified as medium risk objects (Figure 31 and Figure 32), but the uncertainties are large, and scenario 3a is classified close to the high risk zone (red). Scenario 2a also plots relatively high in the transition zone between medium and high risk.

The quality of the risk classification is to a large degree depending on the level of knowledge. Although there have been done relatively extensive investigations, there are still limited knowledge on some issues. Generally, it is important to evaluate the need of the following key areas in order to reduce the uncertainties in the risk evaluation:

- Investigations of the specific scenarios including
    - More displacement data from satellite based and ground-based InSAR
    - Continuous displacement data at some selected areas for the evaluation of seasonal changes
    - Data on the hydrological system and springs

    - More data on structures and possible sliding planes in the steep cliffs and lower areas
- Run-out analysis for some of the scenarios
- Tsunami analysis based on revised input parameters for the most critical scenarios

In the following, a summary of the recommendations from the international expert panel are given. These are followed by more specific recommendations in terms of need of further investigations for reducing uncertainties in the hazard and risk analysis. At the end an evaluation of the need for risk reduction (mitigation) is given.

11.1 Evaluation from the international expert panel

As part of the quality control, the work at Stampa and the present report has been evaluated by an international expert panel for rockslide monitoring. A seminar was held in Flåm in September 2012, including participants for all institutions being involved or performed research/ investigations in the area. The members of the international evaluation have been Corey Froese (Manager at the Aberta Geological Survey, Canada), Giovanni Crosta (Professor at the University of Milano-Bicocca, Italy) and Alvar Braathen (Professor at the University Centre of Svalbard). The main recommendations and conclusions from this evaluation are given below.

Generally, the expert panel was satisfied with NVEs overall approach and organization of the work, and how the data have been synthetized in the report. The panel means the report provide a solid benchmark for the Flåm-Stampa site. They have the following specific comments related to recommendations given in the first draft report

Future monitoring

Further movement analysis is required before final conclusions can be given in some areas, and they recommend performing a follow-up of the ground based InSAR campaigns. The campaign should build on the 2-months GB-InSAR project already performed, but they recommended a longer time period for the campaign (e.g. one year). The periodic GPS measurements should continue, but with possible longer time intervals.

Mapping

The panel recommend some additional structural geological field studies around the regional geological setting of the Stampa/Flåm area, especially the link between regional extensional detachments and faults and the area of instability. This should be documented in the report by a geological introduction including also geological cross-sections.

A better attention on the interpretation of the geophysical data and the possible effect of graphite were recommended, including the possible information about landslide debris thickness.

A better mapping of the frontal parts of the Stampa instabilities (scenario 3a/2a) should help identify possible sliding surfaces, geometrical characteristics and possible groundwater springs. The panel also stressed the need of a better definition of large slope instabilities within the landslide debris, which could lead to severe consequences.

Surface hydrology

The panel recommend that the low-cost monitoring activity performed by the Sogn & Fjordane University College continues on a yearly basis, allowing gathering of fundamental datasets for the understanding of the hydrogeological system of Stampa and the definition of possible

location for daylighting of failure surfaces. An important issue is also a systematic mapping of springs, and possibly also some further discharge studies.

Proposed groundwater drainage system

The panel also commented on the proposed tunnelling project that would aim at draining the groundwater and potentially the surface water from the Stampa area. With the observations of a low ground water level around Stampa, and many remaining questions around the hydrogeology of the area, the panel concluded that the proposed subsurface drainage project was poorly founded. Before considering such major step of mitigation, better documentation around achieved effects of the project has to be in place. The panel questioned whether there would be any effects at all, and that other methods for collecting and deviating surface waters could be considered.

Risk classification

The expert panel express that the applied risk matrix is a good tool for a uniform application on a regional/national basis to identify moderate to high risk slope objects that requires further considerations and resources from NVE. However, they recommend making the risk classification qualitative instead of quantitative concerning the hazard (probabilities). Generally, for Stampa some more detailed surface mapping and monitoring would constrain better the models for volumes and runouts in order to validate or eliminate the "high" risk ranking for certain scenarios.

11.2 Investigations - recommendations

The need for more investigations in order to reduce the uncertainties in the hazard and risk evaluation is evaluated here. This is done for the different scenarios. In addition there is a need for some field investigations in order to map regional fault zones and graphite-bearing lithologies and their possible link to the instabilities. There have been observed many brittle deformation structures in the area, and also localities with graphite (Helge Henriksen, pers. com.).

11.2.1 Scenario 1

The existing investigations and monitoring data shows that the largest scenarios have a low probability for initiating large rock avalanches (e.g. scenario 1a and 1b). However, the large consequences lead to a medium risk (yellow zone) in the classification (Figure 31). It is recommended to follow up these scenarios with the existing periodic GPS measurements and with satellite-based InSAR. A program for the time intervals of the GPS measurements should be implemented (e.g every 2nd or 3rd year). There is also a need for more field data in the northern part of the rockslide area. Scenario 1 is the scenario that would be highly influenced by pore-water pressure at large depths, and it is recommended that the monitoring activity on surface hydrology (discharge measurements at Stampa) performed by Sogn & Fjordane University College (HSF) continues on a yearly basis. HSF also have plans for an internal project to perform a systematic mapping of springs, start discharge measurements in the river Stampa, and to establish data loggers for conductivity and temperatures at selected sites.

11.2.2 Scenario 2

The scenario 2a and 2b with volumes of 2-5 Mm^3 has also been evaluated to have relatively low hazard score (Figure 31), but there are large uncertainties related to the active displacements. The steep area north of the Stampa area has for example displacements of about 1 cm/year, but it is still questionable if this is representative for the entire scenario 2a. The scenarios, as outlined in this report, may be influenced of water pressure since the depth of sliding planes can

be as deep as 100 m. The resistivity data show a distinct change from high resistivity to much lower values at these depths that could be interpreted to be an effect of water-saturated areas. More data is needed on these scenarios in order to reduce the uncertainties, see also the recommendations from the expert panel (11.1). This should include data from satellite-based InSAR and ground-based InSAR in order to evaluate the extent of the scenarios. A further processing should be performed on the 2011 and 2012 GB InSAR data in order to possibly see interannual deformations. The GB InSAR campaigns demonstrate a very good coverage on scenario 2a, and a longer campaign will be a good solution in order to better document possible displacements in this area. A denser net of GPS points for periodic measurements, or possible reflectors for satellite based InSAR could also be considered. A more detailed geological field mapping with focus on structural elements and possible sliding planes in the steep cliff areas is needed. Some new geophysical profiles (2D resistivity; refraction seismics) could be performed by performing these measurements further to the west compared to the existing once. The need for more investigations in terms of deep drillings should be considered after more knowledge on the displacement pattern has been achieved. A continuation and increased focus on the hydrological system, as described under scenario 1, will also be important for the evaluation of scenario 2.

11.2.3 Scenario 3

The smallest scenarios (3a, 3c, 3d) are evaluated to be the most critical in terms of probabilities and risk (Figure 32). Scenario 3a has displacements of about 1 cm/year and should be the most important area to follow up (Figure 29). Scenario 3b has larger displacements, but the area here has a gentle slope gradient, and it is questionable if a collapse here will have the potential to reach the fjord. A run-out analysis is thus needed before the consequences can be evaluated. More data is needed on displacements in scenario 3 in order to see if the GPS points indicating movements are representative. These data should resolve the temporal variations of displacement and cover more widespread areas than the GPS network. Ground-based InSAR should be used in order to evaluate the extent and should be performed by a longer time period, especially during the entire snow-melt season (see also recommendations from the expert panel). Furthermore, detailed geological field mapping should be performed in areas where data are still missing, especially in the steep cliff areas, in order to define the scenario more accurately (see also recommendations for scenario 2). The failure surface is relatively shallow in these scenarios and the influence of water pressure is limited. The scenarios need to be followed up in terms of run-out modelling, including both onshore and into the fjord, in case that significant change to the existing models can be expected. This should be followed by tsunami modelling. Especial focus should be put on the large volumes of active landslide debris in the run-out zone, and the effect of collapse of landslide debris and entrainment (see also recommendations from the expert panel).

11.2.4 Scenario 4

Large areas have relatively gentle slope gradients and are covered by landslide debris which in some areas has relatively large displacements. They will most probably continue without being critical in terms of rapid and destructive rock avalanches (scenario 4). However, such creeping landslides can have considerable destructive effect on buildings and infrastructures. The area of shallow creeping deformations needs to be dealt with in the process of land use planning in the municipality. The expert panel recommend that these areas should be better mapped.

11.3 Mitigation - recommendations

Mitigation in order to reduce the risk for large rockslides is normally performed by passive measures like monitoring and early warning or by moving people and infrastructure out of the hazard area. The prioritization of mitigation measures needs to be based on a risk analysis, and the recommendations given in this report needs to be seen in a national cost-benefit perspective. In this case there is still a need for some more investigations related to displacements, structural field data and run-out modelling in order to reduce the uncertainties related to the risk classification.

11.3.1 Monitoring and early warning

Better knowledge on some of the scenarios are needed before any decision of implementing permanent monitoring and early warning can be done. At the moment, with relatively small movements and without any signals of increased deformations, the follow-up in terms of existing displacement measurements (periodic GPS with more focus on critical areas, InSAR and GB InSAR) is considered to be sufficient in order to cope with the risk situation in the Stampa area. The most important area for follow-up is scenario 3a.

11.3.2 Physical mitigation

In some occasions, risk reduction can be done by physical mitigation, for example by performing large-scale drainage if water pressure is controlling the movements. Mitigation in terms of large scale drainage of surface water or through deep tunnels and drainage boreholes would possibly have an effect on the largest scenarios (e.g scenario 1 and possibly 2). However, the present data show limited displacements and most of the scenarios plot with relatively low hazard score. The knowledge of the unstable area is also still too limited in order to evaluate the effect of drainage. The coupling between the hydrological system, displacement and stability needs to be much better understood. International experience of large-scale drainage of active rockslide areas is good, but it requires an extensive investigation and monitoring program before the implementation. The international example also involves rockslide areas with large active displacements with one order of higher movement rates than those documented from the Stampa area. As another example, the possibility for risk reduction in terms of drainage has also been evaluated for the Åknes rockslide in Møre & Romsdal county (Blikra, 2012). Although extensive investigations have been done in terms of deep boreholes and instrumentation to map movements and water level at Åknes, there is still too limited knowledge on the hydrological conditions to recommend large-scale drainage.

The international expert panel evaluation of the proposed groundwater drainage project is as follows:

The local communities are considering a tunnelling project that would aim at draining the groundwater and potentially the surface water from the Stampa area. With the observations of a low ground water level around Stampa, and many remaining questions around the hydrogeology of the area, we conclude that the proposed subsurface drainage project is poorly founded. Before considering this rather major step of mitigation, better documentation around achieved effects of the project has to be in place. With the current state-of-the-art of Stampa, it is questionable if there will be any effects at all. Other methods for collecting and deviating surface waters could be considered.

12 Conclusions

A compilation of existing data from the unstable phyllitic rocks in the Flåm-Stampa has been performed. Several institutions have contributed with data to this work, especially NGU and NGI. Large areas have been interpreted to be potentially unstable due to the documentation of large deformations in terms of open fractures and landslide deposits. Several possible scenarios have been evaluated and used for a new risk classification. There are still large uncertainties connected to this classification and there is a need for further investigations in terms of getting better knowledge on displacements, geological structures and run-out.

The risk analysis demonstrates that the scenarios from Stampa have a much lower risk compared with for example the scenarios from the Åknes rockslide. However, the risk analysis shows that the smallest scenario related to the steep cliffs north of Stampa (scenario 3a) classify highest in the risk matrix. This area needs to be followed up in more detail in order to reduce the uncertainties in the risk classification.

At the moment, with relatively small movements and without any signals of increased deformations, the follow-up in terms of a slight revision of the existing displacement measurements is considered to be sufficient in order to handle the risk in the Stampa area. This includes a longer-term ground-based inSAR campaign, continuation of the satellite based InSAR and possibly a denser net of GPS points in the most critical area (scenario 2a and 3a).

Physical mitigation in terms of large scale drainage systems would possibly have an effect on the largest scenarios. However, the present data show limited displacements and the risk analysis indicate low hazard score. The knowledge of the unstable area is also still too limited in order to evaluate the effect of drainage, for example the coupling between the hydrological system, displacement and stability. The international examples showing effective and good results of drainage involves rockslide areas with large active displacements, with one order of higher movement rates than those documented from the Stampa area. Based on the relatively low risk connected to the largest scenarios and the limited knowledge on the hydrological conditions, it is in the present situation not recommended to initiate any mitigation measures in terms of larger drainage systems. This is in agreement with the conclusions from the international expert panel.

The recommendations presented here follows the advice from the international expert panel, and the report will be the basis for future handling both related to investigations and possible future handling, led by the Norwegian Water Resources and Energy Directorate (NVE).

13 Acknowledgements

The editor thanks all contributors for the availability to data and for fruitful discussions both during the seminar in Flåm and during preparation of the present report. We wish to make a special thanks to the international expert panel (Corey Froese, Giovanni Crosta and Alvar Braathen) for an in-depth evaluation of both specific issues and for recommendation for further handling of the unstable rocks in the Flåm-Stampa area.

14 References

Andersen, T.B. & Jamtveit, B. 1990. Uplift of deep crust during orogenic extensional collapse: a model based on field studies in the Sogn-Sunnfjord region, W. Norway. Tectonics 9, 1097–1111.

Andersen, T.B., Torsvik, T.H., Eide, E.A., Osmundsen, P.T. & Faleide, J.I. 1999: Permian and Mesozoic extensional faulting within the Caledonides of central south Norway. Journal of Geological Society, London, 156, 1073-1080.

Aurland Havn 2012. Skipsanløp 2012, http://aurlandhavn.no/cruise/skipsanlop-2012/, accessed: 16 July 2012.

Blikra, L.H., Anda, E., Høst, J. & Longva, O. 2006a. Åknes/Tafjord-prosjektet: Sannsynlighet og risiko knyttet til fjellskred og flodbølger fra Åknes og Hegguraksla. Geological Survey of Norway. Report 2006.039.

Blikra, L.H., Longva, O., Braathen, A., Anda, E., Dehls, J.F., Stalsberg, K., 2006b. Rock Slope Failures in Norwegian Fjord Areas: Examples, Spatial Distribution and Temporal Pattern, in: Evans,S.G., Scarascia Mugnozza,G., Strom,A. and Hermanns,R.L. (Eds.), Landslides from Massive Rock Slope Failure; NATO Science Series, IV. Earth and Environmental Sciences, Vol 49. Springer,Dodrecht, Netherlands, pp. 475-496.

Blikra, L.H. 2012: Evaluering av drenering som risikoreduserende tiltak ved Åknes. Åknes report 06.2012.

Böhme, M., Hermanns, R.L., Oppikofer, T., Fisher, L., Bunkholt, H.S.S., Eiken, T., Pedrazzini, A., Derron, M.-H., Jaboyedoff, M., Blikra, L.H. & Nilsen, B. (2013): Analysing complex rock slope deformation at Stampa, western Norway, by integrating geomorphology, kinematics and numerical modelling. Engineering Geology 154, 116-130.

Braathen, A., Blikra, L.H., Berg, S.S., Karlsen, F., 2004. Rock-slope failure in Norway; type, geometry, deformation mechanisms and stability. Norw. J. Geol. 84(1), 67-88.

Brenne, E., Ellingsen, S. & Nes, S. 2011: Vannførings- og reoradarundersøkelser på Joasete, Aurland kommune. Bachelor thesis, University College of Sogn & Fjordane.

Bryhni, I., Sturt, B.A., 1985. Caledonides of southwestern Norway. In: Gee, D., Sturt, B.A. (Eds.), The Caledonide Orogen—Scandinavia and Related areas. John Wiley & Sons, Chichester, pp. 89–106.

Crosta, G.B. & Agliardi, F. 2003: Failure forecast of large rock slides by surface displacement measurements. Can. Geotech. J. 40, 176-191.

Dehls, J., Fisher, L., Bøhme, M., Saintot, A., Hermanns, R., Oppikofer, T., Lauknes, T.R., Larsen, Y., Blikra, L.H., & Kristensen, L. 2012: Landslide monitoirng in western Norway using high resolution TerraSAR-X and Radarsat-2 InSAR. In: Landslides and Engineered Slopes: Protecting Society through Improved Understanding – Eberhardt et al. (eds). 2012 Taylor & Francis Group, London.

Domaas, U., Rosenvold, B.S., Blikra, L.H., Johansen, H., Grimstad, E., Sørlie, J.E., Gunleiksrud, O., Engen, A. & Lægreid, O. 2002: Studie av fjellskred og dalsidestabilitet i fyllittområder (Report to the Norwegian Research Council). *Norwegian Geotechnical Institute Report 20001132-32.*

Domaas, U. & Glimsdal, S. 2009: Skred og flodbølger ved Flåm, Aurland kommune. Norges Geotekniske Institutt Rapport 20081693-1.

Fossen, H. 2000. Extensional tectonics in the Caledonides: synorogenic or post-orogenic? Tectonics. 19. 2. 213-224.

Fossen, H. & Hurich, C.A. 2005: The Hardangerfjord Shear Zone in SW Norway and the North Sea: a large-scale low-angle shear zone in the Caledonian crust. Journal of the Geological Society, London, 162, 675-687.

Grimstad, E. 2008.: Utredning av ustabile dalsider i fyllitt. Aurland. NGI rapport 20081254-1.

Henderson, I.H.C. & Blikra, L.H. 2008: Ustabile fjellparti i fyllittområdene i Flåm – Aurland. Norges geologiske undersøkelse Rapport 208.033. 16 p.

Hermanns, R.L., Fischer, L., Oppikofer, T., Böhme, M., Dehls, J.F., Henriksen, H., Booth, A., Eilertsen, R., Longva, O., Eiken, T., 2011b. Mapping of unstable and potentially unstable slopes in Sogn og Fjordane (work report 2008-2010). NGU report 2011.55, Geological Survey of Norway, Trondheim, Norway.

Hermanns, R.L., Oppikofer, T., Anda, A., Blikra, L.H., Böhme, M., Bunkholt, H., Crosta, G.B., Dahle, H., Devoli, G., Fischer, L., Jaboyedoff, M., Loew, S., Sætre, S. & Molina, F.Y. (2012): Recommended hazard and risk classification system for large unstable rock slopes in Norway. Geological Survey of Norway Report 2012.029. 53 p.

Hungr, O. 2010: Geotechnical Engineering Inc., 2010, DAN 3D. Dynamic Analysis of Landslides in Three Dimensions, User Guide. Vancouver.

Jaboyedoff, M., Baillifard, F., Couture, R., Locat, J. & Locat, P. 2004. Toward preliminary hazard assessment using DEM topographic analysis and simple mechanical modeling by means of sloping local base level. In: Lacerda, W.A., Ehrlich, M., Fontoura, A.B. & Sayão, A. (eds), Landslides: Evaluation and Stabilization, Taylor & Francis, London, p. 199–205.

Kristensen, L. 2011: Ground based radar measurements at Joasete/Furekamben in Flåm, Sogn og Fjordane. Åknes report 09.2011.

Kristensen, L. 2012: GB radar measurements at Joasete/Furekamben in Flåm, Sogn og Fjordane, 2012. Åknes report 07.2012.

Osmundsen, P.T., E.A. Eide, N.E. Haabesland, D. Roberts, T.B. Andersen, M. Kendrick, B., Bingen, A. Braathen and T.F. Redfield. 2006. Kinematics of the Høybakken detachment zone and the Møre–Trøndelag Fault Complex, central Norway. Journal of the Geological Society, London, Vol. 163, 2006, pp. 303–318.

Osmundsen, P.T., Redfield, T.F., Anda, E., Hendriks, B., Henderson, I., Dehls, J., Lauknes, T.R., Fredin, O. & Davidsen, B. 2010. The tectonic significance of Alpine landscapes in Norway. *Journal of the Geological Society, London.* Vol. 167, 1, pp. 83–98. doi: 10.1144/0016-76492009-019.

Osmundsen, P.T., Henderson, I., Lauknes, T.R., Larsen, Y., Redfield, T.F. & Dehls, J. 2009. Tectonic controls on topography and mass-wasting processes in Northern Norway, *Geology*. 37. 135-138. doi:10.1130/G25208A.1

Perla, R., Cheng, TT, McClung and D.M., 1980, A two-parameter model of snow-avalanche motion. Journal of Glaciology, 26: 197-207.

Pfaffhuber, A.A., Bazin, S., Domaas, U. & Grimstad, E. 2011: Electrical resistivity topography to follow up an airborne EM rock slide mapping survey – Linking rock quality with resistivity.

Pfaffhuber, A.A., Grimstad, E. & Domaas, U., Auken, E., Foged, N. & Halkjær, M. 2010: Airborne EM mapping for rockslides and tunneling hazards. The Leading Edge 29 (8), 936-939

Redfield, T. F. & Osmundsen, P. T. 2009. The Tjellefonna fault system of Western Norway: Linking late-Caledonian extension,post-Caledonian normal faulting, and Tertiary rock column uplift with the landslide-generated tsunami event of 1756. *Tectonophysics* .474. 106–123.

Redfield, T.F., Osmundsen, P.T. & Hendriks, B.W.H. 2005. The role of fault reactivation and growth in the uplift of western Fennoscandia. Journal of the Geological Society, London, 162, 1013–1030.

Redfield, T (2012): Regional geological background, Stampa – Flåm. Internal document, NGU.

Vatn, J., Grimstad, E. & Holmøy, K.H. 2009: Utvikling av risikomodell for fjellskred i Aurland kommune. SINTEF Notat nr 3.

Vatn, J. 2011: Perspektiver på risikofastsetting: fjellskred i Aurland kommune. SINTEF notat nr 4.

Skotheim, A.Å. 1993: Statens vegvesen Sogn og Fjordane. RV 50 Hp 03 Aurland Aust – Kolakaien. Parsell Otternes – Kolakaien. Grunnundersøking. GEOVEST rapport nr. 3.

Appendix 1: Run out modeling for a potential catastrophic rockslope failure in Flåm

Freddy Yugsi Molina, NGU

A 3D run out simulation has been carried out in the area of Stampa-Joasete for a small rock cliff of approximately 280000 m^3 consider as the potential source area of a rock avalanche (Figure 1). The area has been evaluated with a high probability for rock avalanche occurrence in previous reports (NGI, 2009; NGU, 2011).

Other reports have presented 2D run out analysis results for the area (NGI, 2009). Modelling was done to calculate input parameters for tsunami wave modeling (Volume and velocity) using the PCM model (Perla et al., 1980); the model is a variation of the Voellmy's (1955) method widely used for snow avalanche run out assessment. DAN 3D Beta Version 2 (Hungr Geotechnical Engineering Inc., 2010) has been used in the preparation of the present report trying to include the effects of lateral spreading of the rock mass along the potential run out track. DAN 3D uses frictional rheology for the rock mass and a set of different rheology models for the basal surface including Voellmy (1955). DAN 3D has been successfully used to simulate rock avalanches in the past (e. g.: Sosio et al., 2008; Hungr & McDougall, 2009).

Input parameters

Several models were produced to include all possible conditions during the potential rock avalanche event. Four different materials were used in the simulation (Figure 2), based on physical properties and maximum depth of erosion. Voellmy was selected to better represent basal rheology for the scree deposits whereas frictional rheology was chosen for the rock exposures. Characteristics of the materials are presented on Table 1. Models simulate conditions with different basal rheology parameter values and different maximum depth of erosion (Table 2). Maximum depth of erosion was estimated based on thickness of talus deposits calculated by Oppikofer et al. (Other sections of this report) using the SLBL method (Jaboyedoff et al., 2004).

No model calibration for the run out properties based on back analysis of previous rock slope failures in the area was possible. Location of previous rock avalanche events (source areas) was not evident from either aerial photographs or DEM analysis. Characteristic values found in literature for other rock avalanche events (Sosio et al., 2008, Table 3) were used to define basal rheology parameters. Values for other physical and mechanical properties of the rock mass were defined based on Boehme et al. (submitted).

A 1,35 m resolution DEM was used to represent topography; the elevation model was obtained by resampling the existent 1m airborne-based LIDAR DEM. Resampling was necessary due to maximum size allowed by the software (1000*1000 pixels).No submarine

topography was used during simulations as it was considered that DAN 3D cannot simulate sub-aquatic flow (it does not take in consideration the landslide-water friction conditions). Current topography was adapted to the run out conditions removing the volume of the rock mass involved in scenario 1 following the geometry proposed by Boehme et al. (submitted). 2000 independent particles represent the unstable rock block in order to simulate the level of fragmentation undergone by the rock block during failure.

Results

16 different starting conditions were simulated taking in account input parameters presented in the previous section (Figures 3 to 6). Results presented in this section are for the arrival time of the mass into the fjord. A summary of the results are presented on Table 4. The results show important differences respect to results obtained on the analysis done in the past (NGI, 2009) in terms of both block geometry and velocity at the fjord impact time. Differences can be explained due to lateral spread of the rock mass during the run out, presence of topographical asperities along the track, material entrainment and longitudinal expansion due to topographic roughness.

Most of the cases analyzed show peak velocity values located in the proximity of the toe of the run out lobes. Simulations with the highest maximum velocity values correspond to friction coefficient (m) of 0.1 and turbulence coefficient (j) of 1000 for all main conditions (as presented on Table 2). Highest average thickness values are for simulations with m=0.25 and j=450 (except for the case of differential erosion). Extremely low values of thickness at the toe of the mass are a common result for all simulations.

A significant change in the run out trajectory occurs at a narrow rock cliff underneath the unstable source area (at the upper part of the run out track), it acts as a spur that splits the whole mass in three separated compartments. Two compartments, continue the run out down-slope with a clear independent behavior (even running at different velocities and having different entrainment rates), reaching the shoreline at different times but near to each other. A larger portion of the mass goes into the southern mass (Figure 7). The third compartment stops at the spur with only a short run out distance.

References

Boehme, M., Hermann, R. L., Oppikofer, T., Fischer, L., Eiken, T., Bunkholt, H. Pedrazzini, A., Derron, M.-H., Jaboyedoff, M., Blikra, L. H., Nilsen, B. Submitted. Analyzing complex rock slope deformation at Stampa, western Norway, by integrating geomorphology, kinematics and numerical modelling. Engineering Geology.

Domaas, U. and Glimsdal, S., 2009, Beregning og flodbølger for tre potensielle fjellskred fra Stampa, Report, Norwegian Geotechnical Institute, Oslo, 49 p.

Hermanns, R.L., Bunkholt, H., Boehme, M., Fischer, L., Oppikofer, T., Rønning, J.R. and Eiken, T., 2011, Foreløpig fare- og risikovurdering av ustabile fjellparti ved Joasete-Furekamben-Ramnanosi, Aurland kommune, Report, Geological Survey of Norway, Trondheim, 46 p.

Hungr, O., McDougall and S., 2009, Two numerical models for landslide dynamic analysis. Computers & Geosciences, 35: 978-992.

Jaboyedoff, M., Baillifard, F., Couture, R., Locat, J., Locat and P., 2004, Toward preliminary hazard assessment using DEM topographic analysis and simple mechanical modeling by means of sloping local base level. Landslides Evaluation and stabilization. Balkema, S: 191-197.

O.Hungr Geotechnical Engineering Inc., 2010, DAN 3D. Dynamic Analysis of Landslides in Three Dimensions, User Guide. Vancouver.

Perla, R., Cheng, TT, McClung and D.M., 1980, A two-parameter model of snow-avalanche motion. Journal of Glaciology, 26: 197-207.

Sosio, R., Crosta, G.B., Hungr and O., 2008, Complete dynamic modeling calibration for the Thurwieser rock avalanche (Italian Central Alps). Engineering Geology, 100: 11-26.

Voellmy and A., 1955, Über die Zerstörungskraft von Lawinen. Schweizerische Bauzeitung, 73: 212-285.

Material	Unit weight (kN/m3)	Rheology type	Internal friction angle (°)	Max. Erosion depth (m)
Phyllite	25.2	Frictional	26	0
Shallow Colluvium	15	Voellmy	35	5
Thick Colluvium	15	Voellmy	35	10
Water	9.81	Frcitional	0	0

Table 1. Material Input parameters.

Main Condition	*Initial Volume (m^3)*	*Final Volume (m^3)*	*Max. Erosion Shallow talus (m)*	*Max erosion Thick talus (m)*	*No. particles*	*Erosion rate*
No erosion	282125	282125	0	0	2000	0
Shallow erosion	282125	400000	0	10	2000	0.00045
Maximum erosion	282125	500000	0	10	2000	0.00072
Differential erosion	282125	500000	5	10	2000	0.00069

Table 2. Input parameters related to entrainment (main condition).

	Internal rheology	Frictional rheology	Voellmy rheology	
	Friction angle, ϕ_i	Bulk friction angle, ϕ_b	Frictional coefficient, μ	Turbulent coefficient, ξ
	[°]	[°]	[-]	[ms^{-2}]
Rock avalanches	35–40	10–30	0.1–0.25	450–1000
Debris avalanches	35	23–30	0.07–0.1	200–250
Rockslide-debris avalanches	35	8–31	0.05–0.2	200–400
Ice-rock avalanches	20–35	10–20	0.03–0.1	1000
Debris flows	35	22–29	0.05–0.2	200–500
Volcanic-rock avalanches	30–35	9–13	0.05–0.1	100–140

Table 3. Characteristic rheology parameter values for rock avalanches (from Sosio et al., 2008)

Main Condition	Rheology parameters		Arrival time (s)	Max velocity (m/s)	Volume (m3)	Length (m)	Width (m)	Toe thickness (m)	Average thickness (m)
	m	j							
No erosion	0.1	450	56	22	282125	1021	626	1.50E-05	0.9
	0.25	450	71	21.3	282125	906	512	1.80E-05	1.1
	0.1	1000	47	29.71	282125	1108	717	1.20E-05	0.83
	0.25	1000	62	23.5	282125	1045	575	7.00E-06	0.99
Shallow erosion	0.1	450	55	24.04	344718	1068	655	2.50E-05	1.05
	0.25	450	70	20.85	349498	910	530	1.70E-05	1.26
	0.1	1000	46	30.35	338687	1075	720	9.90E-05	0.99
	0.25	1000	62	24.41	349428	890	539	4.40E-05	1.19
Maximum erosion	0.1	450	54	25.92	386121	1033	634	8.70E-05	1.16
	0.25	450	70	20.18	399715	910	519	8.70E-05	1.35
	0.1	1000	46	30.92	382247	1075	763	1.50E-05	1.07
	0.25	1000	61	25.73	398660	890	560	2.00E-05	1.37
Differential erosion	0.1	450	53	25.75	451993	1084	630	2.50E-05	1.33
	0.25	450	71	21.28	350509	895	560	3.50E-05	1.25
	0.1	1000	45	31.87	444742	1060	765	3.80E-05	1.21
	0.25	1000	60	30.06	457393	885	628	2.20E-05	1.55

Table 4. Summary of results for all simulations

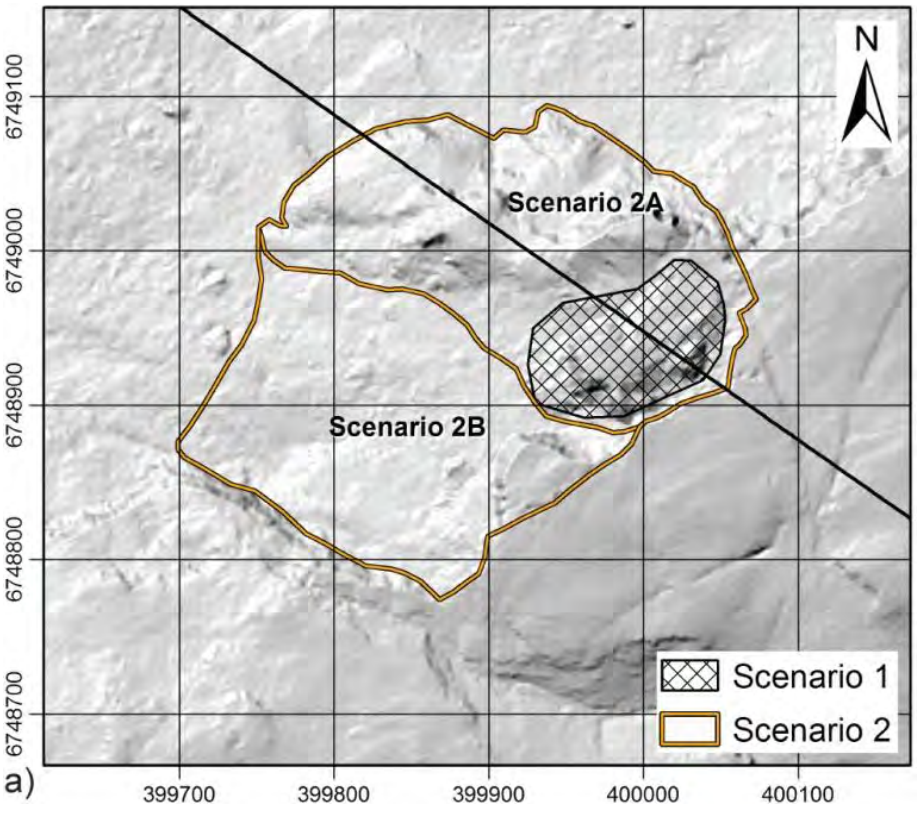

Figure 1. Location area (scenario 1; taken from Oppikofer, previous sections this report)

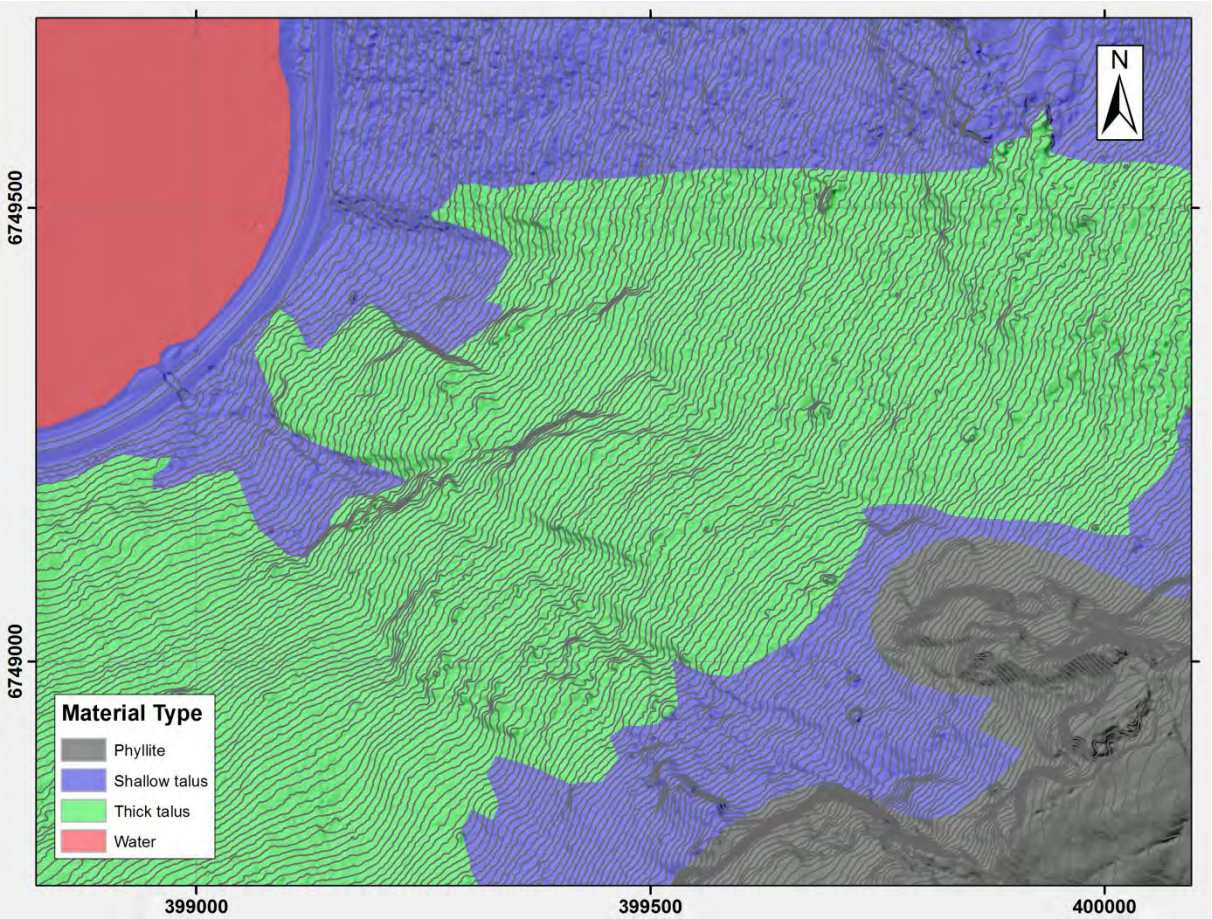

Figure 2. Material Type map. Talus deposits were devided in two units based on their thickness.

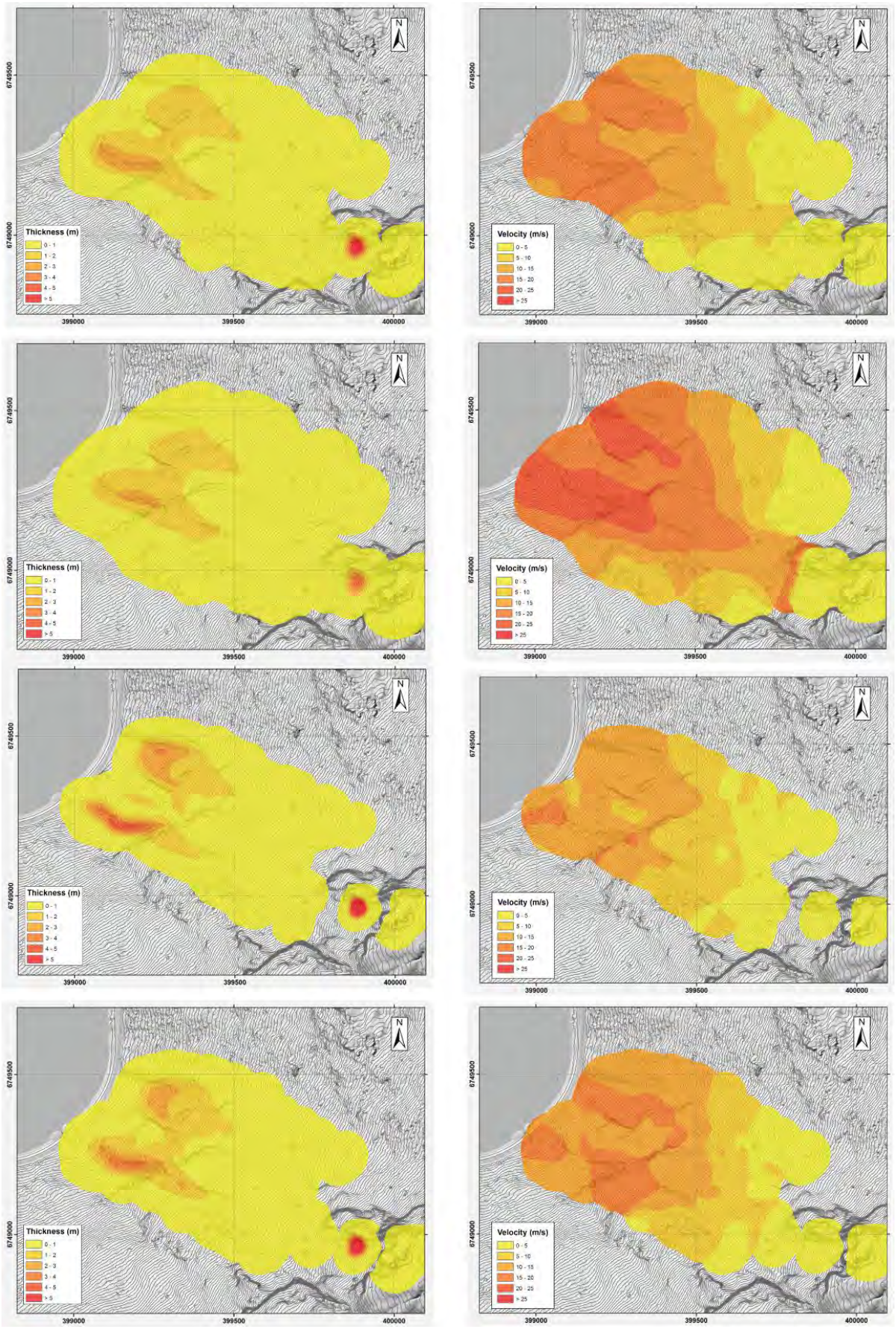

Figure 3. Results for simulations not including entrainment conditions. Uppermost row figures correspond to m=0.1 and j=450, second row m=0.1 and j=1000, third row m=o.25 and j=450, last row m=0.25 and j=1000.

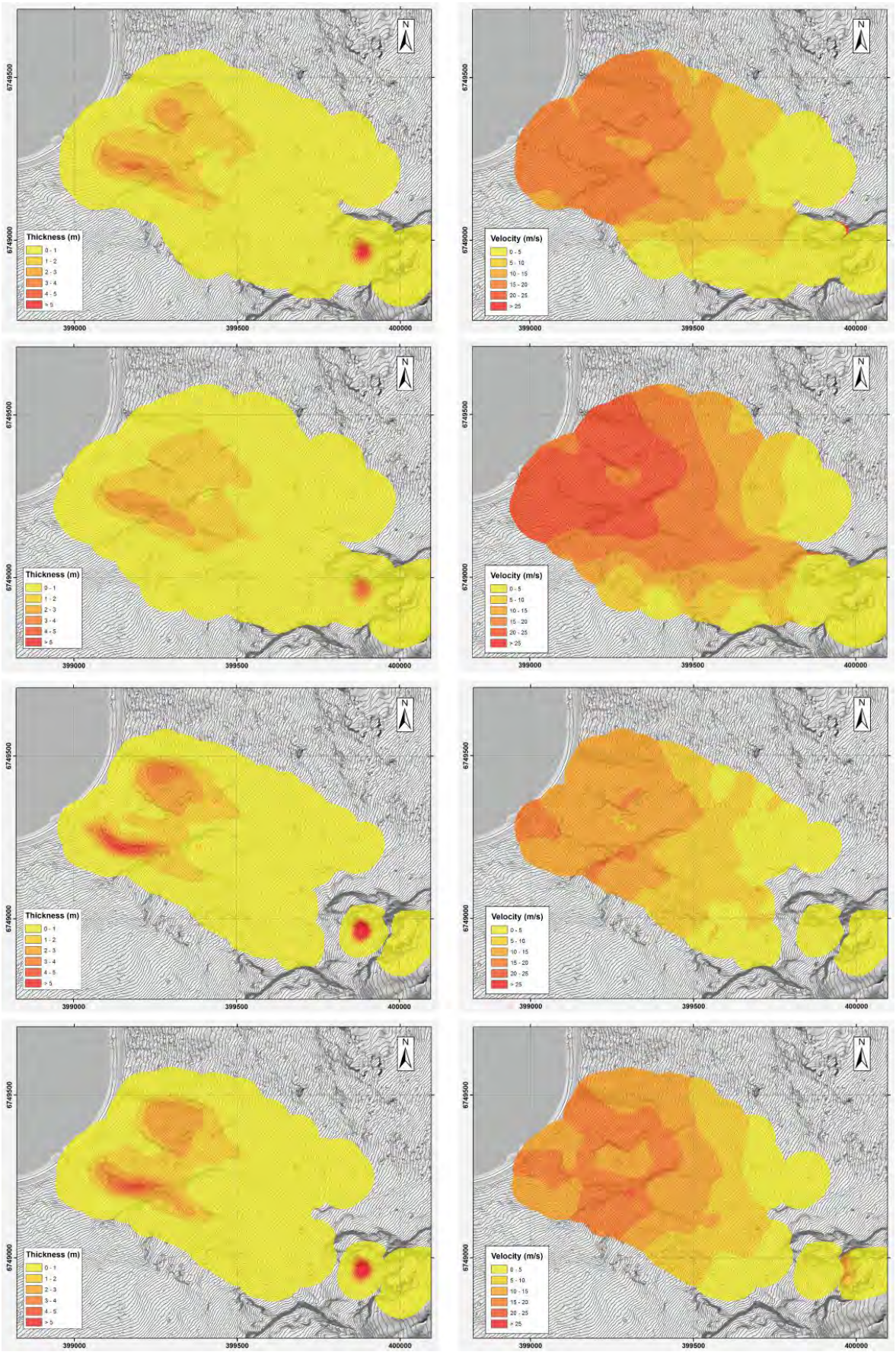

Figure 4. Results for simulations including a maximum erosion depth of 10 m for the Thick talus units and a maximum volume of 500000 m^3. Order similar to Fig. 3.

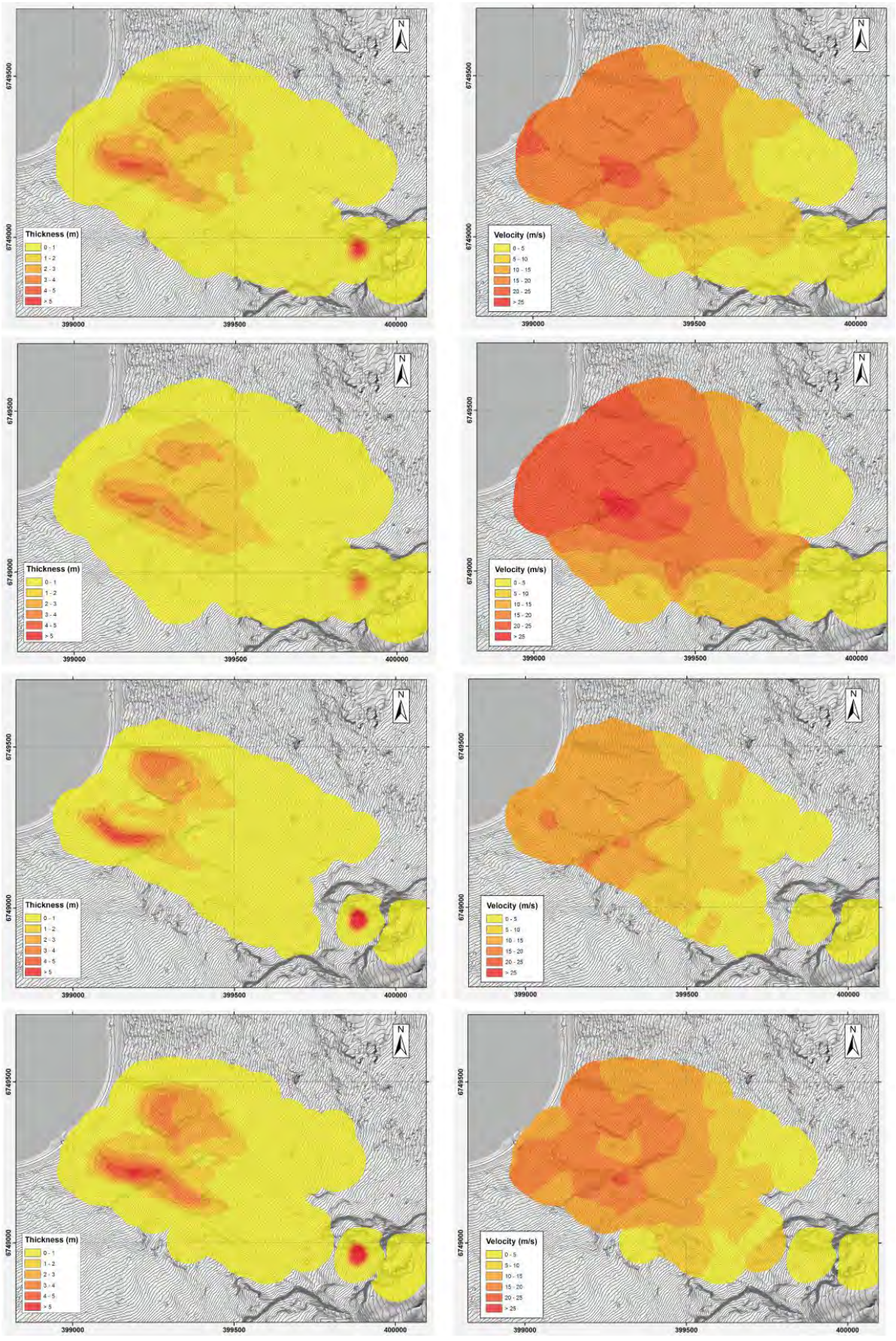

Figure 5. Results for simulations including a maximum erosion depth of 5 m for the Shallow talus unit, 10 m for the Thick talus unit, and a maximum volume of 500000 m^3. Order similar to Fig. 3.

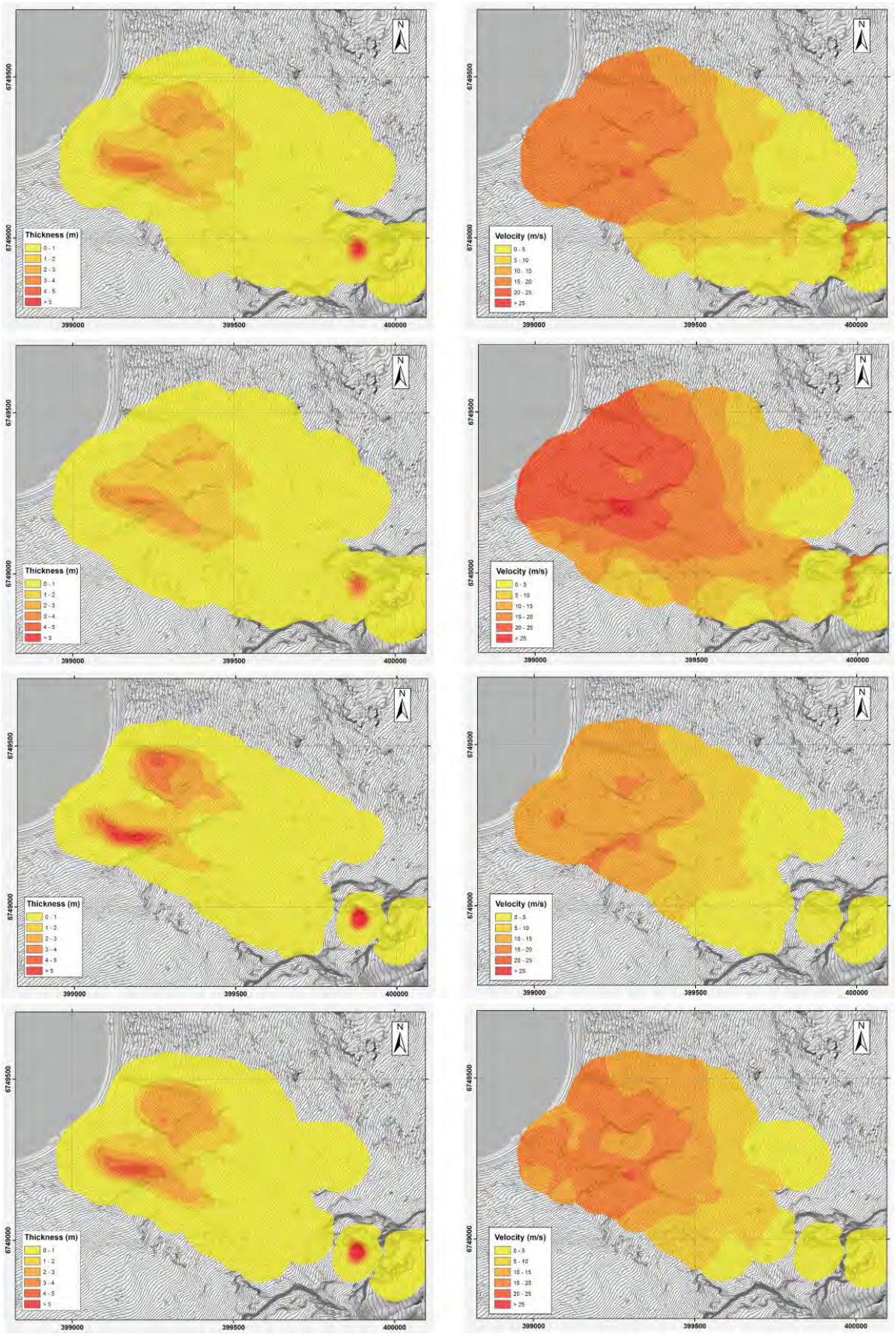

Figure 6. Results for simulation including a maximum erosion depth of 10 m for the Thick talus unit and a maximum volume of 500000 m^3. Order similar to Fig. 3.

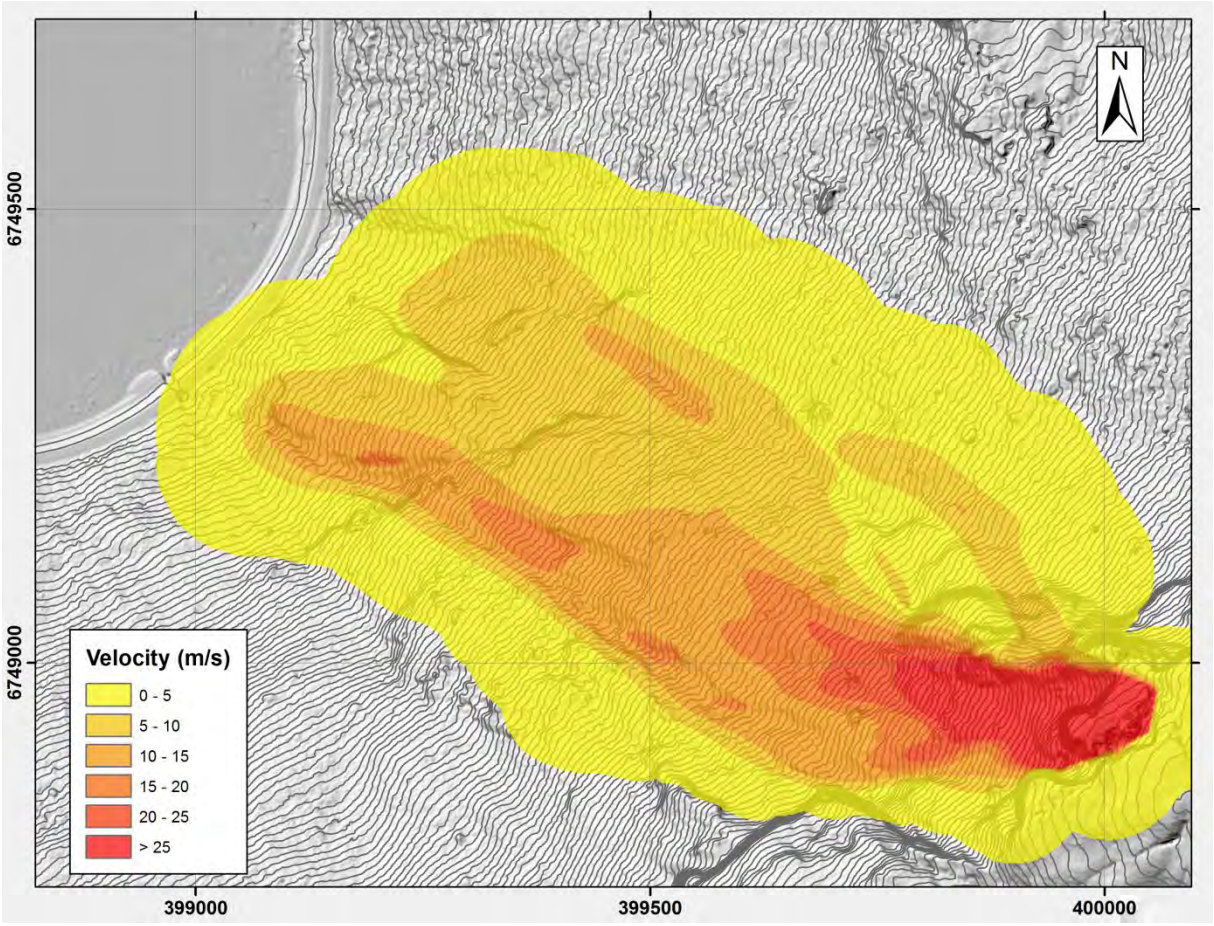

Figure 7. Maximum thickness along the run out track for the case of sliding mass with no entrainment. Friction coefficient 0.1, Turbulence coefficient 450.

Appendix 2: Risk classification, the geological input data and the specific input parameters for each scenario.

Reginald Hermanns (NGU) and Lars Harald Blikra (ÅTB)

The risk classification is based on Hermanns et al. (2012). For each scenario, the risk classification matrix, the hazard score and the summary is given as presented in the individual Excel sheets.

Scenario 1a

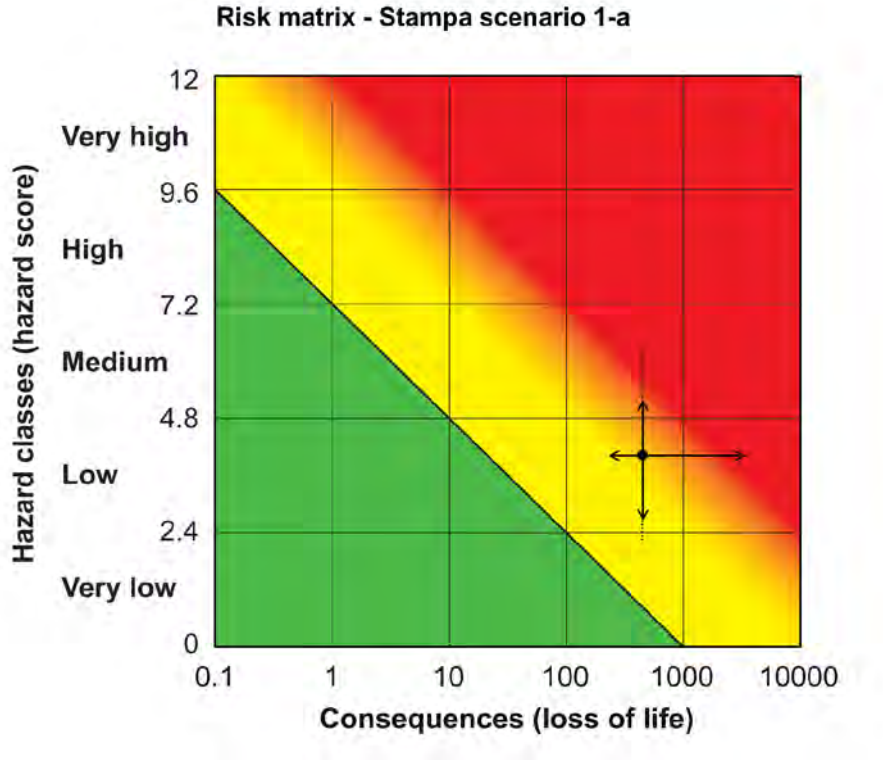

Hazard assessment of unstable rock slopes in Norway

Site name:	Stampa 1a	**Made by:**	Reginald Hermanns / Lars Blikra	**Date:**	22.04.2013

Hazard classes	Class upper limit	Probability	Cumulative probability
Very low	2,4	0,6 %	0,6 %
Low	4,8	88,4 %	89,0 %
Medium	7,2	11,0 %	100,0 %
High	9,6	0,0 %	100,0 %
Very high	12,0	0,0 %	100,0 %

Basic statistics	
Min	2,3
Max	6,3
Mode	4,3
Mean	4,0
5th percentile	2,7
95th percentile	5,2

Fitted normal distribution	
Mean μ	3,9
St. dev. σ	0,8
Mean - 2σ	5
Mean + 2σ	5,45
Corr. coeff.	0,9984
K-S-test (max. diff.)	9,4 %

1. Back-scarp	Score	Rel. prob.	Norm. prob.
Not developed	0	0	0,0 %
Partly open over length of slide body (few cm to m)	0,5	20	20,0 %
Fully open over length of slide body (few cm to m)	1	80	80,0 %

2. Potential sliding structures	Score	Rel. prob.	Norm. prob.
No penetrative structures dip out of the slope	0	10	10,0 %
Penetrative structures dip on average < 20 degree or steeper than the slope	0,5	80	80,0 %
Penetrative structures dip on average > 20 degree and daylight with the slope	1	10	10,0 %

3. Lateral release surfaces	Score	Rel. prob.	Norm. prob.
Not developed	0	0	0,0 %
Partly developed on 1 side	0,25	0	0,0 %
Fully developed or free slope on 1 side or partly developed on 2 sides	0,5	0	0,0 %
Fully developed or free slope on 1 side and partly developed on 1 side	0,75	100	100,0 %
Fully developed or free slope on 2 sides	1	0	0,0 %

4. Kinematic feasibility test	Score	Rel. prob.	Norm. prob.
Kinematic feasibility test does not allow for planar, wedge sliding or toppling	0	0	0,0 %
Failure is partly kinematically possible (movement direction is more than ± 30° to slope orientation)	0,5	100	100,0 %
Failure is partly kinematically possible (movement direction is more than ± 30° to slope orientation)	0,75	0	0,0 %
Failure is partly kinematically possible on persistent discontinuities (movement direction is more than ± 30° to slope orientation)	0,75	0	0,0 %
Failure is kinematically possible on persistent discontinuities (movement direction is less than ± 30° to slope orientation)	1	0	0,0 %

5. Morphologic expression of the rupture surface	Score	Rel. prob.	Norm. prob.
No indication on slope morphology	0	75	75,0 %
Slope morphology suggests formation of a rupture surface (bulging, concavity-convexity, springs)	0,5	25	25,0 %
Continuous rupture surface is suggested by slope morphology and can be mapped out	1	0	0,0 %

6. Displacement rates	Score	Rel. prob.	Norm. prob.
No significant movement	0	50	50,0 %
0.2 - 0.5 cm/year	1	50	50,0 %
0.5 - 1 cm/year	2	0	0,0 %
1 - 4 cm/year	3		0,0 %
4 - 10 cm/year	4		0,0 %
> 10 cm/year	5	0	0,0 %

7. Acceleration (if velocity is >0.5 cm/yr and <10 cm/yr)	Score	Rel. prob.	Norm. prob.
No acceleration or change in slope deformation	0	0	50,0 %
Increase in slope deformation	1	0	50,0 %

8. Increase of rock fall activity	Score	Rel. prob.	Norm. prob.
No increase of rock fall activity	0	75	75,0 %
Increase of rock fall activity	1	25	25,0 %

9. Past events	Score	Rel. prob.	Norm. prob.
No post-glacial events of similar size	0	0	0,0 %
One or several events older than 5000 years of similar size	0,5	100	100,0 %
One or several events younger than 5000 years of similar size	1	0	0,0 %

Summary scenario 1a

Consequences analysis			
	Minimum	Mean	Maximum
Consequences	228	446	3378

Hazard score	
Minimum	2,25
Maximum	6,25
Mode	4,25
Mean	4,03
5th percentile	2,66
95th percentile	5,19

Risk matrix	Consequences	Hazard
Mean	446	4,03
Minimum consequences	228	4,03
Maximum consequences	3378	4,03
Minimum hazard score	446	2,25
Maximum hazard score	446	6,25
5th percentile hazard score	446	2,66
95th percentile hazard score	446	5,19

Scenario 1b

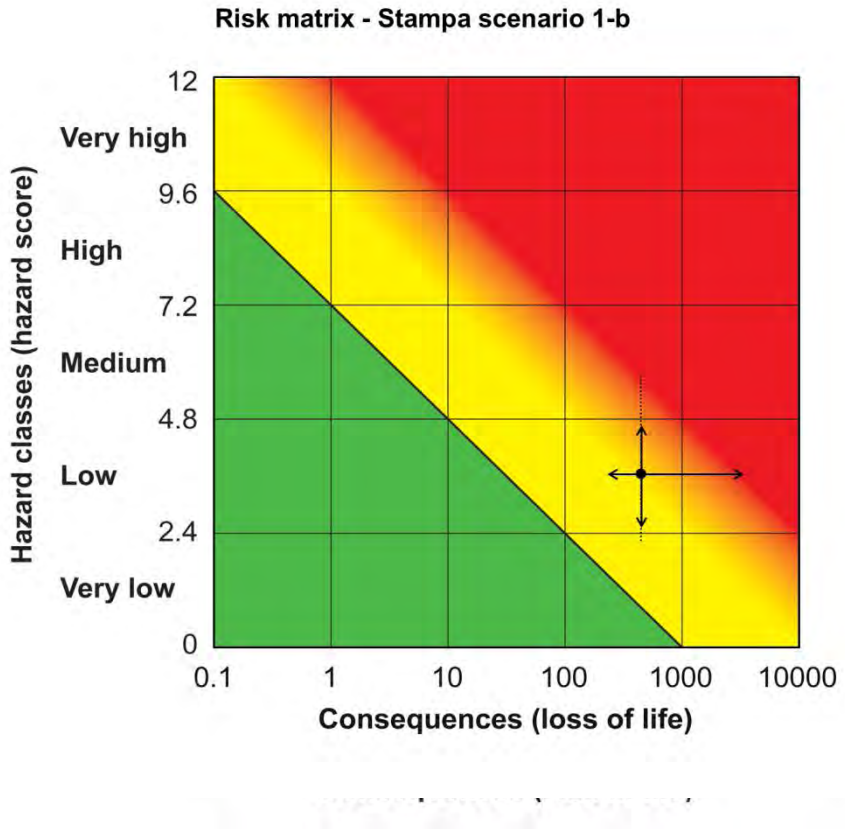

Hazard assessment of unstable rock slopes in Norway

Site name:	Stampa 1b	Made by:	Reginald Hermanns / Lars Blikra	Date:	13.02.2013

Hazard classes	Class upper limit	Probability	Cumulative probability
Very low	2,4	3,5 %	3,5 %
Low	4,8	93,6 %	97,2 %
Medium	7,2	2,8 %	100,0 %
High	9,6	0,0 %	100,0 %
Very high	12,0	0,0 %	100,0 %

Basic statistics	
Min	2,3
Max	5,8
Mode	3,3
Mean	3,7
5th percentile	2,5
95th percentile	4,7

Fitted normal distribution	
Mean μ	3,5
St. dev. σ	0,7
Mean - 2σ	2,0
Mean + 2σ	5,0
Corr. coeff.	0,9984
K-S-test (max. diff.)	8,0 %

1. Back-scarp	Score	Rel. prob.	Norm. prob.
Not developed	0	0	0,0 %
Partly open over length of slide body (few cm to m)	0,5	35	35,0 %
Fully open over length of slide body (few cm to m)	1	65	65,0 %

2. Potential sliding structures	Score	Rel. prob.	Norm. prob.
No penetrative structures dip out of the slope	0	0	0,0 %
Penetrative structures dip on average < 20 degree or steeper than the slope	0,5	100	100,0 %
Penetrative structures dip on average > 20 degree and daylight with the slope	1	0	0,0 %

3. Lateral release surfaces	Score	Rel. prob.	Norm. prob.
Not developed	0	0	0,0 %
Partly developed on 1 side	0,25	0	0,0 %
Fully developed or free slope on 1 side or partly developed on 2 sides	0,5	0	0,0 %
Fully developed or free slope on 1 side and partly developed on 1 side	0,75	100	100,0 %
Fully developed or free slope on 2 sides	1	0	0,0 %

4. Kinematic feasibility test	Score	Rel. prob.	Norm. prob.
Kinematic feasibility test does not allow for planar, wedge sliding or toppling	0	0	0,0 %
Failure is partly kinematically possible (movement direction is more than ± 30° to slope orientation)	0,5	100	100,0 %
Failure is partly kinematically possible (movement direction is more than ± 30° to slope orientation)	0,75	0	0,0 %
Failure is partly kinematically possible on persistent discontinuities (movement direction is more than ± 30° to slope orientation)	0,75	0	0,0 %
Failure is kinematically possible on persistent discontinuities (movement direction is less than ± 30° to slope orientation)	1	0	0,0 %

5. Morphologic expression of the rupture surface	Score	Rel. prob.	Norm. prob.
No indication on slope morphology	0	75	75,0 %
Slope morphology suggests formation of a rupture surface (bulging, concavity-convexity, springs)	0,5	25	25,0 %
Continuous rupture surface is suggested by slope morphology and can be mapped out	1	0	0,0 %

6. Displacement rates	Score	Rel. prob.	Norm. prob.
No significant movement	0	50	50,0 %
0.2 - 0.5 cm/year	1	50	50,0 %
0.5 - 1 cm/year	2	0	0,0 %
1 - 4 cm/year	3	0	0,0 %
4 - 10 cm/year	4	0	0,0 %
> 10 cm/year	5	0	0,0 %

7. Acceleration (if velocity is >0.5 cm/yr and <10 cm/yr)	Score	Rel. prob.	Norm. prob.
No acceleration or change in slope deformation	0	90	90,0 %
Increase in slope deformation	1	10	10,0 %

8. Increase of rock fall activity	Score	Rel. prob.	Norm. prob.
No increase of rock fall activity	0	90	90,0 %
Increase of rock fall activity	1	10	10,0 %

9. Past events	Score	Rel. prob.	Norm. prob.
No post-glacial events of similar size	0	30	30,0 %
One or several events older than 5000 years of similar size	0,5	70	70,0 %
One or several events younger than 5000 years of similar size	1	0	0,0 %

Summary scenario 1b

Consequences analysis			
	Minimum	Mean	Maximum
Consequences	228	446	3378

Hazard score	
Minimum	2,25
Maximum	5,75
Mode	3,25
Mean	3,65
5th percentile	2,52
95th percentile	4,68

Risk matrix	Consequences	Hazard
Mean	446	3,65
Minimum consequences	228	3,65
Maximum consequences	3378	3,65
Minimum hazard score	446	2,25
Maximum hazard score	446	5,75
5th percentile hazard score	446	2,52
95th percentile hazard score	446	4,68

Scenario 2a

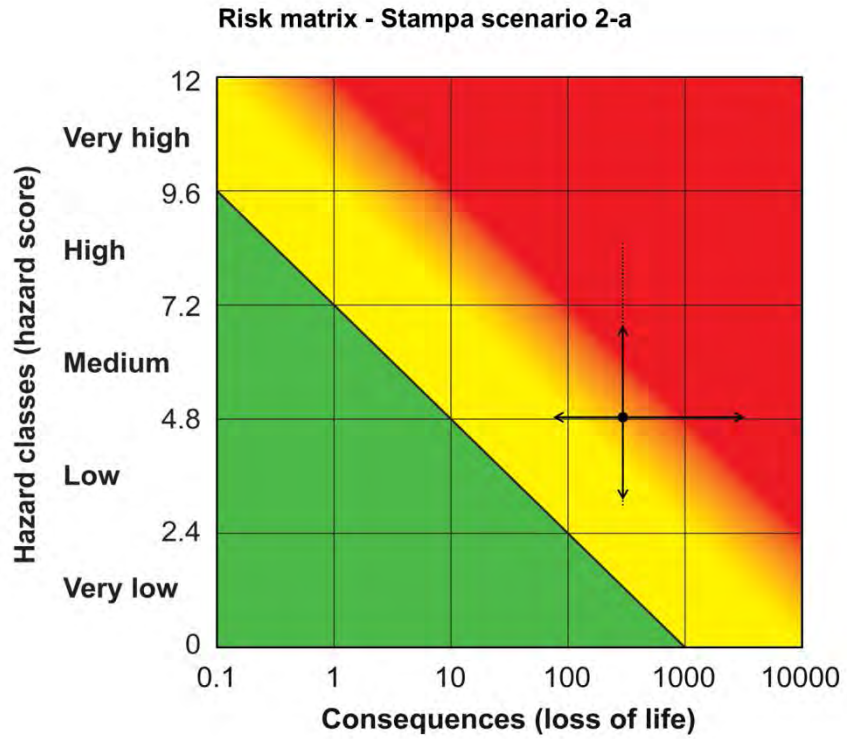

Hazard assessment of unstable rock slopes in Norway

Site name:	Stampa 2a	Made by:	Reginald Hermanns / Lars Blikra	Date:	13.02.2013

Hazard classes	Class upper limit	Probability	Cumulative probability
Very low	2,4	0,0 %	0,0 %
Low	4,8	55,8 %	55,8 %
Medium	7,2	41,9 %	97,7 %
High	9,6	2,3 %	100,0 %
Very high	12,0	0,0 %	100,0 %

Basic statistics	
Min	3,00
Max	8,50
Mode	4,50
Mean	4,84
5th percentile	3,11
95th percentile	6,78

Fitted normal distribution	
Mean μ	4,62
St. dev. σ	1,25
Mean - 2σ	2,11
Mean + 2σ	7,12
Corr. coeff.	0,9989
K-S-test (max. diff.)	8,00 %

1. Back-scarp	Score	Rel. prob.	Norm. prob.
Not developed	0	0	0,0 %
Partly open over length of slide body (few cm to m)	0,5	80	80,0 %
Fully open over length of slide body (few cm to m)	1	20	20,0 %

2. Potential sliding structures	Score	Rel. prob.	Norm. prob.
No penetrative structures dip out of the slope	0	0	0,0 %
Penetrative structures dip on average < 20 degree or steeper than the slope	0,5	100	100,0 %
Penetrative structures dip on average > 20 degree and daylight with the slope	1	0	0,0 %

3. Lateral release surfaces	Score	Rel. prob.	Norm. prob.
Not developed	0	0	0,0 %
Partly developed on 1 side	0,25	0	0,0 %
Fully developed or free slope on 1 side or partly developed on 2 sides	0,5	10	10,0 %
Fully developed or free slope on 1 side and partly developed on 1 side	0,75	40	40,0 %
Fully developed or free slope on 2 sides	1	50	50,0 %

4. Kinematic feasibility test	Score	Rel. prob.	Norm. prob.
Kinematic feasibility test does not allow for planar, wedge sliding or toppling	0	0	0,0 %
Failure is partly kinematically possible (movement direction is more than ± 30° to slope orientation)	0,5	100	100,0 %
Failure is partly kinematically possible (movement direction is more than ± 30° to slope orientation)	0,75	0	0,0 %
Failure is partly kinematically possible on persistent discontinuities (movement direction is more than ± 30° to slope orientation)	0,75	0	0,0 %
Failure is kinematically possible on persistent discontinuities (movement direction is less than ± 30° to slope orientation)	1	0	0,0 %

5. Morphologic expression of the rupture surface	Score	Rel. prob.	Norm. prob.
No indication on slope morphology	0	75	75,0 %
Slope morphology suggests formation of a rupture surface (bulging, concavity-convexity, springs)	0,5	25	25,0 %
Continuous rupture surface is suggested by slope morphology and can be mapped out	1	0	0,0 %

6. Displacement rates	Score	Rel. prob.	Norm. prob.
No significant movement	0	33	33,3 %
0.2 - 0.5 cm/year	1	33	33,3 %
0.5 - 1 cm/year	2	33	33,3 %
1 - 4 cm/year	3	0	0,0 %
4 - 10 cm/year	4	0	0,0 %
> 10 cm/year	5	0	0,0 %

7. Acceleration (if velocity is >0.5 cm/yr and <10 cm/yr)	Score	Rel. prob.	Norm. prob.
No acceleration or change in slope deformation	0	0	50,0 %
Increase in slope deformation	1	0	50,0 %

8. Increase of rock fall activity	Score	Rel. prob.	Norm. prob.
No increase of rock fall activity	0	90	90,0 %
Increase of rock fall activity	1	10	10,0 %

9. Past events	Score	Rel. prob.	Norm. prob.
No post-glacial events of similar size	0	0	0,0 %
One or several events older than 5000 years of similar size	0,5	0	0,0 %
One or several events younger than 5000 years of similar size	1	100	100,0 %

Summary scenario 2a

Consequences analysis			
	Minimum	Mean	Maximum
Consequences	74	293	3224

Hazard score	
Minimum	3,00
Maximum	8,50
Mode	4,50
Mean	4,84
5th percentile	3,11
95th percentile	6,78

Risk matrix	Consequences	Hazard
Mean	293	4,84
Minimum consequences	74	4,84
Maximum consequences	3224	4,84
Minimum hazard score	293	3,00
Maximum hazard score	293	8,50
5th percentile hazard score	293	3,11
95th percentile hazard score	293	6,78

Scenario 2b

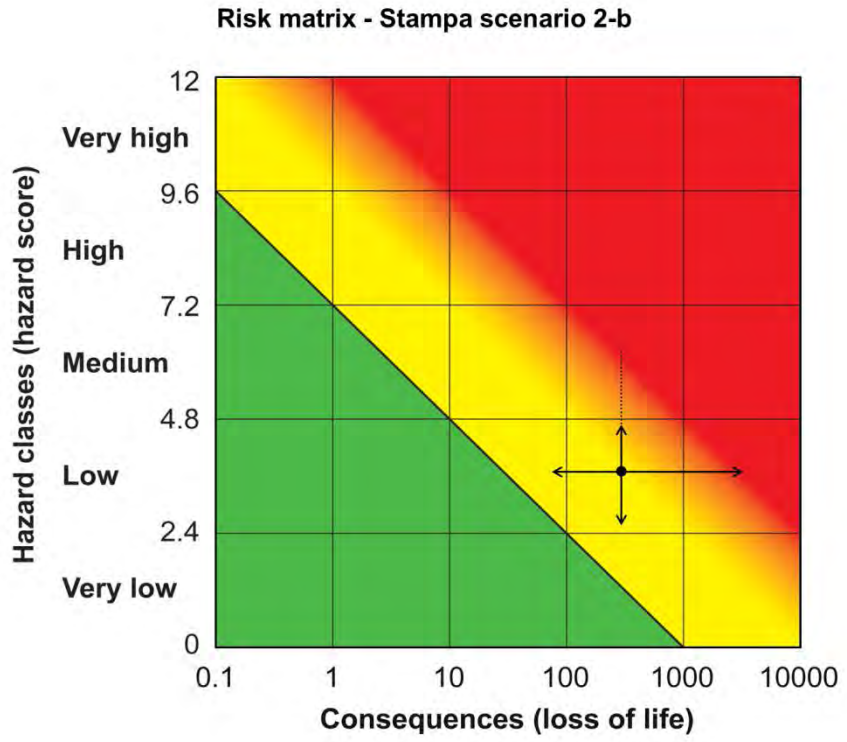

Hazard assessment of unstable rock slopes in Norway

Site name:	Stampa 2b	Made by:	Reginald Hermanns / Lars Blikra	Date:	13.02.2013

Hazard classes	Class upper limit	Probability	Cumulative probability
Very low	2,4	0,0 %	0,0 %
Low	4,8	96,3 %	96,3 %
Medium	7,2	3,7 %	100,0 %
High	9,6	0,0 %	100,0 %
Very high	12,0	0,0 %	100,0 %

Basic statistics	
Min	2,8
Max	6,3
Mode	3,8
Mean	3,7
5th percentile	2,6
95th percentile	4,7

Fitted normal distribution	
Mean μ	3,6
St. dev. σ	0,7
Mean - 2σ	2,1
Mean + 2σ	5,0
Corr. coeff.	0,9991
K-S-test (max. diff.)	6,8 %

1. Back-scarp	Score	Rel. prob.	Norm. prob.
Not developed	0	0	0,0 %
Partly open over length of slide body (few cm to m)	0,5	60	60,0 %
Fully open over length of slide body (few cm to m)	1	40	40,0 %

2. Potential sliding structures	Score	Rel. prob.	Norm. prob.
No penetrative structures dip out of the slope	0	0	0,0 %
Penetrative structures dip on average < 20 degree or steeper than the slope	0,5	100	100,0 %
Penetrative structures dip on average > 20 degree and daylight with the slope	1	0	0,0 %

3. Lateral release surfaces	Score	Rel. prob.	Norm. prob.
Not developed	0	0	0,0 %
Partly developed on 1 side	0,25	70	70,0 %
Fully developed or free slope on 1 side or partly developed on 2 sides	0,5	20	20,0 %
Fully developed or free slope on 1 side and partly developed on 1 side	0,75	10	10,0 %
Fully developed or free slope on 2 sides	1	0	0,0 %

4. Kinematic feasibility test	Score	Rel. prob.	Norm. prob.
Kinematic feasibility test does not allow for planar, wedge sliding or toppling	0	0	0,0 %
Failure is partly kinematically possible (movement direction is more than ± 30° to slope orientation)	0,5	100	100,0 %
Failure is partly kinematically possible (movement direction is more than ± 30° to slope orientation)	0,75	0	0,0 %
Failure is partly kinematically possible on persistent discontinuities (movement direction is more than ± 30° to slope orientation)	0,75	0	0,0 %
Failure is kinematically possible on persistent discontinuities (movement direction is less than ± 30° to slope orientation)	1	0	0,0 %

5. Morphologic expression of the rupture surface	Score	Rel. prob.	Norm. prob.
No indication on slope morphology	0	90	90,0 %
Slope morphology suggests formation of a rupture surface (bulging, concavity-convexity, springs)	0,5	10	10,0 %
Continuous rupture surface is suggested by slope morphology and can be mapped out	1	0	0,0 %

6. Displacement rates	Score	Rel. prob.	Norm. prob.
No significant movement	0	50	50,0 %
0.2 - 0.5 cm/year	1	50	50,0 %
0.5 - 1 cm/year	2	0	0,0 %
1 - 4 cm/year	3	0	0,0 %
4 - 10 cm/year	4	0	0,0 %
> 10 cm/year	5	0	0,0 %

7. Acceleration (if velocity is >0.5 cm/yr and <10 cm/yr)	Score	Rel. prob.	Norm. prob.
No acceleration or change in slope deformation	0	0	50,0 %
Increase in slope deformation	1	0	50,0 %

8. Increase of rock fall activity	Score	Rel. prob.	Norm. prob.
No increase of rock fall activity	0	90	90,0 %
Increase of rock fall activity	1	10	10,0 %

9. Past events	Score	Rel. prob.	Norm. prob.
No post-glacial events of similar size	0	0	0,0 %
One or several events older than 5000 years of similar size	0,5	0	0,0 %
One or several events younger than 5000 years of similar size	1	100	100,0 %

Summary scenario 2b

Consequences analysis			
	Minimum	Mean	Maximum
Consequences	74	293	3224

Hazard score	
Minimum	2,75
Maximum	6,25
Mode	3,75
Mean	3,70
5th percentile	2,57
95th percentile	4,69

Risk matrix	Consequences	Hazard
Mean	293	3,70
Minimum consequences	74	3,70
Maximum consequences	3224	3,70
Minimum hazard score	293	2,75
Maximum hazard score	293	6,25
5th percentile hazard score	293	2,57
95th percentile hazard score	293	4,69

Scenario 3a

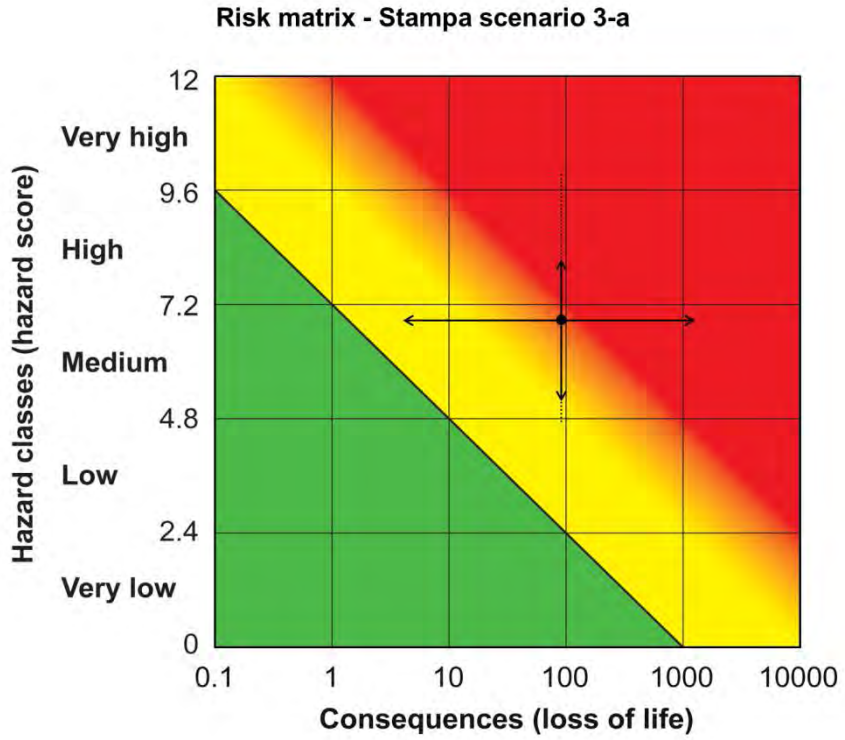

Hazard assessment of unstable rock slopes in Norway

Site name:	Stampa 3a	Made by:	Reginald Hermanns / Lars Blikra	Date:	13.02.2013

Hazard classes	Class upper limit	Probability	Cumulative probability
Very low	2,4	0,0 %	0,0 %
Low	4,8	0,1 %	0,1 %
Medium	7,2	52,3 %	52,4 %
High	9,6	47,5 %	99,9 %
Very high	12,0	0,1 %	100,0 %

Basic statistics	
Min	4,8
Max	10,0
Mode	7,3
Mean	6,9
5th percentile	5,2
95th percentile	8,2

Fitted normal distribution	
Mean μ	6,8
St. dev. σ	0,8
Mean - 2σ	5,1
Mean + 2σ	8,4
Corr. coeff.	0,9987
K-S-test (max. diff.)	9,0 %

1. Back-scarp	Score	Rel. prob.	Norm. prob.
Not developed	0	0	0,0 %
Partly open over length of slide body (few cm to m)	0,5	0	0,0 %
Fully open over length of slide body (few cm to m)	1	100	100,0 %

2. Potential sliding structures	Score	Rel. prob.	Norm. prob.
No penetrative structures dip out of the slope	0	0	0,0 %
Penetrative structures dip on average < 20 degree or steeper than the slope	0,5	100	100,0 %
Penetrative structures dip on average > 20 degree and daylight with the slope	1	0	0,0 %

3. Lateral release surfaces	Score	Rel. prob.	Norm. prob.
Not developed	0	0	0,0 %
Partly developed on 1 side	0,25	0	0,0 %
Fully developed or free slope on 1 side or partly developed on 2 sides	0,5	0	0,0 %
Fully developed or free slope on 1 side and partly developed on 1 side	0,75	10	10,0 %
Fully developed or free slope on 2 sides	1	90	90,0 %

4. Kinematic feasibility test	Score	Rel. prob.	Norm. prob.
Kinematic feasibility test does not allow for planar, wedge sliding or toppling	0	0	0,0 %
Failure is partly kinematically possible (movement direction is more than ± 30° to slope orientation)	0,5	10	10,0 %
Failure is partly kinematically possible (movement direction is more than ± 30° to slope orientation)	0,75	80	80,0 %
Failure is partly kinematically possible on persistent discontinuities (movement direction is more than ± 30° to slope orientation)	0,75	0	0,0 %
Failure is kinematically possible on persistent discontinuities (movement direction is less than ± 30° to slope orientation)	1	10	10,0 %

5. Morphologic expression of the rupture surface	Score	Rel. prob.	Norm. prob.
No indication on slope morphology	0	80	80,0 %
Slope morphology suggests formation of a rupture surface (bulging, concavity-convexity, springs)	0,5	20	20,0 %
Continuous rupture surface is suggested by slope morphology and can be mapped out	1	0	0,0 %

6. Displacement rates	Score	Rel. prob.	Norm. prob.
No significant movement	0	0	0,0 %
0.2 - 0.5 cm/year	1	10	10,0 %
0.5 - 1 cm/year	2	80	80,0 %
1 - 4 cm/year	3	10	10,0 %
4 - 10 cm/year	4	0	0,0 %
> 10 cm/year	5	0	0,0 %

7. Acceleration (if velocity is >0.5 cm/yr and <10 cm/yr)	Score	Rel. prob.	Norm. prob.
No acceleration or change in slope deformation	0	0	50,0 %
Increase in slope deformation	1	0	50,0 %

8. Increase of rock fall activity	Score	Rel. prob.	Norm. prob.
No increase of rock fall activity	0	90	90,0 %
Increase of rock fall activity	1	10	10,0 %

9. Past events	Score	Rel. prob.	Norm. prob.
No post-glacial events of similar size	0	0	0,0 %
One or several events older than 5000 years of similar size	0,5	0	0,0 %
One or several events younger than 5000 years of similar size	1	100	100,0 %

Summary scenario 3a

Consequences analysis			
	Minimum	Mean	Maximum
Consequences	4	91	1264

Hazard score	
Minimum	4,75
Maximum	10,00
Mode	7,25
Mean	6,88
5th percentile	5,18
95th percentile	8,15

Risk matrix	Consequences	Hazard
Mean	91	6,88
Minimum consequences	4	6,88
Maximum consequences	1264	6,88
Minimum hazard score	91	4,75
Maximum hazard score	91	10,00
5th percentile hazard score	91	5,18
95th percentile hazard score	91	8,15

Scenario 3c

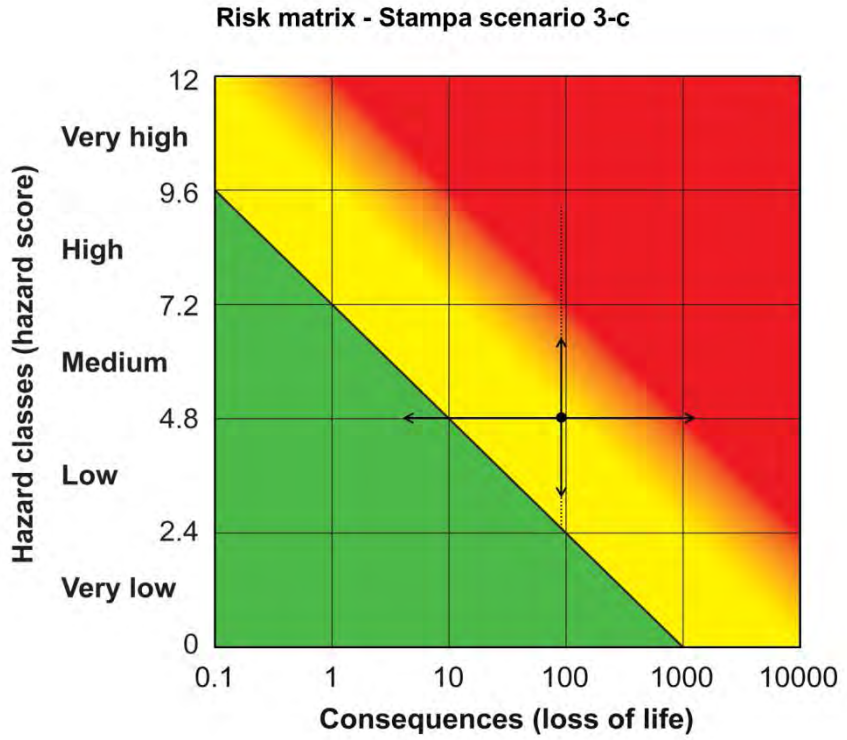

Hazard assessment of unstable rock slopes in Norway

Site name:	Stampa 3c	Made by:	Reginald Hermanns / Lars Blikra	Date:	13.02.2013

Hazard classes	Class upper limit	Probability	Cumulative probability
Very low	2,4	0,0 %	0,0 %
Low	4,8	54,6 %	54,6 %
Medium	7,2	43,0 %	97,6 %
High	9,6	2,4 %	100,0 %
Very high	12,0	0,0 %	100,0 %

Basic statistics	
Min	2,5
Max	9,3
Mode	4,8
Mean	4,8
5th percentile	3,2
95th percentile	6,5

Fitted normal distribution	
Mean μ	4,6
St. dev. σ	1,0
Mean - 2σ	2,7
Mean + 2σ	6,6
Corr. coeff.	0,9999
K-S-test (max. diff.)	2,3 %

1. Back-scarp	Score	Rel. prob.	Norm. prob.
Not developed	0	0	0,0 %
Partly open over length of slide body (few cm to m)	0,5	100	100,0 %
Fully open over length of slide body (few cm to m)	1	0	0,0 %

2. Potential sliding structures	Score	Rel. prob.	Norm. prob.
No penetrative structures dip out of the slope	0	33	33,3 %
Penetrative structures dip on average < 20 degree or steeper than the slope	0,5	33	33,3 %
Penetrative structures dip on average > 20 degree and daylight with the slope	1	33	33,3 %

3. Lateral release surfaces	Score	Rel. prob.	Norm. prob.
Not developed	0	0	0,0 %
Partly developed on 1 side	0,25	0	0,0 %
Fully developed or free slope on 1 side or partly developed on 2 sides	0,5	50	50,0 %
Fully developed or free slope on 1 side and partly developed on 1 side	0,75	50	50,0 %
Fully developed or free slope on 2 sides	1	0	0,0 %

4. Kinematic feasibility test	Score	Rel. prob.	Norm. prob.
Kinematic feasibility test does not allow for planar, wedge sliding or toppling	0	0	0,0 %
Failure is partly kinematically possible (movement direction is more than ± 30° to slope orientation)	0,5	33	33,3 %
Failure is partly kinematically possible (movement direction is more than ± 30° to slope orientation)	0,75	33	33,3 %
Failure is partly kinematically possible on persistent discontinuities (movement direction is more than ± 30° to slope orientation)	0,75	0	0,0 %
Failure is kinematically possible on persistent discontinuities (movement direction is less than ± 30° to slope orientation)	1	33	33,3 %

5. Morphologic expression of the rupture surface	Score	Rel. prob.	Norm. prob.
No indication on slope morphology	0	33	33,3 %
Slope morphology suggests formation of a rupture surface (bulging, concavity-convexity, springs)	0,5	33	33,3 %
Continuous rupture surface is suggested by slope morphology and can be mapped out	1	33	33,3 %

6. Displacement rates	Score	Rel. prob.	Norm. prob.
No significant movement	0	30	30,0 %
0.2 - 0.5 cm/year	1	60	60,0 %
0.5 - 1 cm/year	2	10	10,0 %
1 - 4 cm/year	3	0	0,0 %
4 - 10 cm/year	4	0	0,0 %
> 10 cm/year	5	0	0,0 %

7. Acceleration (if velocity is >0.5 cm/yr and <10 cm/yr)	Score	Rel. prob.	Norm. prob.
No acceleration or change in slope deformation	0	0	50,0 %
Increase in slope deformation	1	0	50,0 %

8. Increase of rock fall activity	Score	Rel. prob.	Norm. prob.
No increase of rock fall activity	0	90	90,0 %
Increase of rock fall activity	1	10	10,0 %

9. Past events	Score	Rel. prob.	Norm. prob.
No post-glacial events of similar size	0	0	0,0 %
One or several events older than 5000 years of similar size	0,5	0	0,0 %
One or several events younger than 5000 years of similar size	1	100	100,0 %

Summary scenario 3c

Consequences analysis			
	Minimum	Mean	Maximum
Consequences	4	91	1264

Hazard score	
Minimum	2,50
Maximum	9,25
Mode	4,75
Mean	4,83
5th percentile	3,15
95th percentile	6,52

Risk matrix	Consequences	Hazard
Mean	91	4,83
Minimum consequences	4	4,83
Maximum consequences	1264	4,83
Minimum hazard score	91	2,50
Maximum hazard score	91	9,25
5th percentile hazard score	91	3,15
95th percentile hazard score	91	6,52

Scenario 3d

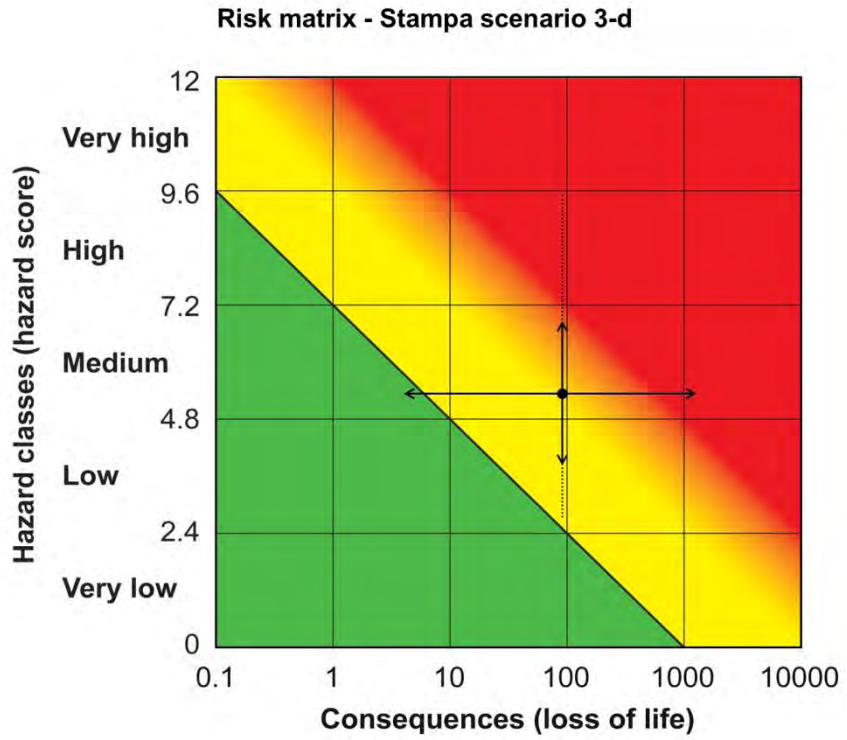

Hazard assessment of unstable rock slopes in Norway

Site name:	Stampa 3d	Made by:	Reginald Hermanns / Lars Blikra	Date:	13.02.2013

Hazard classes	Class upper limit	Probability	Cumulative probability
Very low	2,4	0,0 %	0,0 %
Low	4,8	30,0 %	30,0 %
Medium	7,2	66,1 %	96,1 %
High	9,6	3,9 %	100,0 %
Very high	12,0	0,0 %	100,0 %

Basic statistics	
Min	2,
Max	9,5
Mode	5,0
Mean	5,3
5th percentile	3,8
95th percentile	6,9

Fitted normal distribution	
Mean μ	5,2
St. dev. σ	0,9
Mean - 2σ	3,5
Mean + 2σ	6,9
Corr. coeff.	0,9998
K-S-test (max. diff.)	2,7 %

1. Back-scarp	Score	Rel. prob.	Norm. prob.
Not developed	0	0	0,0 %
Partly open over length of slide body (few cm to m)	0,5	100	100,0 %
Fully open over length of slide body (few cm to m)	1	0	0,0 %

2. Potential sliding structures	Score	Rel. prob.	Norm. prob.
No penetrative structures dip out of the slope	0	33	33,3 %
Penetrative structures dip on average < 20 degree or steeper than the slope	0,5	33	33,3 %
Penetrative structures dip on average > 20 degree and daylight with the slope	1	33	33,3 %

3. Lateral release surfaces	Score	Rel. prob.	Norm. prob.
Not developed	0	0	0,0 %
Partly developed on 1 side	0,25	0	0,0 %
Fully developed or free slope on 1 side or partly developed on 2 sides	0,5	0	0,0 %
Fully developed or free slope on 1 side and partly developed on 1 side	0,75	25	25,0 %
Fully developed or free slope on 2 sides	1	75	75,0 %

4. Kinematic feasibility test	Score	Rel. prob.	Norm. prob.
Kinematic feasibility test does not allow for planar, wedge sliding or toppling	0	0	0,0 %
Failure is partly kinematically possible (movement direction is more than ± 30° to slope orientation)	0,5	33	33,3 %
Failure is partly kinematically possible (movement direction is more than ± 30° to slope orientation)	0,75	33	33,3 %
Failure is partly kinematically possible on persistent discontinuities (movement direction is more than ± 30° to slope orientation)	0,75	0	0,0 %
Failure is kinematically possible on persistent discontinuities (movement direction is less than ± 30° to slope orientation)	1	33	33,3 %

5. Morphologic expression of the rupture surface	Score	Rel. prob.	Norm. prob.
No indication on slope morphology	0	33	33,3 %
Slope morphology suggests formation of a rupture surface (bulging, concavity-convexity, springs)	0,5	33	33,3 %
Continuous rupture surface is suggested by slope morphology and can be mapped out	1	33	33,3 %

6. Displacement rates	Score	Rel. prob.	Norm. prob.
No significant movement	0	10	10,0 %
0.2 - 0.5 cm/year	1	80	80,0 %
0.5 - 1 cm/year	2	10	10,0 %
1 - 4 cm/year	3	0	0,0 %
4 - 10 cm/year	4	0	0,0 %
> 10 cm/year	5	0	0,0 %

7. Acceleration (if velocity is >0.5 cm/yr and <10 cm/yr)	Score	Rel. prob.	Norm. prob.
No acceleration or change in slope deformation	0	0	50,0 %
Increase in slope deformation	1	0	50,0 %

8. Increase of rock fall activity	Score	Rel. prob.	Norm. prob.
No increase of rock fall activity	0	90	90,0 %
Increase of rock fall activity	1	10	10,0 %

9. Past events	Score	Rel. prob.	Norm. prob.
No post-glacial events of similar size	0	0	0,0 %
One or several events older than 5000 years of similar size	0,5	0	0,0 %
One or several events younger than 5000 years of similar size	1	100	100,0 %

Summary scenario 3d

Consequences analysis			
	Minimum	Mean	Maximum
Consequences	4	91	1264

Hazard score	
Minimum	2,75
Maximum	9,50
Mode	5,00
Mean	5,34
5th percentile	3,84
95th percentile	6,87

Risk matrix	Consequences	Hazard
Mean	91	5,34
Minimum consequences	4	5,34
Maximum consequences	1264	5,34
Minimum hazard score	91	2,75
Maximum hazard score	91	9,50
5th percentile hazard score	91	3,84
95th percentile hazard score	91	6,87

Denne serien utgis av Norges vassdrags- og energidirektorat (NVE)

Utgitt i Rapportserien i 2013

Nr. 1 Roller i det nasjonale arbeidet med håndtering av naturfarer for tre samarbeidende direktorat
Nr. 2 Norwegian Hydrological Reference Dataset for Climate Change Studies. Anne K. Fleig (Ed.)
Nr. 3 Anlegging av regnbed. En billedkavalkade over 4 anlagte regnbed
Nr. 4 Faresonekart skred Odda kommune
Nr. 5 Faresonekart skred Årdal kommune
Nr. 6 Sammenfatning av planlagte investeringer i sentral- og regionalnettet for perioden 2012-2021
Nr. 7 Vandringshindere i Gaula, Namsen og Stjørdalselva
Nr. 8 Kvartalsrapport for kraftmarknaden. Ellen Skaansar (red.)
Nr. 9 Energibruk i kontorbygg – trender og drivere
Nr. 10 Flomsonekart Delprosjekt Levanger. Kjartan Orvedal, Julio Pereira
Nr. 11 Årsrapport for tilsyn 2012
Nr. 12 Report from field trip, Ethiopia. Preparation for ADCP testing (14-21.08.2012)
Nr. 13 Vindkraft - produksjon i 2012
Nr. 14 Statistikk over nettleie i regional- og distribusjonsnettet 2013. Inger Sætrang
Nr. 15 Klimatilpasning i energiforsyningen- status 2012. Hvor står vi nå?
Nr. 16 Energy consumption 2012. Household energy consumption
Nr. 17 Bioenergipotensialet i industrielt avfall
Nr. 18 Utvikling i nøkkeltall for strømnettselskapene
Nr. 19 NVEs årsmelding
Nr. 20 Oversikt over vedtak og utvalgte saker. Tariffer og vilkår for overføring av kraft i 2012
Nr. 21 Naturfareprosjektet: Delprosjekt Kvikkleire. Utstrekning og utløpsdistanse for kvikkleireskred basert på katalog over skredhendelser i Norge
Nr. 22 Naturfareprosjektet: Delprosjekt Kvikkleire. Forebyggende kartlegging mot skred langs strandsonen i Norge Oppsummering av erfaring og anbefalinger
Nr. 23 Naturfareprosjektet: Delprosjekt Kvikkleire. Nasjonal database for grunnundersøkelser (NADAG) – forundersøkelse
Nr. 24 Flom og skred i Troms juli 2012. Inger Karin Engen, Graziella Devoli, Knut A. Hoseth, Lars-Evan Pettersson
Nr. 25 Capacity Building in Hydrological Services. ADCP and Pressure Sensor Training Ministry of Water and Energy, Ethiopia 20th – 28th February 2013
Nr. 26 Naturfareprosjektet: Delprosjekt Kvikkleire. Vurdering av kartleggingsgrunnlaget for kvikkleire i strandsonen
Nr. 27 Kvartalsrapport for kraftmarknaden. Ellen Skaansar (red.)
Nr. 28 Flomberegninger for Fedaelva, Kvinesdal kommune, Vest-Agder (025.3A1) Per Alve Glad
Nr. 29 Beregning av energitilsig basert på HBV-modeller. Erik Holmquist
Nr. 30 De ustabile fjellsidene i Stampa – Flåm, Aurland kommune. Sammenstilling, scenario, risiko og anbefalinger.
Nr. 31 Naturfareprosjektet: Delprosjekt 4 Overvåking og varsling Overvåking ved akutte skredhendelser
Nr. 32 Landsomfattende mark- og grunnvannsnett. Drift og formidling 2012. Jonatan Haga
Nr. 33 Naturfareprosjektet: Delprosjekt 6 Kvikkleire. Saltdiffusjon som grunnforsterking i kvikkleire
Nr. 34 Kostnadseffektivitet i distribusjonsnettet – En studie av referentene i kostnadsnormmodellen
Nr. 35 The unstable phyllitic rocks in Stampa – Flåm, western Norway. Compilation, scenarios, risk and recommendations.

Norges
vassdrags- og
energidirektorat

Norges vassdrags- og energidirektorat

Middelthunsgate 29
Postboks 5091 Majorstuen
0301 Oslo

Telefon: 09575
Internett: www.nve.no